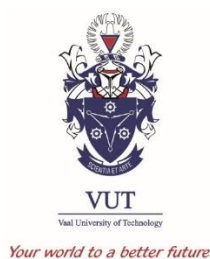


GREEN SYNTHESIS OF COPPER AND SILVER NANOPARTICLES AND THEIR ANTIMICROBIAL ACTIVITY



A Dissertation submitted to the Faculty of Applied and Computer Sciences,
Vaal University of Technology, in fulfilment of the requirement for the degree of
Magister Technologiae: Chemistry.

by

Student Name: Mr. Zondi Nate

Student Number: 212007793

Supervisor :

Prof. Makwena Justice Moloto (VUT, Department of Chemistry)

Co-supervisors:

Dr. Precious Sibiyi (UKZN, School of Physics and Chemistry)

Dr. Pierre Kalenga Mubiayi (VUT, Department of Chemistry)

February 2018

DECLARATION

I, Zondi Nate, student number 212007793, declare that this Dissertation is my work. It has been submitted in partial fulfilment for the degree of Magister technologiae Chemistry in the faculty of Applied and Computer Sciences at the Vaal University of Technology. It has not been submitted for any degree or examination in any other university.

Signature

Date.....

DEDICATION

To my family

PRESENTATIONS

- Oral presentation: 1st VUT interdisciplinary research and postgraduate conference (Vaal University of Technology) (11/2016): Phytochemical screening and antimicrobial activity of *Combretum molle* and *Melia azedarach* leave extracts.
- Oral presentation: SACI young chemist symposium (University of the Witwatersrand) (12/2016): Green synthesis of chitosan capped silver nanoparticles and their antimicrobial activity.
- Poster presentation: SACI inorganic chemistry conference (Cape Town) (07/2017): Green synthesis of silver nanoparticles using *Combretum molle* extracts and their antioxidant and antibacterial activity.
- Oral presentation: 2nd VUT interdisciplinary research and postgraduate conference (Vaal University of Technology) (11/2017): Effect of precursor concentration on the size and shape of silver nanoparticles and their antimicrobial activity.

LIST OF PUBLICATIONS

Submitted manuscript

- Z. Nate, M.J. Moloto, P.K. Mubiayi, P.N. Sibiya, Green synthesis of chitosan capped silver nanoparticles and their antimicrobial activity, MRS advances, (2018) 1-13.
- M.J. Moloto, Z. Nate, P.K. Mubiayi, P.N. Sibiya, Green synthesis of silver nanoparticles using extracts of *Combretum molle* leaves and their antifungal and antioxidant activity. International Journal of Nano and Biomaterials, 2018, under review.

Manuscript under preparation

- M.J. Moloto, Z. Nate, P.K. Mubiayi, P.N. Sibiya, Effect of precursor concentration on the properties of silver nanoparticles.

Additional publication

- T. Xaba, M.J. Moloto, O.B. Nchoe, Z. Nate, N. Moloto, synthesis of silver sulfide nanoparticles through homogeneous precipitation route and the preparation of Ag₂S-Chitosan nanocomposites for the removal of iron (III) ions from wastewater, Chalcogenide letters 14(8) (2017) 337-346.

ABSTRACT

The present study includes the use of a green synthetic method to prepare copper and silver nanoparticles using chitosan, aqueous extracts of *Camellia sinensis*, *Combretum molle* and *Melia azedarach linn* leaves. This study aims to investigate the influence of capping and precursor concentration on the properties of silver nanoparticles with emphasis on the medicinal plants chosen. The effect of capping agent on the properties of copper nanoparticles is also investigated. The phytochemical properties of plant extracts and the antimicrobial activity of the synthesized particles were also studied; this was achieved by using microdilution bioassay. Decoction method was used to extract secondary metabolites from plant leaves. Preliminary phytochemical screening carried out on the aqueous extracts of the plant leaves showed the presence of tannins, proteins, flavonoids, phenols, and carbohydrates. The total phenolic and flavonoids content of the aqueous extract was determined using spectroscopic methods. The highest phenolic content was found in the aqueous extract of *Combretum molle* (135 mg/g), and the highest flavonoid content was found in the aqueous extract of *Camellia sinensis* (0.4 mg/g).

Characterization was done by a combination of spectroscopic, microscopy and XRD techniques. Both the size and shape of the synthesized silver nanoparticles were dependent on the identity of the capping molecule, precursor and capping agent concentration as depicted from their TEM and XRD results. Silver nanoparticles were found to be predominantly spherical. The capping agent concentration was also found to influence the degree of agglomeration, with an increase in capping agent concentration giving lesser agglomeration. FTIR spectral analysis showed that silver nanoparticles interact with bioactive compounds found in the plants through the hydroxyl functional group. Other shapes including diamond were observed for the effect of precursor concentration. The XRD micrographs revealed a face-centered cubic geometry and the phase remained the same with an increase in precursor concentration. The synthesized silver nanoparticles were all blue shifted compared to the bulk material. The TEM results revealed that copper nanoparticles with different sizes and shapes were successfully synthesized.

All the prepared copper and silver nanoparticles showed satisfactory antifungal and antibacterial activity against *Candida albicans*, *Cryptococcus neoformans*, *Staphylococcus aureus*, *Enterococcus faecalis*, *Klebsiella pneumonia* and *Pseudomonas aeruginosa*. The capping molecules used in this study also showed some antibacterial and antifungal activity against the

selected strains. However nanoparticles performed better than these capping molecules. Both silver and copper nanoparticles were found to be more active against gram-negative bacteria compared to gram-positive bacteria. Amongst all the prepared silver nanoparticles *Combretum molle* capped nanoparticles were found to be the most active nanoparticles. Also with copper nanoparticles, it was found that *Combretum molle* capped nanoparticles were the most active nanoparticles. Between the two metal nanoparticles, silver nanoparticles showed high antibacterial and antifungal activity compared to copper nanoparticles.

The antioxidant activity of silver nanoparticles was assessed using 2,2-diphenyl-1-picrylhydrazyl. Silver nanoparticles were found to have some antioxidant activity. However, the capping molecules were found to be more active than the synthesized nanoparticles. This observation is attributed to the presence of some bioactive compounds in the plant extracts.

ACKNOWLEDGEMENTS

The completion of this dissertation is a milestone on my journey of becoming a well-established researcher. I would like to convey my gratitude and appreciation to everyone who assisted and supported me towards achieving this goal. I would also like to express my sincere gratitude to my supervisor Prof Makwena Justice Moloto for his passion, discipline, and dedication. The knowledge and motivation that I gained from you cannot be surpassed, thank you very much Prof MJ Moloto. A special thanks to Dr. PN Sibiya and Dr. PK Mubiayi for co-supervising this work, your contributions to this work is appreciated.

All the glory goes to God, a special thanks to my family for their continuous support and understanding throughout this journey. I would like to thank my colleagues and the NCAP group for their constant support and encouragement. A special thanks to Dikeledi More and Thapelo Mofokeng for their contribution in the preparation of copper nanoparticles. Your suggestions helped me to finish this project. I want to express my deep gratitude to Dr. FM Mtunzi for supplying us with the plant leaves and for his insight in the medicinal plant's aspect. Also, I would like to thank all the BTech postgraduates' students that I worked with; all your projects contributed to this work. A special thank you to Dr. T Xaba for all her contribution to this work.

A special thank you to the department of biotechnology at the Vaal University of Technology, more especially to Samkeliso Takaidza and Angele Munkana for their assistance with the antimicrobial studies. I would also like to acknowledge P Ngoy, B Makgabutlane and the XRD analysis team for their assistance with some analytical instruments. To the 'A-Team' Mahadi Lesaoana, Semakaleng Vivian Kganyago and Daniel Makanyane I cherish your invaluable support and love.

A special mention must be made to a group of people who have contributed to this work. Thank you, Dr. EV Viljoen, Dr. VE Pakade, Dr. P Ejidike, T Selaelo, W, Bout, OB Nchoe, L Maremeni, K Mokubung, SC Nkabinde, N Mabungela, SB Sibokoza, M Thabede, T Ntuli and K Mnqiwu. Finally, I would like to acknowledge the national research foundation, VUT research directorate, department of science and technology and national student financial aid scheme for their financial support.

TABLE OF CONTENTS

DECLARATION.....	II
DEDICATION.....	III
PRESENTATIONS.....	IV
LIST OF PUBLICATIONS	IV
Submitted manuscript	IV
Manuscript under preparation	IV
Additional publication	IV
ABSTRACT.....	V
ACKNOWLEDGEMENTS	VII
LIST OF ABBREVIATIONS	XIII
LIST OF FIGURES	XIV
LIST OF TABLES	XVII
LIST OF SCHEMES	XVII
CHAPTER 1.....	1
1.1 INTRODUCTION.....	1
1.1.1 Background	1
1.1.2 Rationale	3
1.2 AIMS AND OBJECTIVES	5
1.2.1 Aims.....	5
1.2.2 Objectives.....	5
1.3 REFERENCES.....	6
Chapter 2	9
2.1 THE ROLE OF CAPPING MOLECULES IN THE SYNTHESIS OF NANOPARTICLES	
9	
2.2 CHITOSAN AS A CAPPING MOLECULE.....	10

2.2.1	Properties.....	10
2.2.2	Application of chitosan in the preparation of nanomaterials	12
2.3	PLANT EXTRACTS AS STABILIZERS AND REDUCTANTS FOR PREPARING METAL NANOPARTICLES	13
2.3.1	<i>Camellia sinensis</i>	13
2.3.2	<i>Melia azedarach linn</i>	14
2.3.3	<i>Combretum molle</i>	15
2.4	THE INFLUENCE OF pH ON THE PROPERTIES OF BIOACTIVE COMPOUNDS FROM PLANT EXTRACTS	15
2.5	GREEN SYNTHESIS	16
2.6	METHODS OF NANOPARTICLES SYNTHESIS.....	17
2.6.1	Biological approach.....	17
2.6.2	Physical approach	20
2.6.3	Chemical approach	21
2.7	EXTRACTION METHODS	22
2.7.1	Background	22
2.7.2	Maceration and decoction extraction methods.....	23
2.7.3	Microwave and ultrasonic assisted extraction methods	24
2.8	METHODS TO DETECT ANTIBACTERIAL ACTIVITY	25
2.8.1	Background	25
2.8.2	Agar diffusion methods	25
2.8.3	Dilution method.....	26
2.9	ANTIBACTERIAL POTENTIAL OF COPPER AND SILVER METALS NANOPARTICLES AND THEIR BULK COUNTERPARTS	27
2.10	MECHANISM FOR ANTIMICROBIAL RESISTANCE	29
2.11	HIGHLIGHTS FROM THE LITERATURE REVIEW	30

2.12	REFERENCES.....	30
	Chapter 3	42
3.1	MATERIALS	42
3.2	PREPARATION OF PLANT EXTRACT.....	42
3.2.1	Collection of plant leaves	42
3.2.2	Drying of plant leaves	42
3.2.3	Preparation of extracts	43
3.3	PRELIMINARY PHYTOCHEMICAL SCREENING	43
3.3.1	Test for phenolic compounds	43
3.3.2	Test for flavonoids.....	43
3.3.3	Test for carbohydrates.....	43
3.3.4	Test for proteins	43
3.3.5	Test of saponins	44
3.3.6	Test for alkaloids.....	44
3.3.7	Test for glycosides.....	44
3.3.8	Test for diterpenes and triterpenes	44
3.4	PRELIMINARY PHYTOCHEMICAL SCREENING BY THIN LAYER CHROMATOGRAPHY (TLC).....	44
3.5	DETERMINATION OF TOTAL PHENOLIC CONTENTS.....	44
3.6	DETERMINATION OF TOTAL FLAVONOID CONTENTS.....	45
3.7	SYNTHESIS OF NANOPARTICLES	45
3.7.1	Synthesis of silver nanoparticles for effect of capping agent concentration	45
3.7.2	Synthesis of silver nanoparticles for effect of precursor concentration	45
3.7.3	Synthesis of copper nanoparticles for effect of capping agent	46
3.8	CHARACTERIZATION TECHNIQUES.....	46
3.9	BIOLOGICAL STUDIES	46

3.9.1	Bacterial strains.....	46
3.9.2	Fungal strains	47
3.9.3	Antibacterial studies	47
3.9.4	Antifungal studies	47
3.9.5	Antioxidants studies.....	48
3.10	REFERENCES.....	48
	Chapter 4	50
4.1	PHYTOCHEMICAL SCREENING	50
4.1.1	Phytochemical screening, total phenolic, and flavonoid content	50
4.1.2	Uv-vis spectroscopy.....	52
4.1.3	Fourier Infrared Spectroscopy (FTIR).....	53
4.2	EFFECT OF CAPPING AGENT CONCENTRATION ON SILVER NANOPARTICLES CAPPED WITH PLANT EXTRACTS OF <i>CAMELLIA SINENSIS</i> , <i>COMBRETUM MOLLE</i> , AND <i>MELIA AZEDARACH LINN</i>	54
4.2.1	Optical properties	54
4.2.2	Interaction of silver nanoparticles with plant extracts	56
4.2.3	X-ray diffraction analysis.....	58
4.2.4	Transmission electron microscopy (TEM) analysis	59
4.2.5	Biological application.....	62
4.3	EFFECT OF CAPPING AGENT CONCENTRATION ON SILVER NANOPARTICLES CAPPED WITH CHITOSAN.....	67
4.3.1	Optical properties	67
4.3.2	Interaction of silver nanoparticles with chitosan	68
4.3.3	X-ray diffraction analysis.....	70
4.3.4	Transmission electron microscopy analysis.....	71
4.3.5	Biological applications	72

4.4	INFLUENCE OF PRECURSOR CONCENTRATION ON THE PROPERTIES OF SILVER NANOPARTICLES	76
4.4.1	Introduction.....	76
4.4.2	Optical properties	76
4.4.3	FTIR spectral analysis	79
4.4.4	X-Ray diffraction studies.....	80
4.4.5	TEM analysis.....	81
4.5	EFFECT OF CAPPING AGENT CONCENTRATION ON THE PROPERTIES OF COPPER NANOPARTICLES AND THEIR ANTIBACTERIAL ACTIVITY	86
4.5.1	Optical properties	86
4.5.2	FTIR spectral analysis	87
4.5.3	TEM analysis.....	89
4.5.4	Antibacterial activity	90
4.6	REFERENCES.....	91
	Chapter 5	97
5.1	Conclusions.....	97
5.2	Future work and Recommendations	99

LIST OF ABBREVIATIONS

MIC	: Minimum inhibition concentration
TLC	: Thin layer chromatography
HPLC	: High performance liquid chromatography
NMR	: Nuclear magnetic resonance
INT	: p-iodonitrotetrazolium chloride
<i>E Coli</i>	: <i>Escherichia coli</i>
TEM	: Transition electron microscopy
PL	: Photoluminescence
FTIR	: Fourier transform infrared spectroscopy
XRD	: X-ray diffraction
YM	: Yeast malt
MH	: Mueller-Hinton
DPPH	: 2, 2-diphenyl-1-picrylhydrazyl
Sa	: <i>Staphylococcus aureus</i>
Ef	: <i>Enterococcus faecalis</i>
PVP	: Polyvinylpyrrolidone
Kp	: <i>Klebsiella pneumonia</i>
CLSI	: Clinical and laboratories standard institute
Pa	: <i>Pseudomonas aeruginosa</i>
DNA	: Deoxyribonucleic acid

Ca	: <i>Candida albicans</i>
Cm	: <i>Combretum molle</i>
Cn	: <i>Cryptococcus neoformans.</i>
Ma	: <i>Melia azedarach linn</i>
Cs	: <i>Camellia sinensis</i>
FWHM	: Full width at half maximum
EDS	: Energy dispersive spectroscopy

LIST OF FIGURES

Fig 2:1 Chemical structure of chitin and chitosan (Raafat and Sahl, 2009).	11
Fig 2:2 Influence of pH on the molecular structure of chitosan (Kumirska et al., 2011).	12
Fig 4:1 TLC of aqueous extract of <i>Camellia sinensis</i> , <i>Combretum molle</i> and <i>Melia azedarach linn</i> leaves.	50
Fig 4:2 Concentration of total phenolic (i) and flavonoids (ii) content.	51
Fig 4:3 Uv-vis spectra of aqueous extract of (i) <i>Camellia sinensis</i> , (ii) <i>Combretum molle</i> and (iii) <i>Melia azedarach linn</i>	53
Fig 4:4 FT-IR spectra of (i) <i>Camellia sinensis</i> , (ii) <i>Combretum molle</i> and (iii) <i>Melia azedarach linn</i> . Key a= crude, b= aqueous extract	54
Fig 4:5 Uv-vis spectra for Ag nanoparticles capped with (i) <i>Camellia sinensis</i> , (ii) <i>Combretum molle</i> and (iii) <i>Melia azedarach linn</i> aqueous leaves extracts. a= 0.5%, b= 1.0%, c= 2.0% capping agent concentration.	55
Fig 4:6 PL spectra for Ag nanoparticles capped with (i) <i>Camellia sinensis</i> , (ii) <i>Combretum molle</i> and (iii) <i>Melia azedarach linn</i> aqueous leaves extracts. a= 0.5%, b= 1.0%, c= 2.0% capping agent concentration.	56
Fig 4:7 FTIR spectra for Ag nanoparticles capped with (i) <i>Camellia sinensis</i> , <i>Combretum molle</i> and (iii) <i>Melia azedarach linn</i> aqueous leaves extracts a= aqueous extract, b= 0.5%, c=1.0%, d=2.0%	57
Fig 4:8 Proposed interaction of silver ions with plant extracts	58

Fig 4:9 XRD micrographs for Ag nanoparticles capped with (i) <i>Camelia sinensis</i> , (ii) <i>Combretum molle</i> and (iii) <i>Melia azedarach linn</i> aqueous leaves extracts. a= Reference spectrum, b= 0.5%, c= 1.0% d= 2.0%	59
Fig 4:10 TEM micrographs of silver nanoparticles capped with (a) 0.5%, (b) 1% and (c) 2% <i>Camellia sinensis</i> leaves and the corresponding histograms (d, e and f)	60
Fig 4:11 TEM micrographs of silver nanoparticles capped with (a) 0.5%, (b) 1% and (c) 2% <i>Combretum molle</i> leaves and the corresponding histograms (d and e).	61
Fig 4:12 TEM micrographs of silver nanoparticles capped with (a) 0.5%, (b) 1% and (c) 2% <i>Melia azedarach linn</i> leaves and the corresponding histograms (d, e and f).	61
Fig 4:13 Antibacterial activity of silver nanoparticles capped with (i) <i>Camellia sinensis</i> , (ii) <i>Combretum molle</i> and (iii) <i>Melia azedarach linn</i> . S.a = <i>Staphylococcus aureus</i> , E.f = <i>Enterococcus faecalis</i> , P.a = <i>Pseudomonas aeruginosa</i> , K.a = <i>Klebsiella pneumoniae</i>	63
Fig 4:14 Antifungal activity of silver nanoparticles capped with (i) <i>Camellia sinensis</i> , (ii) <i>Combretum molle</i> and (iii) <i>Melia azedarach linn</i> . C.a = <i>Candida albicans</i> , C.n = <i>Cryptococcus neoformans</i>	65
Fig 4:15 Free radical scavenging process.....	66
Fig 4:16 Antioxidant activity of silver nanoparticles capped with (i) <i>Camellia sinensis</i> , (ii) <i>Combretum molle</i> and (iii) <i>Melia azedarach linn</i>	67
Fig 4:17 Uv-vis (i) and PL (ii) spectra of chitosan capped silver nanoparticles. a= 0.5% b= 1.0% c=2.0% capping agent concentration.	68
Fig 4:18 FTIR spectra of chitosan capped silver nanoparticles. a= pure chitosan b= 0.5% c=1.0% d=2.0% capping agent concentration.	69
Fig 4:19 Proposed interaction of silver ions with chitosan.....	70
Fig 4:20 XRD micrographs of chitosan capped silver nanoparticles. a= Reference b= 0.5 % c=1.0% and d=2.0 % capping agent concentration	71
Fig 4:21 TEM micrographs of silver nanoparticles with (a) 0.5%, (b) 1% and (c) 2% chitosan and the corresponding histograms (e and f).....	72
Fig 4:22 Antibacterial activity of silver nanoparticles capped with chitosan. S.a = <i>Staphylococcus aureus</i> , E.f = <i>Enterococcus faecalis</i> , P.a = <i>Pseudomonas aeruginosa</i> , K.a = <i>Klebsiella pneumoniae</i>	73
Fig 4:23 Antifungal activity of silver nanoparticles capped with chitosan. C.a = <i>Candida albicans</i> , C.n = <i>Cryptococcus neoformans</i>	75
Fig 4:24 Antioxidant activity of silver nanoparticles capped with chitosan.....	76

Fig 4:25 Uv-vis spectra for Ag nanoparticles capped with (i) chitosan, (ii) <i>Camellia sinensis</i> , (iii) <i>Combretum molle</i> and (iv) <i>Melia azedarach</i> linn. a= 0.1 M, b= 0.2 M, c= 0.3 M silver nitrate concentration.	77
Fig 4:26 PL spectra for Ag nanoparticles capped with (i) chitosan, (ii) <i>Camellia sinensis</i> , (iii) <i>Combretum molle</i> and (iv) <i>Melia azedarach</i> linn. a= 0.1 M, b= 0.2 M, c= 0.3 M silver nitrate concentration.	78
Fig 4:27 FTIR spectra for Ag nanoparticles capped with (i) chitosan, (ii) <i>Camellia sinensis</i> , (iii) <i>Combretum molle</i> and (iv) <i>Melia azedarach</i> linn. a= capping agent, b= 0.1 M, b= 0.2 M, c= 0.3 M silver nitrate concentration.	79
Fig 4:28 XRD micrographs for Ag nanoparticles capped with (i) chitosan, (ii) <i>Camellia sinensis</i> , (iii) <i>Combretum molle</i> and (iv) <i>Melia azedarach</i> linn. a= Reference, b= 0.1 M, c= 0.2 M, d= 0.3M silver nitrate concentration.	81
Fig 4:29 TEM micrographs and the corresponding histograms (e and f) of chitosan capped silver nanoparticles prepared at different silver nitrate concentrations (a) 0.1 M, (b) 0.2 M and (c) 0.3 M.	82
Fig 4:30 TEM micrographs and the corresponding histograms (d, e and f) of <i>Combretum molle</i> capped silver nanoparticles prepared at different silver nitrate concentrations (a) 0.1 M, (b) 0.2 M and (c) 0.3 M.	83
Fig 4:31 TEM micrographs and the corresponding histograms (d, e and f) of <i>Camellia sinensis</i> capped silver nanoparticles prepared at different silver nitrate concentration (a) 0.1 M, (b) 0.2 M and (c) 0.3 M.	84
Fig 4:32 TEM micrographs and the corresponding histograms (d, e and f) of <i>Melia azedarach</i> linn capped silver nanoparticles prepared at different silver nitrate concentrations (a) 0.1M, (b) 0.2 M and (c) 0.3 M.	85
Fig 4:33 Uv-vis spectra of copper nanoparticles capped with (a) chitosan, (b) <i>Camellia sinensis</i> , (c) <i>Combretum molle</i> and (d) <i>Melia azedarach</i> linn.	87
Fig 4:34 FTIR spectra of copper nanoparticles capped with (i) chitosan, (ii) <i>Camellia sinensis</i> , (iii) <i>Combretum molle</i> , (iv) <i>Melia azedarach</i> linn. a = capping molecules b= copper nanoparticles.	88
Fig 4:35 TEM micrographs and histograms (e and f) of capped copper nanoparticles prepared at different capping agents (a) chitosan, (b) <i>Combretum molle</i> , (c) <i>Camellia sinensis</i> , (d) <i>Melia azedarach</i> linn.	89
Fig 4:36 Antibacterial activity of copper nanoparticles capped with (i) chitosan, (ii) <i>Camellia sinensis</i> , (iii) <i>Combretum molle</i> and (iv) <i>Melia azedarach</i> linn. S.a = <i>Staphylococcus aureus</i> , E.f = <i>Enterococcus faecalis</i> , P.a = <i>Pseudomonas aeruginosa</i> , K.a = <i>Klebsiella pneumoniae</i>	90

LIST OF TABLES

Table 4:1 Phytochemical screening of plant extracts.....	50
Table 4:2 Calibration curve results	52
Table 4:3 Effect of capping agent concentration on FWHM of silver nanoparticles.....	55
Table 4:4 Relationship between average particle sizes estimated using Debye-Scherrer equation and capping agent concentration	59
Table 4:5 Relationship between average particle size from TEM and capping agent concentration.....	60
Table 4:6 Effect of capping agent concentration on FWHM of silver nanoparticles based on UV-vis spectroscopy results	68
Table 4:7 Relationship between characteristic plasmon absorption bands and precursor concentration...	77
Table 4:8 Relationship between precursor concentration and FWHM	79
Table 4:9 Functional groups present in chitosan plant extracts	88
Table 4:10 MIC values for copper nanoparticles	91

LIST OF SCHEMES

Scheme 1:1 Bio-reduction of metallic ions using flavonoids from plant extracts.....	2
Scheme 2:3 Influence of pH on the molecular structure of phenol.....	16
Scheme 2:4 Formation of metal nanoparticles using chemical reduction approach.....	22
Scheme 4:1 Formation of silver nanoparticles at different concentrations.....	86

CHAPTER 1

1.1 INTRODUCTION

1.1.1 Background

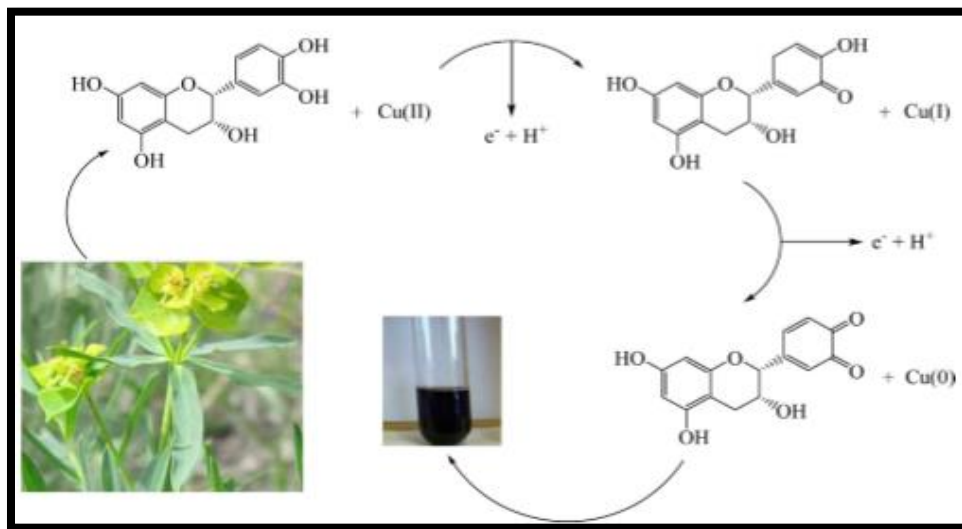
Nanotechnology is an important field in modern research dealing with synthesis, strategy and manipulation of nanomaterials including nanoparticles, nano-sheets, nanowires and nano-rods (Wang and Kong, 2015, Tiwari et al., 2012). Metal nanoparticles are of special importance because they are easier and cheaper to synthesize and are the most promising in applications. Metallic nanoparticles have different physical and chemical properties from their bulk metals. These properties include higher specific surface areas, mechanical strengths, lower melting point and specific optical properties (Marin et al., 2015, Firdhouse and Lalitha, 2015, Beyene et al., 2017). One of the fundamental attractions and characteristics of nanoparticles are their optical properties. The transition from the bulk material size to the nanoparticle size range displays the quantum mechanical properties and also increases the dominance of surface atoms which improves the chemical reactivity of the material (Khalil et al., 2014, Hosseinpour-Mashkani and Ramezani, 2014). The optical properties of silver nanoparticles arise from their high efficiency in absorbing and scattering light (Zhang et al., 2016). When silver nanoparticles interact with light, the conduction electrons on the surface undergo a collective oscillation at a specific wavelength which is defined as surface plasmon resonance.

Metal nanoparticles have attracted considerable attention as antimicrobial agents because of their effectiveness even in small amounts. Copper nanoparticles are mostly used due to their catalytic, optical and electrical conducting properties. Copper is known to have antibacterial and anti-fungal properties, and also it is non-toxic to mammals (Muthukrishnan, 2015, Seil and Webster, 2012). Amongst other noble metals, silver nanoparticles have become the main focus of intensive research due to its wide range of applications in a variety of sectors of life and industry. Silver is an effective antibacterial agent as it is non-toxic to the animal cell and highly toxic to bacteria (Le Ouay and Stellacci, 2015, Losasso et al., 2014).

Due to their unique properties and a wide range of applications different methods are being developed to synthesize metal nanoparticles. Generally, the method used in the synthesis of metal nanoparticles involves the reduction of metal salts in a solution. This is done by the use of reducing

agents such as sodium borohydride which increases the environmental toxicity of the synthesized particles (Rashid et al., 2017, Jalali and Allafchian, 2016). The use of non-biodegradable compounds as reducing agents in the synthesis of metal nanoparticles has a potential hazard to the environment and biological systems. Hence there is an increasing need for clean, less toxic and environmentally friendly methods that follow green chemistry principles. The 12 green chemistry principles include the maximization of atom economy, the use of less hazardous processes and the use of safer solvents (Gałuszka et al., 2013). Other aspects of green synthesis require that the selected reagents are easily accessible, widely distributed, easy to handle and can minimize the waste and be energy cost effective (Gałuszka et al., 2013). By definition, green chemistry is referred as the design, development, and implementation of less-toxic chemical products and processes to reduce the use and generation of substances that are harmful to the environment and human health (Suresh et al., 2014). As part of adhering to the green chemistry guidelines, many researchers have started to use medicinal plants and biodegradable polymers during the synthesis of metal nanoparticles as shown in Scheme 1:1 (Ahmed et al., 2016, Phull et al., 2016).

The current study focuses on the use of chitosan, *Camellia sinensis*, *Combretum molle* and *Melia azedarach linn* as reducing and capping agents in the synthesis of copper and silver nanoparticles. The physical and chemical properties of these four capping agents are discussed in chapter 2.



Scheme 1:1 Bio-reduction of metallic ions using flavonoids from plant extracts (Nasrollahzadeh et al., 2015).

For several decades the resistance of microorganisms to antibiotics has been a growing threat to the treatment of an ever-increasing range of infections caused by bacteria, parasites, viruses, and fungi. Antibiotic resistance occurs when bacteria develop means which reduce the effectiveness of the drug or chemical agent designed to cure or prevent infections (Silver, 2011, Meyer et al., 2011). Since some bacteria have found ways to reduce the effectiveness of antibiotics, the more the antibiotics are used, the more some bacteria become resistant to them. Hence they are adapting to the new environment created by antibiotics (Ventola, 2015, Meyer et al., 2011). Susceptible bacteria are killed, and the resistant bacteria survive and multiply. Hence the need for alternative antibacterial agents is evident.

As part of the ongoing search for a new antimicrobial agent that will have strong antibacterial activity against some resistant microorganism such as *Staphylococcus aureus*, diverse research is being conducted in different fields such as medicinal plants and bio-nanotechnology. Medicinal plants are known to have antimicrobial activity because of the presence of bioactive compounds such as phenols, flavonoids, and tannins. On the other hand nanoparticles of different metals have shown high antimicrobial activity because they possess different chemical and physical properties compared to their bulk counterparts (Philip, 2009, Rajeshkumar, 2016). The properties of metal nanoparticles depend mostly on the size and shape of the material. The high surface to volume ratio of nanoparticles has attracted great interest from most researchers. Since the mechanism of interaction between metal nanoparticles and microorganisms is based on contact between the cell wall and nanoparticles. Therefore the size and shape of the nanoparticles play a crucial role (Reidy et al., 2013, Rajeshkumar, 2016).

1.1.2 Rationale

According to the world health organization, antimicrobial resistance is one of the growing threats to human health. Antimicrobial resistance is estimated to account for more than 700 000 deaths per year worldwide, most of the deaths occur in developing countries which are mostly found in Africa and East Asia (Tadesse et al., 2017). Antimicrobial resistance occurs when bacteria develop means which reduce the effectiveness of the drug or chemical agent designed to cure or prevent infections. Microorganisms have become resistance to mostly used drugs such as cephalosporins,

fluoroquinolones, carbapenems and methicillin; these are first-line drugs for the treatment of urinary tract and blood stream infections. As a result several microorganisms such as *Staphylococcus aureus* are becoming a problem in public hospitals. The common health-care infections that are caused by *Escherichia Coli*, *Klebsiella Pneumoniae*, and *Staphylococcus aureus* are becoming a global problem. *Escherichia Coli* and *Klebsiella Pneumoniae* are associated with urinary tract and blood stream infections while *Staphylococcus aureus* is linked with wound infections. One of the major impacts of antimicrobial resistance is prolonged illness and increased mortality. Antimicrobial resistance is a natural selection phenomenon, and it is accelerated by the selective pressure that arises from the misuse of antimicrobial agents in humans and animals. It is also reported that the resistance is due to the changes in DNA of these organisms and also the concept of Charles Darwin on natural selection which is based on survival of the fittest.

Since the above-mentioned problem affects living organisms such as human beings, several ways have been designed to develop new generations of antimicrobial agents. As part of the ongoing research nanoparticles of noble metals such as copper, gold, and silver are used to treat some of the resistance microorganisms (Durán et al., 2016, Zhang et al., 2015, Bogdanović et al., 2014). The challenge with the use of metal nanoparticles as antimicrobial agents is their method of synthesis since most synthetic methods of metal nanoparticles uses reducing and capping agents that are harmful to humans and the environment. The toxicity of these nanoparticles thus hinders them to be used in biological applications. To address these challenges several studies have been conducted using green synthesis methods, however, despite this, it is still essential to prepare silver and copper nanoparticles of different sizes and shapes since these properties affect the antimicrobial activity of nanoparticles. The particle size and shape plays a crucial role in the physical and chemical properties of nanomaterials, and these two parameters are mostly influenced by the concentration of the precursor and capping agents.

Due to the above-mentioned reasons, the current study, therefore, focuses on the green synthesis of copper and silver nanoparticles using chitosan and medicinal plants (*Camellia Sinensis*, *Combretum Molle* and *Melia Azedarach linn* leave as capping and reducing agents. The biological application of copper and silver nanoparticles is also investigated.

1.2 AIMS AND OBJECTIVES

In summary, the study focuses on the following aims and objectives:

1.2.1 Aims

To synthesize silver nanoparticles using selected plant extracts and chitosan, explore reaction parameters and test the materials for their antimicrobial activities.

1.2.2 Objectives

- To conduct phytochemical screening of aqueous extract of *Camellia Sinensis*, *Combretum Molle*, and *Melia Azedarach linn* leaves and their characterization.
- To examine the effect of capping agent concentration on the properties of silver nanoparticles capped with plant extracts and characterization of nanoparticles using a combination of spectroscopic and microscopic techniques.
- To examine the effect of capping agent concentration on the properties of silver nanoparticles capped with chitosan and characterization of nanoparticles using a combination of spectroscopic and microscopic techniques.
- To study the antibacterial activity of capped silver nanoparticles using two-gram positive bacteria (*Staphylococcus aureus* and *Enterococcus faecalis*) and two-gram negative bacteria (*Klebsiella pneumonia* and *Pseudomonas aeruginosa*).
- To study the antifungal activity of capped silver nanoparticles using *Candida albicans* and *Cryptococcus neoformans*.
- To study the antioxidant activity of capped silver nanoparticles using 2,2-diphenyl-1-picrylhydrazyl.
- To examine the effect of precursor concentration on the size and shape of silver nanoparticles and characterize the nanoparticles using spectroscopic and microscopic techniques.
- To examine the influence of capping agent on the properties of copper nanoparticles and the study of their antibacterial activity.

1.3 REFERENCES

- AHMED, S., AHMAD, M., SWAMI, B. L. & IKRAM, S. 2016. A review on plants extract mediated synthesis of silver nanoparticles for antimicrobial applications: A green expertise. *J Adv Res*, 7, 17-28.
- BEYENE, H. D., WERKNEH, A. A., BEZABH, H. K. & AMBAYE, T. G. 2017. Synthesis paradigm and applications of silver nanoparticles (AgNPs), a review. *Sustainable Materials and Technologies*, 13, 18-23.
- BOGDANOVIĆ, U., LAZIĆ, V., VODNIK, V., BUDIMIR, M., MARKOVIĆ, Z. & DIMITRIJEVIĆ, S. 2014. Copper nanoparticles with high antimicrobial activity. *Materials Letters*, 128, 75-78.
- DURÁN, N., NAKAZATO, G. & SEABRA, A. B. 2016. Antimicrobial activity of biogenic silver nanoparticles, and silver chloride nanoparticles: an overview and comments. *Applied Microbiology and Biotechnology*, 100, 6555-6570.
- FIRDHOUSE, M. J. & LALITHA, P. 2015. Biosynthesis of Silver Nanoparticles and Its Applications. *Journal of Nanotechnology*, 2015, 1-18.
- GALUSZKA, A., MIGASZEWSKI, Z. & NAMIEŚNIK, J. 2013. The 12 principles of green analytical chemistry and the SIGNIFICANCE mnemonic of green analytical practices. *TrAC Trends in Analytical Chemistry*, 50, 78-84.
- HOSSEINPOUR-MASHKANI, S. M. & RAMEZANI, M. 2014. Silver and silver oxide nanoparticles: Synthesis and characterization by thermal decomposition. *Materials Letters*, 130, 259-262.
- JALALI, S. A. H. & ALLAFCHIAN, A. R. 2016. Assessment of antibacterial properties of novel silver nanocomposite. *Journal of the Taiwan Institute of Chemical Engineers*, 59, 506-513.
- KHALIL, M. M. H., ISMAIL, E. H., EL-BAGHDADY, K. Z. & MOHAMED, D. 2014. Green synthesis of silver nanoparticles using olive leaf extract and its antibacterial activity. *Arabian Journal of Chemistry*, 7, 1131-1139.
- LE OUAY, B. & STELLACCI, F. 2015. Antibacterial activity of silver nanoparticles: A surface science insight. *Nano Today*, 10, 339-354.
- LOSASSO, C., BELLUCO, S., CIBIN, V., ZAVAGNIN, P., MIČETIĆ, I., GALLOCCHIO, F., ZANELLA, M., BREGOLI, L., BIANCOTTO, G. & RICCI, A. 2014. Antibacterial

- activity of silver nanoparticles: sensitivity of different Salmonella serovars. *Frontiers in Microbiology*, 5, 227.
- MARIN, S., VLASCEANU, G. M., TIPLEA, R. E., BUCUR, I. R., LEMNARU, M., MARIN, M. M. & GRUMEZESCU, A. M. 2015. Applications and toxicity of silver nanoparticles: a recent review. *Curr Top Med Chem*, 15, 1596-604.
- MEYER, W. G., PAVLIN, J. A., HOSPENTHAL, D., MURRAY, C. K., JERKE, K., HAWKSWORTH, A., METZGAR, D., MYERS, T., WALSH, D., WU, M., ERGAS, R., CHUKWUMA, U., TOBIAS, S., KLENA, J., NAKHLA, I., TALAAT, M., MAVES, R., ELLIS, M., WORTMANN, G., BLAZES, D. L. & LINDLER, L. 2011. Antimicrobial resistance surveillance in the AFHSC-GEIS network. *BMC Public Health*, 11, S8.
- MUTHUKRISHNAN, A. M. 2015. Green Synthesis of Copper-Chitosan Nanoparticles and Study of its Antibacterial Activity. *Journal of Nanomedicine & Nanotechnology*, 06.
- NASROLLAHZADEH, M., SAJADI, S. M., ROSTAMI-VARTOONI, A., BAGHERZADEH, M. & SAFARI, R. 2015. Immobilization of copper nanoparticles on perlite: Green synthesis, characterization and catalytic activity on aqueous reduction of 4-nitrophenol. *Journal of Molecular Catalysis A: Chemical*, 400, 22-30.
- PHILIP, D. 2009. Biosynthesis of Au, Ag and Au-Ag nanoparticles using edible mushroom extract. *Spectrochim Acta A Mol Biomol Spectrosc*, 73, 374-81.
- PHULL, A.-R., ABBAS, Q., ALI, A., RAZA, H., KIM, S. J., ZIA, M. & HAQ, I.-U. 2016. Antioxidant, cytotoxic and antimicrobial activities of green synthesized silver nanoparticles from crude extract of *Bergenia ciliata*. *Future Journal of Pharmaceutical Sciences*, 2, 31-36.
- RAJESHKUMAR, S. 2016. Synthesis of silver nanoparticles using fresh bark of *Pongamia pinnata* and characterization of its antibacterial activity against gram positive and gram negative pathogens. *Resource-Efficient Technologies*, 2, 30-35.
- RASHID, M. I., MUJAWAR, L. H., MUJALLID, M. I., SHAHID, M., REHAN, Z. A., KHAN, M. K. I. & ISMAIL, I. M. I. 2017. Potent bactericidal activity of silver nanoparticles synthesized from *Cassia fistula* fruit. *Microb Pathog*, 107, 354-360.
- REIDY, B., HAASE, A., LUCH, A., DAWSON, K. & LYNCH, I. 2013. Mechanisms of Silver Nanoparticle Release, Transformation and Toxicity: A Critical Review of Current

- Knowledge and Recommendations for Future Studies and Applications. *Materials*, 6, 2295-2350.
- SEIL, J. T. & WEBSTER, T. J. 2012. Antimicrobial applications of nanotechnology: methods and literature. *International Journal of Nanomedicine*, 7, 2767-2781.
- SILVER, L. L. 2011. Challenges of Antibacterial Discovery. *Clinical Microbiology Reviews*, 24, 71-109.
- SURESH, Y., ANNAPURNA, S., SINGH, A. K. & BHIKSHAMACAH, G. 2014. Green synthesis and characterization of the decoction stabilized copper nanoparticles. *International Journal of Innovative research in science, engineering and technology*, 3, 3-6.
- TADESSE, B. T., ASHLEY, E. A., ONGARELLO, S., HAVUMAKI, J., WIJEGOONEWARDENA, M., GONZÁLEZ, I. J. & DITTRICH, S. 2017. Antimicrobial resistance in Africa: a systematic review. *BMC Infectious Diseases*, 17, 616.
- TIWARI, J. N., TIWARI, R. N. & KIM, K. S. 2012. Zero-dimensional, one-dimensional, two-dimensional and three-dimensional nanostructured materials for advanced electrochemical energy devices. *Progress in Materials Science*, 57, 724-803.
- VENTOLA, C. L. 2015. The Antibiotic Resistance Crisis: Part 1: Causes and Threats. *Pharmacy and Therapeutics*, 40, 277-283.
- WANG, A. X. & KONG, X. 2015. Review of Recent Progress of Plasmonic Materials and Nano-Structures for Surface-Enhanced Raman Scattering. *Materials (Basel)*, 8, 3024-3052.
- ZHANG, X. F., LIU, Z. G., SHEN, W. & GURUNATHAN, S. 2016. Silver Nanoparticles: Synthesis, Characterization, Properties, Applications, and Therapeutic Approaches. *Int J Mol Sci*, 17.
- ZHANG, Y., SHAREENA DASARI, T. P., DENG, H. & YU, H. 2015. Antimicrobial Activity of Gold Nanoparticles and Ionic Gold. *J Environ Sci Health C Environ Carcinog Ecotoxicol Rev*, 33, 286-327.

Chapter 2

LITERATURE REVIEW

2.1 THE ROLE OF CAPPING MOLECULES IN THE SYNTHESIS OF NANOPARTICLES

Capping agents are usually employed for nanocrystals prepared by solution-based chemical methods. This is done to prevent nanoparticle overgrowth, aggregation and thus to control the structural characteristics of the resulting nanoparticles in a precise manner (Faleni and Moloto, 2013, Li et al., 2013). The other function of capping molecules is to carry specific functional groups to the surface of the synthesized nanoparticles. This is important since the presence of the functional groups on the surface of the particles contribute to the electrostatic and steric stability of the particles. Capping agents are usually classified as either electrostatic or steric effects. Electrostatic stabilizers are capping agents that coordinate with the metal via the anionic species. As a result, an electrical double layer which is responsible for the coulombic repulsion between nanoparticles is formed (Bauer et al., 2015). Steric stabilizers are bulky capping molecules that bind on the surface of the nanoparticles, and they prevent particles from diffusing together (Bauer et al., 2015).

The role of capping agents on the stability of silver nanoparticles has been investigated by Balaz et al., 2017, Silver nanoparticles were synthesized using a silver nitrate solution, *Origanum vulgare L.* and polyvinylpyrrolidone as a precursor, reducing and capping agent respectively. The uncapped silver nanoparticles were found to be stable for one week while polyvinylpyrrolidone (PVP) capped silver nanoparticles were found to be stable for more than 26 weeks. The increase in stability of the capped nanoparticles was attributed to the presence of PVP on their surface. Previous studies have also demonstrated that the size and shape of nanoparticles are affected by many reaction parameters such as capping agent concentration and temperature (Kumari et al., 2017). Jeyarani et al., 2016 investigated the influence of capping agent concentration on the size of copper oxide nanoparticles, the capping agent concentration was found to be inversely proportional to the particle size. In another study by Sibiyi and Moloto, 2016 the capping agent concentration was found to decrease the particle size of silver selenide nanoparticles, but a further

increase in capping agent concentration resulted in an increase in particle size. This was attributed to the ripening effect.

It is also reported that the identity of the capping agent influences the properties of metal nanoparticles. Li et al., 2013 synthesized silver nanoparticles in the absence of the capping agent, while the other particles were synthesized using oleic acid and polyacrylic acid as capping agents. Nanoparticles with an average size of 479 nm were obtained for particles synthesized without capping agent, while particles with 122 and 13 nm were obtained with polyacrylic acid and oleic acid respectively. In comparison of the two capping agents, oleic acid was found to be a better capping agent compared to polyacrylic acid as it produced a smaller particle sizes. The large size of silver particles obtained when polyacrylic was used may be due to the large quantity of –COOH which interact preferentially with metals thus the formed silver nanoparticles have high possibilities of reforming large particles. Since the properties of nanomaterials depend mostly on the size and shape of the synthesized particles, it is, therefore, necessary to use a suitable capping agent as well as the optimum capping agent concentration for the synthesis of metal nanoparticles.

2.2 CHITOSAN AS A CAPPING MOLECULE

2.2.1 Properties

Chitin is a polymer of the nitrogen-containing polysaccharide $[(C_8H_{13}O_5N)_n]$, and it is the most abundant natural biopolymer after cellulose (Venkatesan and Kim, 2010, Cheung et al., 2015). Chitin is mainly obtained from crustacean, insects and fungi species. The partial deacetylation of chitin results in the production of a very useful polymer called chitosan (1, 4)-(2-amino-2-deoxy- β -D-glucan) (Martins et al., 2014, Martins et al., 2013). Chitosan is known as a high molecular weight linear heteropolysaccharide polymer. It is composed of a β -(1-4) linked two monosaccharides, *N*-acetyl- D-glucosamine, and D-glucosamine. The reactivity of chitosan depends on three functional groups which are the amino group at C-2, the primary and secondary hydroxyl group at C-3 and C-6 respectively as indicated in Fig 2:1 (Furusaki et al., 1996, Dutta et al., 2004).

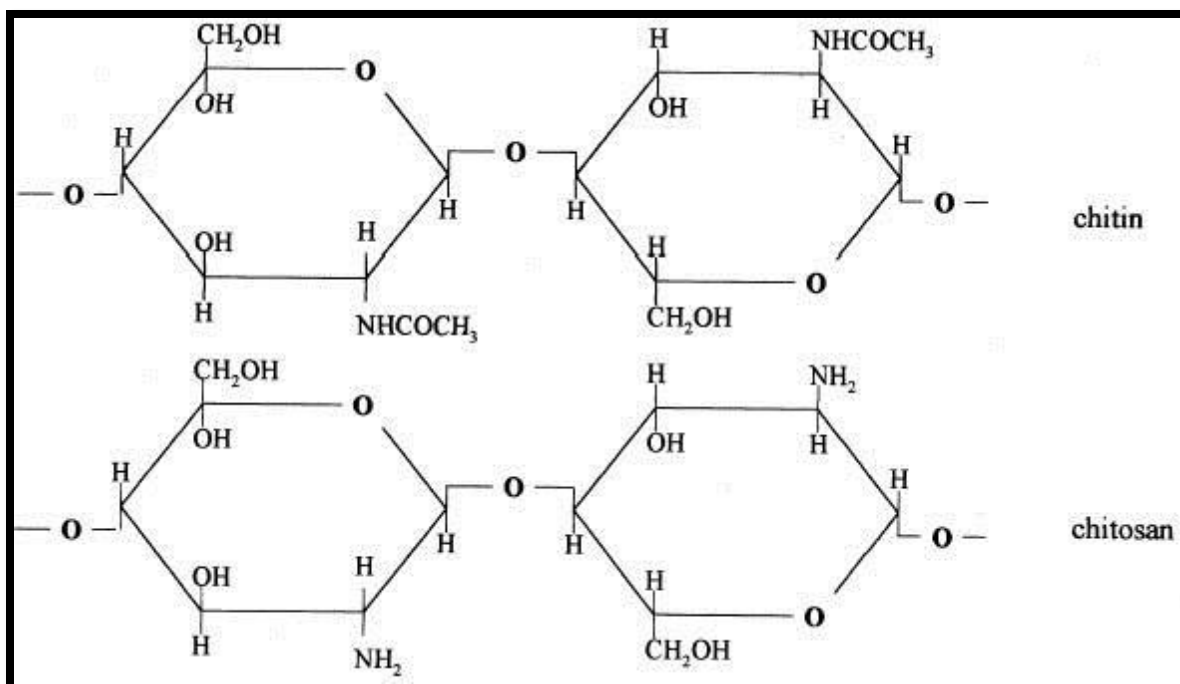


Fig 2:1 Chemical structure of chitin and chitosan (Raafat and Sahl, 2009).

Chitosan is less toxic, inert, hydrophilic, biocompatible and biodegradable. The low toxicity of this biopolymer is its attractive feature, and hence it is mostly used in biological applications. An *in vivo* toxicity assay on chitosan was carried out by Singla and Chawla, 2001, the LD₅₀ of around 16 g/kg was obtained. This value is similar to that of salt and glucose. It is also reported that the degree of deacetylation of chitin affects the toxicity of chitosan (Singla and Chawla, 2001). Another attractive feature of chitosan is its biodegradability. Chitosan can be broken down into small units by enzyme-catalyzed reactions such as lysozymes, lipases, and pepsin. The degradation of chitosan by the enzyme-catalyzed reaction is mainly due to the acetamide groups (Kumirska et al., 2011).

Chitosan is insoluble in water and most common organic solvents, this is attributed to the presence of the amino group which facilitates the solubility of chitosan. It is readily soluble in acidic solutions, at pH > 6.5 chitosan solutions exhibit phase separation, while at pH < 6.5 chitosan is soluble, carrying a positive charge because of the presence of protonated amino groups as shown in Fig 2:2 (Kumirska et al., 2011). At pH between 6.0 and 6.5 in solution, the free amino groups

of chitosan molecules become less protonated, and hydrophobicity along the chitosan chain increases.

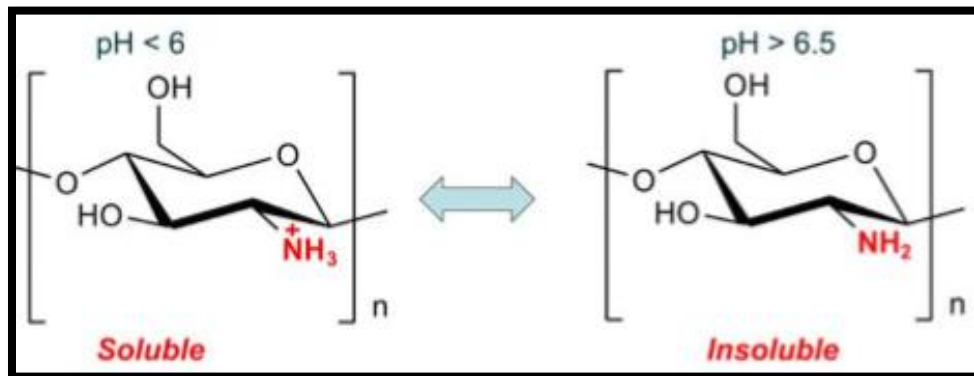


Fig 2:2 Influence of pH on the molecular structure of chitosan (Kumirska et al., 2011).

2.2.2 Application of chitosan in the preparation of nanomaterials

In the synthesis of metal nanoparticles, chitosan serves a dual purpose biopolymer because it acts as a reducing agent as well as a capping agent (Muthukrishnan, 2015). When metal salts dissolve in an acidified chitosan solution, metal ions bind to the polymer chain via amino groups; the reduction of these ions takes place with subsequent oxidation of the hydroxyl group (Praveenkumar et al., 2014). Thus the nanoparticles synthesized are strongly attached to chitosan due to the chemical bond between the electron-rich nitrogen present in the amino groups of the polymer. The hydrophilic side chain of chitosan plays a fundamental role in stabilization and dispersion of metal nanoparticles thus preventing agglomeration (Muthukrishnan, 2015, Praveenkumar et al., 2014). Praveenkumar et al., 2014 used chitosan as a capping and reducing agent for synthesis of silver nanoparticles, the role of capping agent was investigated. The X-ray diffraction pattern of both capped and uncapped silver nanoparticles showed a face centered cubic phase. A difference regarding the sharpness of the X-ray diffraction peaks was also observed, where very sharp peaks were obtained for uncapped silver nanoparticles as compared to chitosan capped silver nanoparticles. This observation was attributed to the difference in particle size.

To understand the reducing and stabilizing ability of chitosan, a study by Muthukrishnan, 2015 was carried out where copper sulfate was used as a source of copper and chitosan was used as reducing and stabilizing agent. A single absorption peak at 536 nm was obtained from the UV-Vis

spectrum; this is the characteristic peak for copper nanoparticles since they exhibit a peak at around 500-600 nm. The reducing and stabilizing of copper nanoparticles was attributed to the ability of chitosan to bind with copper ions via the electron-rich oxygen atoms of polar hydroxyl and ether groups. The above-cited studies by Praveenkumar et al., 2014 and Muthukrishnan, 2015 indicates that chitosan binds with the metal ions via the amino and hydroxyl functional groups. Zain et al., 2014 investigated the effect of capping agent concentration on the synthesis of copper and silver nanoparticles using microwave heating. The chitosan concentration was varied from 1, 2 and 3% (w/v). The mean particle size was found to decrease with an increase in chitosan concentration for both copper and silver nanoparticles. The decrease in particle size was reported to be due to the protective action by chitosan which prevents the growth of nanoparticles by adsorbing on to their surfaces.

2.3 PLANT EXTRACTS AS STABILIZERS AND REDUCTANTS FOR PREPARING METAL NANOPARTICLES

2.3.1 *Camellia sinensis*

Camellia sinensis (L) Kuntze commonly known as green tea belongs to the family of *Theaceae*. The *Theaceae* family is known to be rich in polyphenolic compounds, predominantly catechins. *Camellia Sinensis* is highly soluble in water which is due to high solubility of catechins. One of the interesting features about the leaves of *Camellia Sinensis* is their low toxicity and biodegradability. Polyphenols found in plant material often play a key role in the synthesis of metal nanoparticles since they are good in chelating with metal ions, thus the tea extracts with high polyphenol content act as both reducing and capping agents (Sun et al., 2014, Wang et al., 2014). Suresh et al., 2014 used a tea extract to stabilize copper nanoparticles. Face centered cubic particles with a spherical shape and an average size of 5 nm was obtained. The interesting factor about this study is the stability test since copper nanoparticles are known to oxidize easy and form copper oxide. The synthesized copper nanoparticles were found to be stable for 25 days with no contamination, and this was attributed to the use of the tea extract as a capping agent. Sun et al., 2014 synthesized silver nanoparticles using tea leaf extract as a capping agent and reducing agent. The synthesized silver nanoparticles were nearly spherical with sizes ranging between 20 and 90 nm. The nanoparticles also exhibited a zeta potential of 21.3 mV. Generally, particles that exhibit an absolute zeta potential less than 20 mV are considered unstable, and those that have zeta

potential greater than 20 mV are said to be stable. The stability of the particles was attributed to the presence of the organic functional groups present on the surface of the synthesized particles. Loo et al., 2012 synthesized silver nanoparticles using *Camellia Sinensis* as a capping and reducing agent. From the XRD results, five main characteristic peaks which correspond to (111), (200), (220), (311) and (222) Face-centered cubic silver crystals were obtained. These results confirms, the formation of silver nanoparticles.

2.3.2 *Melia azedarach linn*

Melia azedarach linn belongs to the *Maliaceae* family. The leaves of *Melia azedarach linn* have been used in many applications such as medicine and the synthesis of metal nanoparticles (Khan et al., 2014). This is because of the unique phytochemicals that are found in this plant. Ahmed et al., 2012 did the phytochemical analysis of the leaf extract of *Melia azedarach linn*. The leaves were found to contain some active ingredients such as phenols, flavonoids, alkaloids, tannins, and saponins. The total phenol content was also investigated using the folin-ciocalteu spectroscopic method, and the phenols content in the water extract was found to be 305 ug/mg. The phytochemical studies and the total phenol content is important in the synthesis of metal nanoparticles using medicinal plants, since the active functional groups such as the hydroxyl groups are known to be responsible for reducing metal ions.

Mehmood et al., 2013 synthesized silver nanoparticles using *Melia azedarach linn* aqueous leaf extract, the effect of reducing agent was studied. Bio-reduction of silver ions was monitored by UV-Vis spectroscopy and atomic absorption spectroscopy. When the leaf extract was mixed with a silver nitrate solution, the color changed to dark brown, and this was attributed to the surface plasmon resonance of silver which indicates the formation of silver nanoparticles. The absorption maximum was found to be at 482 nm, indicating that the leaf extract successfully reduced silver ions. Further confirmation was done using atomic absorption spectroscopy, the concentration of silver in the mixture decreased with time from 216 ppm/mL of silver ions at 2 minutes to 53 ppm/mL after 3 hours. These results also indicate the reducing power of *Melia azedarach linn* leaf extract. Ramanibai and Velayutham, 2015 synthesized silver nanoparticles using 2,7-bis [2-diethylamino]-ethoxy] fluorence isolates from *Melia azedarach* leaves. Spherical particles with

size ranging from 3-31 nm were obtained, and the presence of surface plasma resonance at 426 nm also confirmed the formation of silver nanoparticles.

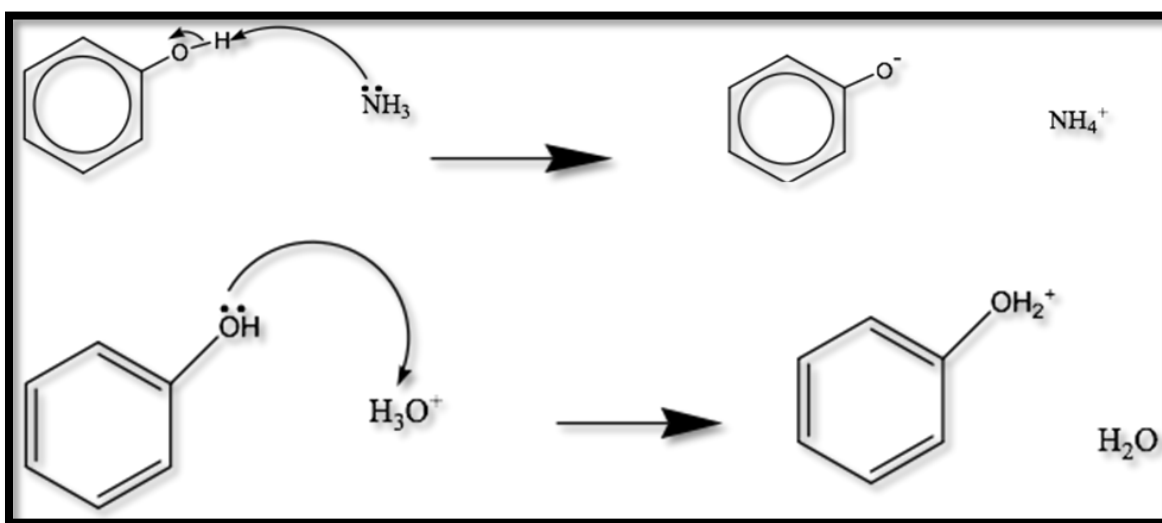
2.3.3 *Combretum molle*

Combretum molle belongs to the *Combretaceae* family, which is a large family of herbs, shrubs, and trees. Vroumsia et al., 2015 studied the phytochemicals present in the acetone extract of *Combretum molle* leaves, the tests showed that the plant leaves contained tannins, proteins, flavonoids, phenols, and glycosides. The phenols were found to be present in a small amount as compared to flavonoids which were found to be present in appreciable quantity. This might be due to the polarity of the solvent used to extract these bioactive compounds because phenols and mono-substituted phenols are hydrophilic compounds with a lower affinity towards less polar solvents. Since *Combretum molle* is known to have phenols and flavonoids, it can, therefore, be used as capping and reducing agent for the synthesis of silver nanoparticles (Singh et al., 2016, El-Kassas and El-Sheekh, 2014). Polyphenols have a strong affinity towards metal ions such as silver ions which is due to the presence of the hydroxyl functional group (El-Kassas and El-Sheekh, 2014, Patil Shrinivas and Kumbhar Subhash, 2017). Silver ions coordinate with the hydroxyl functional group from the phenols, as a result the nucleation of silver nanoparticles is favored.

2.4 THE INFLUENCE OF pH ON THE PROPERTIES OF BIOACTIVE COMPOUNDS FROM PLANT EXTRACTS

The pH of the medium used during the synthesis of metal nanoparticles using bioactive compounds plays a significant role because it influences both the size and crystallinity of the nanoparticles. This is because the pH affects the distribution of the functional groups responsible for reducing and capping metal nanoparticles (Ghodake et al., 2010, Sibiya and Moloto, 2014). The major influence of pH is its ability to change the electrical charges of the bioactive compounds as shown in Scheme 2:1. Sibiya and Moloto, 2014 studied the effect of pH on the size and shape of starch capped silver selenide nanoparticles. Acidic pH was found to change the chemical structure and activity of starch, while basic pH was found to enhance the percentage of starch hydroxyl group species, thus resulting in small particle size. Similar results were obtained by Sathishkumar et al., 2010 in the synthesis of silver nanoparticles using *Curcuma longa tuber* powder. In another study by Khalil et al., 2014b the influence of pH on the size and shape of silver nanoparticles synthesized

using olive leaf extract was investigated. The particle size was found to be large at pH 3, but a decrease in particle size was observed at pH 8. This was due to an increase in a number of nuclei because of the promoted reactivity of the olive leaf extract at basic pH. Ghodake et al., 2010 investigated the effect of pH on the shape of gold nanoparticles synthesized from pear fruit extract. At pH 4 partially formed triangular and hexagonal shaped particles were obtained and this was attributed to inter-particle interactions. As the pH was increased to 10 well defined triangular and hexagonal particles were obtained.



Scheme 2:1 Influence of pH on the molecular structure of phenol

2.5 GREEN SYNTHESIS

The fabrication of metal nanoparticles using natural substances is a very important step in nanotechnology. Useful material can be easily produced because the biomaterial-based routes eliminate the need to use toxic chemicals (Zain et al., 2014). Also, waste products are relatively easier to dispose of because they are mostly composed of leftovers of natural plant extracts such as proteins and glycoside. Ahmed et al., 2016 used *Azedarachia indica* aqueous leaf extract in the synthesis of silver nanoparticles. The plant extract acted as both the reducing and capping agent, an absorption peak at 446 nm was obtained which is a characteristic peak for silver nanoparticles. The functional groups that were responsible for this dual function were found to be the hydroxyl group from the polyphenols and the N-H stretching from the NH_2 . Guagqum, 2012 synthesized silver nanoparticles using an extract of *argemone Mexicana* leaf at room temperature, and the

particle size was found to be in the range of 10-50 nm. Forough and Farhadi, 2012 synthesized silver nanoparticles via a greener method, water was used as a solvent, and the leaf extract of *Euphorbia hirta L* acted as both the reducing and capping agent. Spherical particles with an average of 45 nm were obtained.

The application of nanomaterials into biological systems is dependent on their method of synthesis which influences their toxicity. Different parameters such as particle size, shape, surface area and surface reactivity determine the toxicity of the nanoparticles (Daniel et al., 2010). Yang and Li, 2015 investigated the cytotoxicity of gold nanoparticles prepared using chitosan oligosaccharide as reducing and capping agent on human fibroblasts. There was no significant difference on cell viability at a concentration of 15.6 and 31.3 $\mu\text{g/ml}$, but the dose-dependent cytotoxicity was observed at concentrations above 62.5 $\mu\text{g/ml}$. In another study by Prasad et al., 2016, the cytotoxicity of copper nanoparticles capped with *Broccoli* extract was investigated. The in-vitro cytotoxic study was evaluated by monitoring the change in cell density after 2 hours of exposure to nanoparticles. The cell showed excellent viability in the presence of nanoparticles with a concentration of 1.5 μM . This behavior was attributed to the functionalization of phenolic moieties derived from the plant extract.

2.6 METHODS OF NANOPARTICLES SYNTHESIS

There are several methods that have been used to synthesize metal nanoparticles. These include biological, physical and chemical approaches.

2.6.1 Biological approach

2.6.1.1 Synthesis of nanoparticles using microorganisms

Bio-based protocols have been used for the synthesis of highly stable and well-structured nanoparticles. In the biological synthesis of nanoparticles, organisms such as prokaryotic bacterial cells to eukaryotic fungi and plants were used. These organisms are used as capping agent replacement during the synthesis of nanoparticles (Iravani et al., 2014). Synthesis of metal nanoparticles using microorganisms involves different parameters such as elaborated method of maintaining cell cultures, living things synthesis and multiple steps of purifications (Sharma et al., 2009). The size and morphology of the nanoparticles can be controlled by altering some critical

conditions such as substrate concentration, pH, light, temperature and interaction speed and optimal conditions for all cell growth.

Vigneshwaran et al., 2007 synthesized silver nanoparticles using fungus *Aspergillus flavus*. The reaction temperature was at 37 °C, the choice of the temperature was influenced by the suitable temperature for the growth and survival of *Aspergillus flavus*. From the obtained results an absorption peak at 420 nm was obtained which is a characteristic peak for silver nanoparticles, this was also supported by a face-centered cubic structure of silver that was found from the XRD. The presence of proteins on the surface of the particles as confirmed by Fourier infrared spectroscopy analysis which indicated that the proteins acted as reducing and capping agents. It is reported that proteins have redox potential and that they act as electron shuttles in the metal ion reduction (Shah et al., 2015).

Du et al., 2007 synthesized gold nanoparticles using *Escherichia coli* as a reducing and capping agent. An average particle diameter of 25 ± 8 nm was obtained with mostly spherical shape, and other shapes such as triangles and quasi-hexagons were present. The influence of the bacteria on the size and shape of the particles is still not well understood, therefore it was speculated that the reduction of gold ions might be due to the presence of sugars and enzymes that were present on the surface of the gram-negative *Escherichia coli*. Mendrek et al., 2016 also synthesized silver nanoparticles using two strains of *Bacillus subtilis*.

It is of importance to mention that not all microorganisms are capable of synthesizing nanoparticles. In one study by Ottoni et al., 2017, 20 fungal strains which were isolated from sugar cane plantation soil were used to synthesize silver nanoparticles. The obtained results indicated that only four strains were able to produce silver nanoparticles. The synthesized particles were found to be spherical with a size range of 30-100 nm. The four fungi strains were found to be great producers of extracellular enzymes which are responsible for bio-reduction of metal salts. Rasool and Hemalatha, 2017 also synthesized copper nanoparticles using marine *endophytic actinomycetes* which were isolated from seaweeds. Generally microorganisms with a potential to accumulate heavy metals have the best chance of synthesizing metallic nanoparticles.

The biological approach of synthesizing metal nanoparticles using microorganisms is mostly not used because of some draw backs. Little is known about the mechanistic aspects, the selection of

the best bacteria and the scaling up of the laboratory to the industrial scale. Some key properties of the bacteria that must be well understood before the selection of the best bacteria include growth rate, enzyme activities and biochemical pathways. The separation of cells by filtration and homogenization of the cells to isolate the produced nanoparticles is still a problem in the industrial production of metal nanoparticles using microorganisms.

2.6.1.2 Synthesis of nanoparticles using plant extracts

Different plants components are used such as the leaves, roots, seeds, and stem for the synthesis of metal nanoparticles through the biological approach. The presence of bioactive compounds that have a strong affinity towards the metal ions is key in the selection of the plant material. The choice of the plant tissue to be used also depends on the quantity of the bioactive compounds present in the plant tissues since different compounds can be found in these tissues (Punjabi et al., 2015). The choice of the solvent used during the extraction of bioactive compounds affects the total phenol and flavonoids content as a result the reducing capacity of the extract during the synthesis of nanoparticles is also affected. It is therefore essential to select the solvent that is relevant for the compound of interest present in the plant tissue. Do et al., 2014 investigated the effect of extraction solvent on the bioactive compounds present in *Limnophila aromatic*. The strength of solvent for extraction of total phenolic and flavonoids content was found to be in the following order ethanol > acetone > methanol > water. The low content of phenolic compounds in the water extract was attributed to the ability of water to extract non-phenolic compounds such as carbohydrates and terphene, while the high content in the ethanol extract was due to high polarity of this solvent.

Several studies in the literature have reported the use of medicinal plant extracts as reducing and capping agents during the synthesis of nanoparticles. Loo et al., 2012 described the synthesis of silver nanoparticles using the leaf extract of *Camellia sinensis*, well-dispersed spherical nanoparticles with an average size of 4 nm were obtained. In another study Prasad et al., 2016 synthesized copper nanoparticles using a *Broccoli* extract. The occurrence of bioactive compounds that are responsible for reducing and capping copper nanoparticles was confirmed by FTIR spectroscopy. From the pristine *Broccoli* extract, a peak at 3444 cm^{-1} was attributed to O-H stretching. Also, a peak at 2900 and 2750 cm^{-1} was observed due to the presence of asymmetric and symmetric C-H stretching vibration from flavonoids and phenolic compounds respectively.

The shift in the peak position of the above mentioned functional groups was observed on the surface of the synthesized copper nanoparticles. These results suggested that the oxidized polyphenols were responsible for reducing and capping the copper nanoparticles. Moreover, the extract of various plants including *Camellia sinensis* (Nabikhan et al., 2010) and *Melia dubia* (Kathiravan et al., 2014) have been used to synthesis metal nanoparticles. The main advantage of using plant extract for synthesis of metal nanoparticles over microorganisms such as bacteria and fungi is that it avoids the preparation of well-conditioned cell culture and isolation techniques that tend to be expensive and complicated because of the optimization of culturing parameters which may differ for each organism (Punjabi, 2015); (Kathiravan et al., 2014, Punjabi et al., 2015).

2.6.2 Physical approach

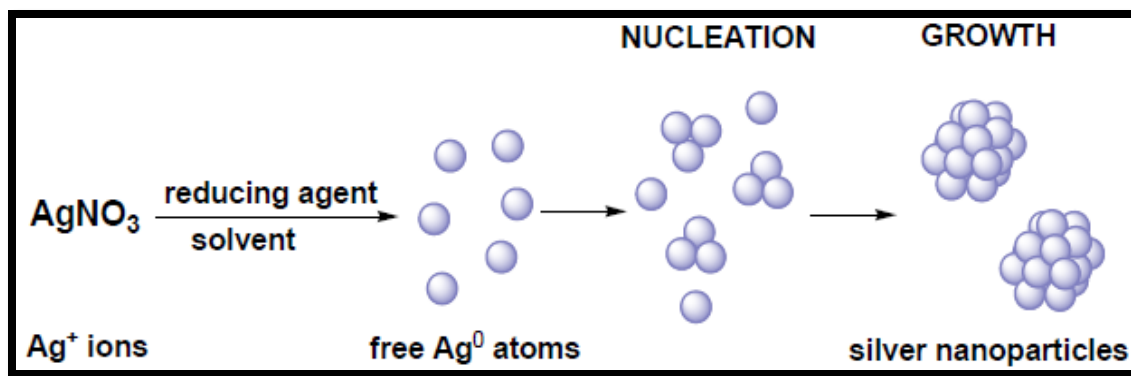
There are two approaches that are used for the synthesis of metal nanoparticles, the top to bottom approach and bottom to up approach. In the top to bottom approach, the bulk material is broken down into small units or fine particles by reduction with various lithographic techniques such as thermal, laser ablation and grinding. This approach has some advantages over other methods, and one of the major advantages is the absence of solvent contamination in the prepared nanoparticles. Khalil et al., 2014a synthesized zinc oxide nanoparticles by thermal decomposition of a curcumin zinc complex. Lattice fringes with 0.25 nm were obtained, and these results were supported by the high crystalline structure in the XRD. Silver nanoparticles can be synthesized via a small ceramic heater with a local heating area, where the heater is used to evaporate source materials. The evaporated vapor can cool at a suitable rapid rate thus makes possible the formation of small nanoparticles in high concentration. The particle generated is very stable because the temperature of the heater surface does not fluctuate with time (Iravani et al., 2014, Tran et al., 2013). Some of the drawbacks with this approach include the usage of a tube furnace which should occupy large space, consume a great amount of energy while raising the environmental temperature around the source material and requires a lot of time to achieve thermal stability (Iravani et al., 2014, Tran et al., 2013).

The synthesis of nanomaterials using laser ablation has been reported in the literature as one of the mostly used physical approaches. The main advantage of laser ablation is that it is a clean process which has a high spatial resolution (Thakka and Mhsatre, 2010). Also, its simplicity and

effectiveness is advantageous since it does not involve several steps and long processing times. The properties of nanoparticles synthesized using this approach are affected by several reaction parameters which include the wavelength of the laser impinging the metallic target, duration of the laser pulses and laser fluency (Bauer et al., 2015). Valverde-Alvaa et al., 2015 synthesized silver nanoparticles using laser ablation where the effect of laser pulse energy was investigated. A decrease in particle size with an increase in laser pulse energy was observed and spherical particles with an average size of 11.8, 10.9 and 8.7nm were obtained for 10, 60 and 100 mJ/pulse. A plasmon resonance peak at 400 nm which corresponds to spherical nanoparticles was also obtained. Some of the drawbacks of laser ablation include the reduced duration of nanoparticles as a result of the raise in a number of laser shots which increases the density of the solution (Valverde-Alvaa et al., 2015).

2.6.3 Chemical approach

The most common approach for the synthesis of metal nanoparticles is the chemical reduction by organic and inorganic reducing agents. In the wet chemical reduction techniques, the metal ion is reduced in aqueous and non-aqueous solutions. Typically, the reducing agent may reduce silver metal (Ag^+) to silver metallic (Ag^0), which is followed by agglomeration into algometric clusters. The clusters eventually lead to the formation of colloidal silver nanoparticles as shown in Scheme 2:2 (Iravani et al., 2014, Tran et al., 2013). The advantages of wet chemical techniques include cost-effectiveness, low impurity factor, thermal stability and control over growth rate. These advantages are attributed to the use of stabilizing agents. This approach is also mostly used because it is cost-effective and easy to setup. Khanna et al., 2007 synthesized copper nanoparticles via the chemical reduction method where polyvinyl alcohol and sodium formaldehyde sulfoxylate were used as capping and reducing agent respectively. An absorption peak at 600 nm was obtained, this was attributed to surface resonance phenomenon of copper nanoparticles.



Scheme 2:2 The formation of metal nanoparticles using chemical reduction approach (Aguihotri et al., 2014).

2.7 EXTRACTION METHODS

2.7.1 Background

Medicinal plants are gaining interest as an alternative medicine to treat various diseases such as fever and malaria. The application of medicinal plants is dependent on the yield and phytochemical constituents that are present in the plant. The phytochemical constituents also influence the application of medicinal plants as reducing and capping agents in the synthesis of nanoparticles. There are several parameters that influence the phytochemical constituents; these parameters include extraction method, plant tissue as starting material and choice of solvent (Grujic et al., 2012, Xu et al., 2017). Concerning medicinal plants chemistry, extraction is defined as the separation of a medicinally active portion of the plant using standard procedures (Vinatoru et al., 2017). The main function of extraction is to separate plant metabolites that are soluble in a selected solvent. It is important to note that during extraction, solvents diffuse into the solid plant material and solubilize compounds with similar polarity. Different extraction methods are used to extract bioactive compounds from plant extracts. These methods include maceration, decoction, Soxhlet extraction, microwave-assisted extraction, ultrasonic assisted extraction and accelerated solvent extraction (Chua, 2013, Duval et al., 2016). Some of these methods are discussed in this section. The difference in extraction methods normally depends on the following factors: solvent used, pH of the solvents, temperature, length of extraction period and particle size of the plant tissue.

2.7.2 Maceration and decoction extraction methods

Maceration is the technique that is mostly used in the extraction of plant material because it is simple to setup and cheap to maintain (Lu et al., 2017, Chen et al., 2016). This technique involves the soaking of plant material into a solvent at room temperature for 72 hours with continuous agitation. After 72 hours the mixture is strained by filtration. The soaking and continuous agitation of the plant material breaks the plant cell wall to release secondary metabolites that are present in the plant. The advantage of this method is that it is good at handling thermolabile phytochemicals. Some of the drawbacks of this method are the use of the large volume of organic solvents, as a result proper waste management is needed. This method is also time-consuming as it requires a minimum of 3 days for the single extraction process. Deng et al., 2017 investigated the influence of extraction method on the phenolic compounds present in fresh olives, Maceration and ultrasonic assisted extraction methods were used. From the high-performance liquid chromatography (HPLC) results 14 main compounds were identified from both methods however ultrasonic assisted extraction exhibited more amount of phenolic content compared to maceration. This high phenolic content is attributed to a high extraction efficiency of the ultrasonic assisted method. In a review by Setford et al., 2017 factors that influence the total phenolic content in red wine extracted by maceration method were investigated. Physical factors such as solvent diffusion into the porous solid and solute dissolution into the solvent were found to play an important role. Albuquerque et al., 2017 investigated the effectiveness of three extraction methods using *Arbutus unedo L.* fruits, Catechin was the compound of interest. Maceration and microwave-assisted extraction was found to be the most effective methods compared to the ultrasonic method. However, microwave extraction was more effective compared to maceration. Similar results were also obtained by Castro-Lopez et al., 2017 where the maceration method was found to be more effective than ultrasonic extraction method.

Another method of extraction that is mostly used is decoction; this method uses the same principle as maceration. However, with decoction, the plant material is boiled to accelerate the extraction of phytochemicals. Water soluble and heat stable phytochemicals are mostly extracted by this method. Fotakis et al., 2016 investigated the metabolic and antioxidant profile of herbal infusions and decoctions. From the nuclear magnetic resonance spectroscopy (NMR) results more phenolic compounds were obtained by infusion compared to decoction method. It was also observed that

the total phenolic content was more in infusion than decoction. This observation may be attributed to the fact that decoction method is mostly suitable for non-thermolabile compounds. In another study by Vongsak et al., 2013 the effect of decoction method on total phenolic and flavonoids content of *Moringa oleifera* leaf was investigated. The total phenolic content was found to be more than the total flavonoid content. Decoction method is mostly used in the green synthesis of metal nanoparticles using plant extracts (Ahmed et al., 2015, Ajitha et al., 2016, Ravichandran et al., 2016).

2.7.3 Microwave and ultrasonic assisted extraction methods

Microwave-assisted extraction is a process of using microwave energy to heat solvents in contact with the sample to partition analytes from sample matrix into a solvent (Sparr Eskilsson and Björklund, 2000, Ekezie et al., 2017). Briefly, the extraction procedure takes about 3-30 minutes, and it uses small solvent volumes in the range of 10-30 ml. The use of small volumes is one of the advantages of this approach since it minimizes the disposal of larger organic waste, which is a problem in other methods such as maceration extraction method. The reduction in extraction time is attributed to the difference in heating principle. The microwave heats the solution directly while conventional methods heat the vessel first before the sample hence more time is needed (Sparr Eskilsson and Björklund, 2000, Kala et al., 2016).

Calinescu et al., 2017 used microwave assisted extraction to extract polyphenols from sea buckthorn leaves. From the obtained results microwaves method performed better than conventional methods with regards to total phenolic content and antioxidant capacity. In another study by Tongkham et al., 2017 the effect of microwave power was investigated on the extraction of pectin from dragon fruit peels. Microwave power of 300, 450 and 600 W were investigated, high pectin yield was found at 600W. However, a decrease in viscosity of pectin was observed. This decrease in viscosity is attributed to degradation of pectin at 600 W. Although microwave assisted extraction is considered as the fastest way to extract phytochemicals from the plant material, it has some drawbacks such as waiting time for the vessels to cool down. Since microwaves are being used as a source of energy, therefore, the solvent that is used, it must be able to absorb microwaves. Microwave-assisted extraction is limited to extraction of small molecules such as phenolic acids; this is mainly because these molecules are stable at microwave heating of

about 100 °C for 20 minutes (Lovrić et al., 2017, Li et al., 2017). This method is usually not recommended for extraction of secondary metabolites from plant extracts since some phytochemicals are subjected to degradation at high temperatures.

Other methods such as ultrasonic assisted extractions are also being used in the extraction of plant material. Ultrasonic extraction disrupts the plant cell wall using ultrasound (Chemat et al., 2017, Saini and Keum, 2018). This allows the breaking down of the cell wall as a result most secondary metabolites are released from the plant material into the solvent. The advantages of this method are similar to those of microwave extraction method which is a reduction in extraction time and solvent consumption. The use of ultrasonic sound that is greater than 20 kHz may have some negative effect on the phytochemicals because at this frequency some molecules can form free radicals (Zhang et al., 2017a).

2.8 METHODS TO DETECT ANTIBACTERIAL ACTIVITY

2.8.1 Background

Several methods are used to test the antibacterial activity of different antibacterial agents such as antibiotics and nanomaterials. The clinical and laboratories standards institutes (CLSI) for measuring *in vitro* susceptibility of bacteria to antimicrobial agents used in clinical settings recommends two main methods that can be used. The most popular techniques that are used include agar diffusion methods (disk or well diffusion) and dilution methods (agar dilution or broth microdilution). The selection of appropriate method depends mostly on the intended degree of accuracy, urgency and technical expertise (CLSI, 2012).

2.8.2 Agar diffusion methods

The disk diffusion susceptibility method is a simple and well-standardized method. With this approach, the effectiveness of the drug is related to the diameter of the zone of inhibition. The bigger the diameter of the inhibition zone, the more susceptible is the microorganism to the antibacterial agent. Several authors reported successful testing of antibacterial agents using this approach. Briefly, the disk diffusion method includes the preparation of a bacterial inoculum of approximately 1×10^8 CFU/ml. The bacterial inoculum is then applied on the Mueller-Hinton agar plate. Prepared or commercial antibacterial agents are then placed on the inoculum agar surface

and the plates are incubated for 16 to 24 hours at 35 °C. For optimum results there are factors that need to be considered such as the agar thickness, inoculum concentration, incubation temperature and exposure time (Dafale et al., 2016, Dafale et al., 2015). The optimum incubation temperature is around 35-37 °C, at elevated temperatures the credibility of the results is compromised since large zone of inhibition will be obtained because most pathogens will be affected by the high temperature of the system. If a temperature lower than 35 °C is used, then the growth rate will be affected. Some drawbacks about the disk diffusion method are that it is unable to generate the minimum inhibitory concentration (MIC). Also the difference in the zone of inhibition sometimes is attributed to the unequal exposure of individual plates at the top and bottom of the stacks. This problem may affect the credibility of the results. Several interventions are made to solve the above-mentioned problems. (Liu et al., 2016, Fehlberg et al., 2016).

In several previous studies, the disk diffusion method was used to determine the antimicrobial activity of different medicinal plants and nanomaterials. Phongtongpasuk et al., 2016 investigated the antibacterial activity of silver nanoparticles synthesized through the green approach. The antibacterial screening of silver nanoparticles was carried out against gram-positive bacteria (*Staphylococcus aureus*) and two-gram negative bacteria (*Escherichia coli* and *Pseudomonas aeruginosa*). The highest zone of inhibition was 9.2 mm for *Staphylococcus aureus*, followed by *Escherichia coli* with 8 mm and *Pseudomonas aeruginosa* at 7.3 mm. Ethiraj et al., 2016 studied the antibacterial activity of silver nanoparticles using the agar well diffusion method. Five test microorganisms (*Escherichia coli*, *Pseudomonas aeruginosa*, *Staphylococcus sp*, *Bacillus sp* and *Klebsiella sp.*) were used. The prepared silver nanoparticles were found to be active against all the tested microorganisms, but the highest activity was observed in *Klebsiella sp* with a zone of inhibition of 36 mm and the lowest was in *Staphylococcus sp*. The antibacterial activity was attributed to the size of silver nanoparticles since small particles have the ability to reach bacterial proximity easily.

2.8.3 Dilution method

The dilution methods are usually used to detect the antibacterial activity of different antibacterial agents. Unlike the diffusion method, the dilution method is a quantitative assessment of antibacterial agents. With this approach, the lowest concentration capable of inhibiting the growth

of the tested organisms can be determined. In a typical study, the dilution method by either broth or agar dilution involves subjecting the isolates to a series of concentrations of the antibacterial agent. The microdilution bioassay involves dilution of the bacterial strain with Mueller-Hinton broth to give an inoculum of approximately 10^6 CFU/ml. The antibacterial agent is diluted to different concentrations, and then the bacterial growth is usually detected by the use of a p-iodonitrotetrazolium chloride (INT) (CLSI, 2012). The use of dilution methods to determine the antibacterial activity of different drugs has been reported in the literature (Tchinda et al., 2017). Jalali and Allafchian, 2016 tested the antibacterial activity of silver nano-composite against four bacterial strains. The minimum inhibitory concentration was found to be 6.25, 6.25, 25 and 50 $\mu\text{g/ml}$ for *Escherichia coli*, *Salmonella typhimurium*, *Staphylococcus aureus* and *Bacillus cereus* respectively. The difference in antibacterial activity between the gram-negative and gram-positive bacteria was attributed to their cell walls.

2.9 ANTIBACTERIAL POTENTIAL OF COPPER AND SILVER METALS NANOPARTICLES AND THEIR BULK COUNTERPARTS

Bulk copper and silver metals are being used as an antibacterial agent, and this has been the case since ancient times (Seil and Webster, 2012). The antibacterial property of heavy metals is mostly explained using the oligodynamic effect (Guggenbichler et al., 1999). The oligodynamic action is the ability of small amount of heavy metals to exert a lethal effect on bacterial cells. Among all the metals that are known to have antibacterial activity, silver is known to be the best because it is less toxic to the mammals and highly toxic to bacterial cells. The high antibacterial activity of silver is also due to the strong affinity that silver ions have on sulfur and thiol-containing compounds. There are several mechanisms that are proposed in which bulk silver interacts with bacteria. The mechanism of action includes protein inactivation, DNA association, and penetration of the cell wall (Yamanaka et al., 2005). The protein inactivation involves two proposed mechanisms. The first postulation is based on the formation of a stable Ag-S bond with thiol-containing compounds that are found in the cell membrane of the bacteria. The second postulation is also based on the thiol functional groups in the cell membrane.

Silver ions may easily catalyze the oxidation of the oxygen molecules and the hydrogen atoms on the thiol group. As a result the disulfide bonds between the two thiol groups are formed (Klueh et

al., 2000). The formation of the disulfide bonds may, therefore, alter the function of the cell membrane by changing the shape of the cellular enzymes. The antibacterial activity of bulk copper has been reported in the literature by (Villapún et al., 2016, Grass et al., 2010).

Silver nanoparticles are known to have antibacterial activity; this is due to their unique physical and chemical properties. The enhanced antibacterial activity of silver nanoparticles as compared to their bulk counter parts is explained by their high surface to volume ratio and their shape. Raza et al., 2016 investigated the effect of size and shape on the antibacterial activity of silver nanoparticles. The antibacterial activity of spherical and triangular particles with different sizes was investigated against two gram-negative bacteria (*Escherichia coli* and *Pseudomonas aeruginosa*). Both spherical and triangular silver nanoparticles were found to be active against the tested bacterial strains. The activity showed to be shape dependent as high activity was observed with spherical particles as compared to triangular particles. The obtained results also suggested that the antibacterial activity is size dependent since small spherical particles were found to have high activity as compared to large spherical particles. Since the particles interact with the cell wall of the microorganisms, therefore the shape plays a major role in the antibacterial efficiency because different morphologies provide different area to interact with microorganisms. The high antibacterial activity of small-sized particles is also attributed to the ability of these particles to release more silver cation than larger particles. In another study by Rajeshkumar, 2016 the antibacterial activity of silver nanoparticles prepared via a green synthesis approach was investigated against two bacterial strains. The minimum zone of inhibition of 15 mm and 13 mm were obtained for *Klebsiella planticola* and *Staphylococcus aureus* respectively.

The penetration of the cell membrane by silver ions is the mostly used explanation for their antibacterial activity. Since this is size dependent, it is therefore of importance that the effect of size is studied on the antibacterial activity of silver nanoparticles. The antibacterial activity of copper nanoparticles has been reported in the literature by Rasool and Hemalatha, 2017, Prasad et al., 2016, Muthukrishnan, 2015 and Yoon et al., 2007.

2.10 MECHANISM FOR ANTIMICROBIAL RESISTANCE

The world health organization (WHO) and other public health bodies classify antimicrobial resistance as one of the most serious health threats. This is because some pathogens are now resistance to multiple classes of antimicrobial agents (Sefton, 2002). Antimicrobial resistance occurs when microorganisms such as bacteria, fungi, and viruses change in ways that make the antimicrobial agent used to cure infections to be ineffective. Since antimicrobial resistance is a global problem, it is therefore of importance to understand the mechanism of resistance to develop new or improved antimicrobial agents that will not be affected by the current strategies used by microorganisms to hinder the effectiveness of antimicrobial agents. In an attempt to understand how microorganism become resistant to antimicrobial agents different mechanism are proposed. Before the mechanism for antimicrobial resistance can be discussed in it of importance to firstly understand how antimicrobial agents work. The mechanism of action for antimicrobial agents can be divided into two categories either as bacteriostatic or bactericidal. With bacteriostatic the antimicrobial agent inhibits the growth or multiplication of the bacteria as a result the immune system of the host is given the task to clear the bacteria from the system (Byarugaba, 2009). If the antimicrobial agent is bactericidal, then it can kill the bacteria completely without giving any task to the immune system of the host (Sefton, 2002, Byarugaba, 2009).

Antimicrobial resistance can be described in two ways either as intrinsic or acquired. Intrinsic resistance is a natural phenomenon where microorganisms do not possess target sites for the drug. Therefore they are not affected by the drug (Feng et al., 2016). The increase in antimicrobial resistance is mainly due to acquired antimicrobial resistance. This type of resistance can be described using five different mechanisms which include modification of existing targets, reduced cell permeability, production of drug-inactivating enzymes, acquisition of a target by-passing system and drug removal from the cell. Zhang et al., 2017b studied the antimicrobial resistance of *Escherichia coli* from chicken and swine in 8 years. A total of 15130 *Escherichia coli* were isolated from chicken and swine in different provinces around China. Nine antimicrobial agents were used in this study which included among others florfenicol, sulfisoxazole, and Enrofloxacin. The findings of this study revealed that a multi-drug resistance was highly prevalent in *E. coli*, the *E. coli* isolates showed a high resistant rate of 78% to several old drugs including ampicillin and sulfisoxazole. *E. coli* from different provinces showed different resistant patterns. In another study

by Yang et al., 2016 the genetic characterization of antimicrobial resistance in *Staphylococcus aureus* isolated from bovine mastitis was studied. A total number of 44 *S. aureus* were isolated for antimicrobial resistance testing. The results revealed that *S. aureus* isolates were resistant to penicillin (84.09%), erythromycin (20.45%) and tetracycline (15.91%).

2.11 HIGHLIGHTS FROM THE LITERATURE REVIEW

The application of nanoparticles into biological systems is dependent on their method of synthesis. This study focuses on the use of chemical reduction method to synthesize both copper and silver nanoparticles. Based on the above literature review, chemical reduction method is mostly used in the synthesis of nanoparticles because it is inexpensive, easy to setup and, the parameters that affect the size and shape of nanoparticles can be optimized easily. However with this approach toxic chemicals such as sodium borohydride and hydrazine are usually used as reducing and capping agents, thus they hinder the synthesized nanoparticles to be used in biological application. In this study a green synthesis approach is used where chitosan, plant leaves (*Camelia sinensis*, *Combretum molle* and *Melia azedarach*) are being used as capping and reducing agents. The choice of chitosan is based on its ability to bind with the metal ions via the amino groups, thus the nanoparticles synthesized are strongly attached to the chitosan due to the chemical bond between the electron-rich nitrogen present in the amino groups of the polymer. Plant extracts are known to contain secondary metabolites, the selected plant leaves are rich in polyphenolic compounds therefore they are suitable to be used as reducing and capping agent during the synthesis of metal nanoparticles.

2.12 REFERENCES

- AHMED, M. F., SRINIVASA RAO, A. & IBRAHIM, M. 2012. Phytochemical studies and antioxidant activity of *Melia azedarach* leaves by DPPH scavenging assay. *International Journal of pharmaceutical applications*, 3, 271-276.
- AHMED, M. J., MURTAZA, G., MEHMOOD, A. & BHATTI, T. M. 2015. Green synthesis of silver nanoparticles using leaves extract of *Skimmia laureola*: Characterization and antibacterial activity. *Materials Letters*, 153, 10-13.

- AHMED, S., SAIFULLAH, AHMAD, M., SWAMI, B. L. & IKRAM, S. 2016. Green synthesis of silver nanoparticles using *Azadirachta indica* aqueous leaf extract. *Journal of Radiation Research and Applied Sciences*, 9, 1-7.
- AGUIHOTRI, S., MUKHERJI, S. & MUKHERJI, S. 2014. Size-controlled silver nanoparticles over the range 5-100 nm using the same protocol and their antimicrobial efficacy *RSC Adv*, 4, 3974.
- AJITHA, B., ASHOK KUMAR REDDY, Y., RAJESH, K. M. & SREEDHARA REDDY, P. 2016. *Sesbania grandiflora* leaf extract assisted green synthesis of silver nanoparticles: Antimicrobial activity. *Materials Today: Proceedings*, 3, 1977-1984.
- ALBUQUERQUE, B. R., PRIETO, M. A., BARREIRO, M. F., RODRIGUES, A., CURRAN, T. P., BARROS, L. & FERREIRA, I. C. F. R. 2017. Catechin-based extract optimization obtained from *Arbutus unedo* L. fruits using maceration/microwave/ultrasound extraction techniques. *Industrial Crops and Products*, 95, 404-415.
- BALAZ, M., BALAZOVA, L., DANEU, N., DUTKOVA, E., BALAZOVA, M., BUJNAKOVA, Z. & SHPOTYUK, Y. 2017. Plant-Mediated Synthesis of Silver Nanoparticles and Their Stabilization by Wet Stirred Media Milling. *Nanoscale Res Lett*, 12, 83.
- BAUER, M., RIECH, S., BRANDES, I. & WAESCHLE, R. M. 2015. [Advantages and disadvantages of different methods for the implementation and the support of standard operating procedures: From PDF files to an app- and webbased SOP management system]. *Anaesthesist*, 64, 874-883.
- BYARUGABA, D. 2009. Mechanisms of Antimicrobial Resistance. *Antimicrobial Resistance in Developing Countries*, 1, 1-13.
- CALINESCU, I., LAVRIC, V., ASOFIEI, I., GAVRILA, A. I., TRIFAN, A., IGHIGEANU, D., MARTIN, D. & MATEI, C. 2017. Microwave assisted extraction of polyphenols using a coaxial antenna and a cooling system. *Chemical Engineering and Processing: Process Intensification*, 122, 373-379.
- CASTRO-LOPEZ, C., VENTURA-SOBREVILLA, J. M., GONZALEZ-HERNANDEZ, M. D., ROJAS, R., ASCACIO-VALDES, J. A., AGUILAR, C. N. & MARTINEZ-AVILA, G. C. G. 2017. Impact of extraction techniques on antioxidant capacities and phytochemical composition of polyphenol-rich extracts. *Food Chem*, 237, 1139-1148.

- CHEMAT, F., ROMBAUT, N., SICAIRE, A. G., MEULLEMIESTRE, A., FABIANO-TIXIER, A. S. & ABERT-VIAN, M. 2017. Ultrasound assisted extraction of food and natural products. Mechanisms, techniques, combinations, protocols and applications. A review. *Ultrason Sonochem*, 34, 540-560.
- CHEN, Q., FUNG, K. Y., LAU, Y. T., NG, K. M. & LAU, D. T. W. 2016. Relationship between maceration and extraction yield in the production of Chinese herbal medicine. *Food and Bioproducts Processing*, 98, 236-243.
- CHEUNG, R. C., NG, T. B., WONG, J. H. & CHAN, W. Y. 2015. Chitosan: An Update on Potential Biomedical and Pharmaceutical Applications. *Mar Drugs*, 13, 5156-86.
- CHUA, L. S. 2013. A review on plant-based rutin extraction methods and its pharmacological activities. *Journal of Ethnopharmacology*, 150, 805-817.
- CLSI 2012. Methods for Dilution Antimicrobial Susceptibility Tests for Bacteria That Grow Aerobically; Approved Standard. 9 ed.: Clinical and Laboratory Standards Institute
- DAFALE, N. A., SEMWAL, U. P., AGARWAL, P. K., SHARMA, P. & SINGH, G. N. 2015. Development and validation of microbial bioassay for quantification of Levofloxacin in pharmaceutical preparations. *Journal of Pharmaceutical Analysis*, 5, 18-26.
- DAFALE, N. A., SEMWAL, U. P., RAJPUT, R. K. & SINGH, G. N. 2016. Selection of appropriate analytical tools to determine the potency and bioactivity of antibiotics and antibiotic resistance. *Journal of Pharmaceutical Analysis*, 6, 207-213.
- DANIEL, S. C. G. K., THARMARAJ, V., SIRONMANI, T. A. & PITCHUMANI, K. 2010. Toxicity and immunological activity of silver nanoparticles. *Applied Clay Science*, 48, 547-551.
- DENG, J., XU, Z., XIANG, C., LIU, J., ZHOU, L., LI, T., YANG, Z. & DING, C. 2017. Comparative evaluation of maceration and ultrasonic-assisted extraction of phenolic compounds from fresh olives. *Ultrasonics Sonochemistry*, 37, 328-334.
- DO, Q. D., ANGKAWIJAYA, A. E., TRAN-NGUYEN, P. L., HUYNH, L. H., SOETAREDJO, F. E., ISMADJI, S. & JU, Y.-H. 2014. Effect of extraction solvent on total phenol content, total flavonoid content, and antioxidant activity of *Limnophila aromatica*. *Journal of Food and Drug Analysis*, 22, 296-302.

- DU, L., JIANG, H., LIU, X. & WANG, E. 2007. Biosynthesis of gold nanoparticles assisted by *Escherichia coli* DH5 α and its application on direct electrochemistry of hemoglobin. *Electrochemistry Communications*, 9, 1165-1170.
- DUTTA, P. K., DUTTA, J. & TRIPATHI, V. S. 2004. Chitin and chitosan: chemistry, properties and application. *Journal of scientific and industrial research* 63, 20-31.
- DUVAL, J., PECHER, V., POUJOL, M. & LESELLIER, E. 2016. Research advances for the extraction, analysis and uses of anthraquinones: A review. *Industrial Crops and Products*, 94, 812-833.
- EKEZIE, F.-G. C., SUN, D.-W. & CHENG, J.-H. 2017. Acceleration of microwave-assisted extraction processes of food components by integrating technologies and applying emerging solvents: A review of latest developments. *Trends in Food Science & Technology*, 67, 160-172.
- EL-KASSAS, H. Y. & EL-SHEEKH, M. M. 2014. Cytotoxic Activity of Biosynthesized Gold Nanoparticles with an Extract of the Red Seaweed *Corallina officinalis* on the MCF-7 Human Breast Cancer Cell Line. *Asian Pacific Journal of Cancer Prevention*, 15, 4311-4317.
- ETHIRAJ, A. S., JAYANTHI, S., RAMALINGAM, C. & BANERJEE, C. 2016. Control of size and antimicrobial activity of green synthesized silver nanoparticles. *Materials Letters*, 185, 526-529.
- FALENI, N. & MOLOTO, M. J. 2013. effect of glucose as stabilizer of ZnO and CdO nanoparticles on the morphology and optical properties *IJRRAS*, 14, 1-9.
- FEHLBERG, L. C., NICOLETTI, A. G., RAMOS, A. C., RODRIGUES-COSTA, F., DE MATOS, A. P., GIRARDELLO, R., MARQUES, E. A. & GALES, A. C. 2016. In vitro susceptibility of *Burkholderia cepacia* complex isolates: Comparison of disk diffusion, Etest(R), agar dilution, and broth microdilution methods. *Diagn Microbiol Infect Dis*, 86, 422-427.
- FENG, Y., QI, W., XU-RONG, W., LING, W., XIN-PU, L., JIN-YIN, L., SHI-DONG, Z. & HONG-SHENG, L. 2016. Genetic characterization of antimicrobial resistance in *Staphylococcus aureus* isolated from bovine mastitis cases in Northwest China. *Journal of Integrative Agriculture*, 15, 2842-2847.

- FOROUGH, M. & FARHADI, K. 2012. Biological and green synthesis of silver nanoparticles. .
Turkish Journal of engineering and Environmental science, 34, 281-287.
- FOTAKIS, C., TSIGRIMANI, D., TSIACA, T., LANTZOURAKI, D. Z., STRATI, I. F.,
MAKRIS, C., TAGKOULI, D., PROESTOS, C., SINANOGLU, V. J. &
ZOUμποULAKIS, P. 2016. Metabolic and antioxidant profiles of herbal infusions and
decoctions. *Food Chemistry*, 211, 963-971.
- FURUSAKI, E., UENO, Y., SAKAIRI, N., NISHI, N. & TOKURA, S. 1996. Facile preparation
and inclusion ability of a derivative bearing carboxymethyl-β-cyclodextrin. *Carbohydrate
polymers* 9, 29-34.
- GHODAKE, G. S., DESHPANDE, N. G., LEE, Y. P. & JIN, E. S. 2010. Pear fruit extract-assisted
room-temperature biosynthesis of Au nanoplates. *Coll. Surf B Biointerfaces*, 75, 584-9.
- GRASS, G., RENSING, C. & SOLIOZ, M. 2010. Metallic Copper as an Antimicrobial Surface.
Applied and Environmental Microbiology, 77, 1541-1547.
- GRUJIC, N., LEPOJEVIC, Z., SRDJENOVIC, B., VLADIC, J. & SUDJI, J. 2012. Effects of
different extraction methods and conditions on the phenolic composition of mate tea
extracts. *Molecules*, 17, 2518-28.
- GUAGQUM, L. 2012. Fungus-mediated green synthesis of silver nanoparticles *International
Journal of Current Molecular Science*, 13, 446-476.
- GUGGENBICHLER, J. P., BOSWALD, M., LUGAUER, S. & KRALL, T. 1999. A New
Technology of Microdispersed Silver in Polyurethane Induces Antimicrobial Activity in
Central Venous Catheters. *Infection*, 27, 16-23.
- IRAVANI, S., KORBKANDI, H., MIRMOHAMMADI, S. V. & ZOLFAGHARI, B. 2014.
Synthesis of silver nanoparticles: chemical, physical and biological methods. *Res Pharm
Sci*, 9, 385-406.
- JALALI, S. A. H. & ALLAFCHIAN, A. R. 2016. Assessment of antibacterial properties of novel
silver nanocomposite. *Journal of the Taiwan Institute of Chemical Engineers*, 59, 506-513.
- JEYARANI, W. J., TENKYONG, T., BACHAN, N., KUMAR, D. A. & SHYLA, J. M. 2016. An
investigation on the tuning effect of glucose-capping on the size and bandgap of CuO
nanoparticles. *Advanced Powder Technology*, 27, 338-346.

- KALA, H. K., MEHTA, R., SEN, K. K., TANDEY, R. & MANDAL, V. 2016. Critical analysis of research trends and issues in microwave assisted extraction of phenolics: Have we really done enough. *TrAC Trends in Analytical Chemistry*, 85, 140-152.
- KATHIRAVAN, V., RAVI, S. & KUMAR, S. A. 2014. Synthesis of silver nanoparticles from Meliadubia leaf extract and their in vitro anticancer activity. *Spectrochim Acta Part A: Mol Biomol Spectrosc*, 130, 116-121.
- KHALIL, M. I., AL-QUNAIBIT, M. M., AL-ZAHM, A. M. & LABIS, J. P. 2014a. Synthesis and characterization of ZnO nanoparticles by thermal decomposition of a curcumin zinc complex. *Arabian Journal of Chemistry*, 7, 1178-1184.
- KHALIL, M. M. H., ISMAIL, E. H., EL-BAGHDADY, K. Z. & MOHAMED, D. 2014b. Green synthesis of silver nanoparticles using olive leaf extract and its antibacterial activity. *Arabian Journal of Chemistry*, 7, 1131-1139.
- KHAN, M. F., RAWAT, A. K., PAWAR, B., GAUTAM, S., SRIVASTAVA, A. K. & NEGI, D. S. 2014. Bioactivity-guided chemical analysis of Melia azedarach L. (Meliaceae), displaying antidiabetic activity. *Fitoterapia*, 98, 98-103.
- KHANNA, P. K., GAIKWAD, S., ADHYAPAK, P. V., SINGH, N. & MARIMUTHU, R. 2007. Synthesis and characterization of copper nanoparticles. *Materials Letters* 61, 61, 4711-4714.
- KLUEH, U., WAGNER, V., KELLY, S., JOHNSON, A. & BRYERS, J. D. 2000. Efficacy of Silver-Coated Fabric to Prevent Bacterial Colonization and Subsequent Device-Based Biofilm Formation. *Journal of Biomedical Materials Research Part B: Applied Biomaterials.*, 53, 621-631.
- KUMARI, M., PANDEY, S., GIRI, V. P., BHATTACHARYA, A., SHUKLA, R., MISHRA, A. & NAUTIYAL, C. S. 2017. Tailoring shape and size of biogenic silver nanoparticles to enhance antimicrobial efficacy against MDR bacteria. *Microb Pathog*, 105, 346-355.
- KUMIRSKA, J., WEINHOLD, M. X., THÖMING, J. & STEPNOWSKI, P. 2011. Biomedical Activity of Chitin/Chitosan Based Materials—Influence of Physicochemical Properties Apart from Molecular Weight and Degree of N-Acetylation. *Polymers*, 3, 1875-1901.
- LI, C.-C., CHANG, S.-J., SU, F.-J., LIN, S.-W. & CHOU, Y.-C. 2013. Effects of capping agents on the dispersion of silver nanoparticles. *Colloids and Surfaces A: Physicochemical and Engineering Aspects*, 419, 209-215.

- LI, Y., LI, S., LIN, S.-J., ZHANG, J.-J., ZHAO, C.-N. & LI, H.-B. 2017. Microwave-Assisted Extraction of Natural Antioxidants from the Exotic *Gordonia axillaris* Fruit: Optimization and Identification of Phenolic Compounds. *Molecules*, 22, 1481.
- LIU, H., TAYLOR, T. H., JR., PETTUS, K., JOHNSON, S., PAPP, J. R. & TREES, D. 2016. Comparing the disk-diffusion and agar dilution tests for *Neisseria gonorrhoeae* antimicrobial susceptibility testing. *Antimicrob Resist Infect Control*, 5, 46.
- LOO, Y. Y., CHIENG, B. W., NISHIBUCHI, M. & RADU, S. 2012. Synthesis of silver nanoparticles by using tea leaf extract from *Camellia sinensis*. *Int J Nanomed*. 7, 4263-7.
- LOVRIĆ, V., PUTNIK, P., KOVAČEVIĆ, D. B., JUKIĆ, M. & DRAGOVIĆ-UZELAC, V. 2017. Effect of Microwave-Assisted Extraction on the Phenolic Compounds and Antioxidant Capacity of Blackthorn Flowers. *Food Technology and Biotechnology*, 55, 243-250.
- LU, M., HO, C.-T. & HUANG, Q. 2017. Extraction, bioavailability, and bioefficacy of capsaicinoids. *Journal of Food and Drug Analysis*, 25, 27-36.
- MARTINS, A. F., BUENO, P. V., ALMEIDA, E. A., RODRIGUES, F. H., RUBIRA, A. F. & MUNIZ, E. C. 2013. Characterization of N-trimethyl chitosan/alginate complexes and curcumin release. *Int J Biol Macromol*, 57, 174-84.
- MARTINS, A. F., FACCHI, S. P., FOLLMANN, H. D., PEREIRA, A. G., RUBIRA, A. F. & MUNIZ, E. C. 2014. Antimicrobial activity of chitosan derivatives containing N-quaternized moieties in its backbone: a review. *Int J Mol Sci*, 15, 20800-32.
- MEHMOOD, A., MURTAZA, G., BHATTI, T. M. & KAUSAR, R. 2013. Phyto-mediated synthesis of silver nanoparticles from *Melia azedarach* L. leaf extract: Characterization and antibacterial activity. *Arabian Journal of Chemistry*.
- MENDREK, B., CHOJNIK, J., LIBERA, M., TRZEBICKA, B., BERNAT, P., PARASZKIEWICZ, K. & PŁAZA, G. 2016. Silver nanoparticles formed in bio- and chemical syntheses with biosurfactant as the stabilizing agent. *Journal of Dispersion Science and Technology*, 38, 1647-1655.
- MUTHUKRISHNAN, A. M. 2015. Green Synthesis of Copper-Chitosan Nanoparticles and Study of its Antibacterial Activity. *Journal of Nanomedicine & Nanotechnology*, 06.
- NABIKHAN, A., KANDASAMY, K., RAJ, A. & ALIKUNHI, N. M. 2010. Synthesis of antimicrobial silver nanoparticles by callus and leaf extracts from saltmarsh plant, *Sesuvium portulacastrum* L. *Colloids Surf B Biointerfaces*, 79, 488-93.

- OTTONI, C. A., SIMOES, M. F., FERNANDES, S., DOS SANTOS, J. G., DA SILVA, E. S., DE SOUZA, R. F. B. & MAIORANO, A. E. 2017. Screening of filamentous fungi for antimicrobial silver nanoparticles synthesis. *AMB Express*, 7, 31.
- PATIL SHRINIWAS, P. & KUMBHAR SUBHASH, T. 2017. Antioxidant, antibacterial and cytotoxic potential of silver nanoparticles synthesized using terpenes rich extract of *Lantana camara* L. leaves. *Biochemistry and Biophysics Reports*, 10, 76-81.
- PHONGTONGPASUK, S., POADANG, S. & YONGVANICH, N. 2016. Environmental-friendly method for synthesis of silver nanoparticles from dragon fruit peel extract and their antibacterial activities. *Energy Procedia*, 89, 237-247.
- PRASAD, P. R., KANCHI, S. & NAIDOO, E. B. 2016. In-vitro evaluation of copper nanoparticles cytotoxicity on prostate cancer cell lines and their antioxidant, sensing and catalytic activity: One-pot green approach. *J Photochem Photobiol B*, 161, 375-82.
- PRAVEENKUMAR, K., ROBINAL, M. K., KALASAD, M. D., SANKARAPPA, T. & MASSHESH, D. 2014. Chitosan capped silver nanoparticles used as pressure sensors. *Journal of applied physics* 5, 43-51.
- PUNJABI, K. 2015. Biosynthesis of Nanoparticles : A Review. 30, 219-226.
- PUNJABI, K., CHOUDHARY, P., SAMANT, L., MUKHERJEE, S., VAIDYA, S. & CHOWDHARY, A. 2015. Biosynthesis of Nanoparticles : A Review. *Int. J. Pharm. Sci. Rev. Res.*, 30, 219-226.
- RAAFAT, D. & SAHL, H. G. 2009. Chitosan and its antimicrobial potential -a critical literature survey. *Microbial Biotechnology* 2, 186-201.
- RAJESHKUMAR, S. 2016. Synthesis of silver nanoparticles using fresh bark of *Pongamia pinnata* and characterization of its antibacterial activity against gram positive and gram negative pathogens. *Resource-Efficient Technologies*, 2, 30-35.
- RAMANIBAI, R. & VELAYUTHAM, K. 2015. Bioactive compound synthesis of Ag nanoparticles from leaves of *Melia azedarach* and its control for mosquito larvae. *Res Vet Sci*, 98, 82-8.
- RASOOL, U. & HEMALATHA, S. 2017. Marine endophytic actinomycetes assisted synthesis of copper nanoparticles (CuNPs): Characterization and antibacterial efficacy against human pathogens. *Materials Letters*, 194, 176-180.

- RAVICHANDRAN, V., VASANTHI, S., SHALINI, S., ALI SHAH, S. A. & HARISH, R. 2016. Green synthesis of silver nanoparticles using *Atrocarpus altilis* leaf extract and the study of their antimicrobial and antioxidant activity. *Materials Letters*, 180, 264-267.
- RAZA, M. A., KANWAL, Z., RAUF, A., SABRI, A. N. & RIAZ, S. 2016. Size- and Shape-Dependent Antibacterial Studies of Silver Nanoparticles Synthesized by Wet Chemical Routes. *Nanomaterials* 6, 74.
- SAINI, R. K. & KEUM, Y.-S. 2018. Carotenoid extraction methods: A review of recent developments. *Food Chemistry*, 240, 90-103.
- SATHISHKUMAR, M., SNEHA, K. & YUN, Y. S. 2010. Immobilization of silver nanoparticles synthesized using *Curcuma longa* tuber powder and extract on cotton cloth for bactericidal activity. *Bioresour Technol*, 101, 7958-65.
- SEFTON, A. 2002. Mechanisms of Antimicrobial Resistance Their Clinical Relevance in the New Millennium. *Drugs*, 62, 557-566.
- SEIL, J. T. & WEBSTER, T. J. 2012. Antimicrobial applications of nanotechnology: methods and literature. *Int J Nanomedicine*, 7, 2767-81.
- SETFORD, P. C., JEFFERY, D. W., GRBIN, P. R. & MUHLACK, R. A. 2017. Factors affecting extraction and evolution of phenolic compounds during red wine maceration and the role of process modelling. *Trends in Food Science & Technology*, 69, 106-117.
- SHAH, M., FAWCETT, D., SHARMA, S., TRIPATHY, S. & POINERN, G. 2015. Green Synthesis of Metallic Nanoparticles via Biological Entities. *Materials*, 8, 7278-7308.
- SHARMA, V. K., YNGARD, R. A. & LIN, Y. 2009. Silver nanoparticles: green synthesis and their antimicrobial activities. *Adv Colloid Interface Sci*, 145, 83-96.
- SIBIYA, P. N. & MOLOTO, M. J. 2014. Effect of precursor concentration and pH on the shape and size of starch capped silver Selenide nanoparticles. *Chalcogenide letters* 11, 577-588.
- SIBIYA, P. N. & MOLOTO, M. J. 2016. Starch-Capped Silver Selenide Nanoparticles: Effect of Capping Agent Concentration and Extraction Time on Size. *Asian Journal of Chemistry*, 28, 1315-1320.
- SINGH, P., KIM, Y. J., ZHANG, D. & YANG, D. C. 2016. Biological Synthesis of Nanoparticles from Plants and Microorganisms. *Trends Biotechnol*, 34, 588-99.
- SINGLA, A. K. & CHAWLA, M. 2001. Chitosan: some pharmaceutical and biological aspects-an update. *Journal of Pharmacy and Pharmacology*, 53, 1047-1067.

- SPARR ESKILSSON, C. & BJÖRKLUND, E. 2000. Analytical-scale microwave-assisted extraction. *Journal of Chromatography A*, 902, 227-250.
- SUN, Q., CAI, X., LI, J., ZHENG, M., CHEN, Z. & YU, C.-P. 2014. Green synthesis of silver nanoparticles using tea leaf extract and evaluation of their stability and antibacterial activity. *Colloids and Surfaces A: Physicochemical and Engineering Aspects*, 444, 226-231.
- SURESH, Y., ANNAPURNA, S., SINGH, A. K. & BHIKSHAMACAH, G. 2014. Green synthesis and characterization of the decoction stabilized copper nanoparticles. *International Journal of Innovative research in science, engineering and technology*, 3, 3-6.
- TCHINDA, C. F., VOUKENG, I. K., BENG, V. P. & KUETE, V. 2017. Antibacterial activities of the methanol extracts of *Albizia adianthifolia*, *Alchornea laxiflora*, *Laportea ovalifolia* and three other Cameroonian plants against multi-drug resistant Gram-negative bacteria. *Saudi J Biol Sci*, 24, 950-955.
- THAKKA, K. N. & MHSATRE, S. S. 2010. Biological synthesis of metallic nanoparticle. *Journal of NanoMedical Nanotechnology*, 6, 257-262.
- TONGKHAM, N., JUNTASALAY, B., LASUNON, P. & SENGKHAMPARN, N. 2017. Dragon fruit peel pectin: Microwave-assisted extraction and fuzzy assessment. *Agriculture and Natural Resources*.
- TRAN, Q. H., NGUYEN, V. Q. & LE, A.-T. 2013. Silver nanoparticles: synthesis, properties, toxicology, applications and perspectives. *Advances in Natural Sciences: Nanoscience and Nanotechnology*, 4, 033001.
- VALVERDE-ALVAA, M. A., GARCÍA-FERNÁNDEZB, T. M., VILLAGRÁN-MUNIZC, M., SÁNCHEZ-AKÉC, C., CASTAÑEDA-GUZMÁN, R., ESPARZA-ALEGRÍAD, E. & SÁNCHEZ-VALDÉSE, C. F. 2015. Synthesis of silver nanoparticles by laser ablation in ethanol: A pulsedphotoacoustic study. *Applied Surface Science*, 355, 341-349.
- VENKATESAN, J. & KIM, S. K. 2010. Chitosan composites for bone tissue engineering--an overview. *Mar Drugs*, 8, 2252-66.
- VIGNESHWARAN, N., ASHTAPUTRE, N. M., VARADARAJAN, P. V., NACHANE, R. P., PARALIKAR, K. M. & BALASUBRAMANYA, R. H. 2007. Biological synthesis of silver nanoparticles using the fungus *Aspergillus flavus*. *Materials Letters*, 61, 1413-1418.

- VILLAPÚN, V., DOVER, L., CROSS, A. & GONZÁLEZ, S. 2016. Antibacterial Metallic Touch Surfaces. *Materials*, 9, 736.
- VINATORU, M., MASON, T. J. & CALINESCU, I. 2017. Ultrasonically assisted extraction (UAE) and microwave assisted extraction (MAE) of functional compounds from plant materials. *TrAC Trends in Analytical Chemistry*, 97, 159-178.
- VONGSAK, B., SITHISARN, P., MANGMOOL, S., THONGPRADITCHOTE, S., WONGKRAJANG, Y. & GRITSANAPAN, W. 2013. Maximizing total phenolics, total flavonoids contents and antioxidant activity of Moringa oleifera leaf extract by the appropriate extraction method. *Industrial Crops and Products*, 44, 566-571.
- VROUMSIA, T., SAOTOING, P., DAWE, A., DJAOUDA, M., EKANEY, M. & MUA, B. A. 2015. The sensitivity of Escherichia coli to extracts of Combretum fragrans, Combretum micranthum and Combretum molle locally used in the treatment of Diarrheal diseases in the far north region of cameroon *international Journal of Current Microbiology and Applied Sciences* 2, 399-411.
- WANG, T., LIN, J., CHEN, Z., MEGHARAJ, M. & NAIDU, R. 2014. Green synthesized iron nanoparticles by green tea and eucalyptus leaves extracts used for removal of nitrate in aqueous solution. *Journal of Cleaner Production*, 83, 413-419.
- XU, C.-C., WANG, B., PU, Y.-Q., TAO, J.-S. & ZHANG, T. 2017. Advances in extraction and analysis of phenolic compounds from plant materials. *Chinese Journal of Natural Medicines*, 15, 721-731.
- YAMANAKA, M., HARA, K. & KUDO, J. 2005. Bactericidal Actions of a Silver Ion Solution on Escherichia coli, Studied by Energy-Filtering Transmission Electron Microscopy and Proteomic Analysis
Applied and Environmental Microbiology, 71, 7.
- YANG, F., WANG, Q., WANG, X.-R., WANG, L., LI, X.-P., LUO, J.-Y., ZHANG, S.-D. & LI, H.-S. 2016. Genetic characterization of antimicrobial resistance in Staphylococcus aureus isolated from bovine mastitis cases in Northwest China. *Journal of Integrative Agriculture*, 15, 2842-2847.
- YANG, N. & LI, W.-H. 2015. Preparation of gold nanoparticles using chitosan oligosaccharide as a reducing and capping reagent and their in vitro cytotoxic effect on Human fibroblasts cells. *Materials Letters*, 138, 154-157.

- YOON, K. Y., HOON BYEON, J., PARK, J. H. & HWANG, J. 2007. Susceptibility constants of *Escherichia coli* and *Bacillus subtilis* to silver and copper nanoparticles. *Sci Total Environ*, 373, 572-5.
- ZAIN, N. M., STAPLEY, A. G. & SHAMA, G. 2014. Green synthesis of silver and copper nanoparticles using ascorbic acid and chitosan for antimicrobial applications. *Carbohydr Polym*, 112, 195-202.
- ZHANG, L., ZHOU, C., WANG, B., YAGOUB, A. E. A., MA, H., ZHANG, X. & WU, M. 2017a. Study of ultrasonic cavitation during extraction of the peanut oil at varying frequencies. *Ultrason Sonochem*, 37, 106-113.
- ZHANG, P., SHEN, Z., ZHANG, C., SONG, L., WANG, B., SHANG, J., YUE, X., QU, Z., LI, X., WU, L., ZHENG, Y., ADITYA, A., WANG, Y., XU, S. & WU, C. 2017b. Surveillance of antimicrobial resistance among *Escherichia coli* from chicken and swine, China, 2008–2015. *Veterinary Microbiology*, 203, 49-55.

Chapter 3

RESEARCH METHODOLOGY

3.1 MATERIALS

Silver nitrate (99.8%) and cupric acetate (99.5%) were purchased from Merk (South Africa). Acetone (99.8%), ammonia solution (32%), ascorbic acid (99.5), gallic acid (97.5%), quercetin (>95.5), aluminum chloride (97%), folin-ciocalteus phenol reagent, sodium carbonate (99%), methanol (99.5), 2,2-diphenyl-1-picrylhydrazyl, hydrochloric acid (37%), Dragendorff's reagent, formic acid (98%), iron (III) chloride hexa-hydrate (99%), pyridine (99.8), sodium hydroxide (99%), sodium nitroprusside, vanillin, Fehling's reagent I for sugars, Fehling's reagent II for sugars and nitric acid (> 65%) were purchased from Sigma Aldrich (South Africa). Chitosan, p-iodonitrotetrazolium chloride (INT), neomycin and amphotericin B were purchased from Sigma-Aldrich (South Africa). Ethyl acetate and sulfuric acid were purchased from Glass world. Muller-Hinton broth was purchased from Neogen (South Africa). *Staphylococcus aureus*, *Enterococcus Faecalis*, *Klebsiella pneumonia*, *Pseudomonas aeruginosa*, *Candida albicans* and *Cryptococcus neoformans* were bought from Anatech (South Africa). All chemicals were used as purchased, without any further purification.

3.2 PREPARATION OF PLANT EXTRACT

3.2.1 Collection of plant leaves

The leaves of *Melia azedarach linn* were harvested at Vanderbijlpark, Gauteng province. Identification was done by botanists at North-West University where the voucher specimen (CHE DVU 1) was deposited. The leaves of *Combretum molle* were harvested in the Lowveld National Botanical Garden in Nelspruit, Mpumalanga. A voucher specimen for this leaves is present in the herbarium of this Botanical Garden. *Camellia sinensis* which is commonly known as green tea was purchased from a local Pick n Pay supermarket in Vanderbijlpark.

3.2.2 Drying of plant leaves

The plant leaves were washed with distilled water to remove impurities which may be deposited on the leaves by natural factors such as wind, birds, insects, etc. The washed leaves were then placed in a ventilated oven at 30 °C for 96 hours. This was followed by grinding into a fine powder using commercial laboratory blender (Salton elite, SEBS13).

3.2.3 Preparation of extracts

Aqueous extracts of *Combretum molle*, *Camellia sinensis*, and *Melia azedarach linn* were prepared from powdered plant leaves. For each plant material 0.5, 1.0 or 2.0 g of powder was dissolved in 100 ml of water and heated at 90 °C for 15 min. The aqueous extracts were then filtered through Whatman No.1 filter paper with a pore size of 11 µm. The process was repeated three times in order to ensure maximum extraction of the plant extracts (Remington, 2008).

3.3 PRELIMINARY PHYTOCHEMICAL SCREENING

The extracts were concentrated using water as a solvent and were subjected to phytochemical screening using standard procedures. The compounds were analyzed for phenols, flavonoids, carbohydrates, proteins, saponins, alkaloids, glycosides, diterpenes and triterpenes using the following methods.

3.3.1 Test for phenolic compounds

This was done using Ferric Chloride test where 5 ml of the plant extract was allowed to react with 1 ml of 5 % ferric chloride solution. The observation of greenish black colour showed the presence of phenols (Tiwari et al., 2011).

3.3.2 Test for flavonoids

The evidence of flavonoids was shown through the addition of a few drops of sodium hydroxide solution on plant extract followed by addition of diluted hydrochloric acid. The formation of intense yellow colour, which becomes colorless on the addition of dilute hydrochloric acid indicated the presence of flavonoids (Onwukaeme et al., 2007).

3.3.3 Test for carbohydrates

Fehling's test was done to check the presence of carbohydrates. This was done by mixing 5 ml of the plant extract with 5 ml Fehling's solution (an equal mixture of Fehling's solution A which is made up of copper (II) sulfate pentahydrate and solution B which is made up of aqueous potassium sodium tartrate) and boiled. Development of red brick precipitate showed the presence of reducing sugars (Tiwari et al., 2011).

3.3.4 Test for proteins

Evidence of proteins in extracts was done by using xanthoproteic test. The plant extract was treated with a few drops of concentrated nitric acid. The formation of a yellow colour indicated the presence of protein (Tiwari et al., 2011)

3.3.5 Test of saponins

This was done using froth test where the extract was diluted with 200 ml of distilled water in a 500 ml graduated cylinder and shaken for about 15 minutes using a graduated cylinder. The formation of 1 cm foam layer above the solution indicated the presence of saponins (Parekh and Chanda, 2007).

3.3.6 Test for alkaloids

A drop of the extract was spotted on a small piece of pre-coated thin layer chromatography (TLC) plate, and the plate was sprayed with a modified Dragendorff's reagent. The change in colour of the spot to orange indicated the presence of alkaloids (Ahmed et al., 2012).

3.3.7 Test for glycosides

Plant extract (0.1 ml) was mixed with 2 ml of pyridine, into which 2 ml of sodium nitroprusside solution was added. The mixture was made alkaline by adding sodium hydroxide. The formation of a pink to red coloured solution indicated the presence of glycosides (Deepa and Padmaja, 2014).

3.3.8 Test for diterpenes and triterpenes

Extracts were dissolved in water and treated with 3-4 drops of copper acetate solution. The formation of emerald green colour indicated the presence of diterpenes and triterpenes (Tiwari et al., 2011).

3.4 PRELIMINARY PHYTOCHEMICAL SCREENING BY THIN LAYER CHROMATOGRAPHY (TLC)

Chemical constituents of the extracts were analyzed by thin layer chromatography (TLC) using aluminum-backed TLC plates (Merck, silica gel 60 F₂₅₄). Ethyl acetate-methanol-water (30:5:4) was used as the solvent system. The plates were sprayed with vanillin-sulfuric acid spray and viewed under visible light (Masoko and Eloff, 2007b).

3.5 DETERMINATION OF TOTAL PHENOLIC CONTENTS

Total phenolic contents in the extracts of *Camellia sinensis*, *Combretum molle*, and *Melia azedarach linn* leaves was determined by the modified Folin-Ciocalteu method with some modifications (Al-Jadidi and Hossain, 2016). Briefly, an aliquot of the extract (1 ml) was mixed with Folin-Ciocalteu reagent (0.5 ml) and 20% of sodium carbonate solution (1.5 ml) in a tube.

The tube was vortexed for 15 s, and then it was allowed to settle at 40 °C for 30 min to develop a colour. The absorbance was then measured at 720 nm using UV-Vis spectrometer. The total phenolic content was calculated as the concentration of garlic acid (mg/g) using the equation based on the calibration curve.

3.6 DETERMINATION OF TOTAL FLAVONOID CONTENTS

Total flavonoid content was determined using the spectrophotometric method based on the formation of the flavonoid complex with aluminum (Al-Jadidi and Hossain, 2016). An aluminum chloride-methanol solution (0.5 ml) was added to the plant extract (0.5 ml) solution, and the mixture was allowed to stay at room temperature for 1 hour, after which the absorbance was measured at 412 nm. Total flavonoid content was calculated as the concentration of quercetin (mg/g) using the equation based on the calibration curve.

3.7 SYNTHESIS OF NANOPARTICLES

3.7.1 Synthesis of silver nanoparticles for effect of capping agent concentration

Silver nitrate (AgNO_3) aqueous solution was prepared by dissolving AgNO_3 salt (0.1 M) in 20 ml of ultra-pure water in a round bottomed flask. A 50 ml chitosan solution, *Camellia sinensis*, *Combretum molle* and *Melia azedarach linn* leaves aqueous extracts of various concentrations (0.5, 1.0, and 2.0 %) were each added dropwise into different 20 ml AgNO_3 solution while stirring. The pH of the solution was adjusted to 10 using ammonium hydroxide. The mixture was kept stirring at room temperature for 2 hours under nitrogen gas. After 2 hours, acetone was poured to the mixture and the solution was then centrifuged.

3.7.2 Synthesis of silver nanoparticles for effect of precursor concentration

A 50 ml chitosan solution, aqueous extracts of *Camellia sinensis*, *Combretum molle* and *Melia azedarach linn* were each added to different concentrations (0.1, 0.2 and 0.3 M) of 20 ml AgNO_3 solution. The pH of the solution was adjusted to 10 using ammonium hydroxide. The mixture was kept stirring at room temperature for 2 hours under nitrogen gas. After 2 hours, acetone was poured to the mixture and the solution was then centrifuged.

3.7.3 Synthesis of copper nanoparticles for effect of capping agent

Copper acetate ($\text{Cu}(\text{CH}_3\text{COO})_2$) aqueous solution was prepared by dissolving $\text{Cu}(\text{CH}_3\text{COO})_2$ (0.1 M) in 15 ml of distilled water in a round bottomed flask. A 40 mL chitosan solution, aqueous extract of *Camellia sinensis*, *Combretum molle* and *Melia azedarach linn* leaves were each added dropwise into different solutions of $\text{Cu}(\text{CH}_3\text{COO})_2$ solution while stirring. The mixture was kept stirring at 85 °C for 6 hours under nitrogen gas. After 6 hours, acetone was poured to the mixture and the solution was then centrifuged. 85 °C was used as the reaction temperature because at room temperature copper oxide nanoparticles were formed.

3.8 CHARACTERIZATION TECHNIQUES

The optical properties of the synthesized copper and silver nanoparticles were studied using Perkin Elmer Lambda 25 UV/Vis spectrometer which collects spectra in the wavelength range 180-1100 nm using a spectral bandwidth of 0.5 nm (variable slit). Photoluminescence analysis was performed at room temperature using Jasco Spectrofluorimeter FP-8600 equipped with XE lamp at 150 W. The bandwidth excitation slit was at 5 nm, and the emission was used in the range of 200-1010 nm. The chemical structures of capped silver and copper nanoparticles were determined using Perkin-Elmer Spectrum 400 FT-IR/FT-NIR Spectrometer, universal ATR with the diamond detector with a wavelength range of 650 cm^{-1} to 4000 cm^{-1} . Transition electron microscopy A JEOL JEM-2100 transmission electron microscope operating at 200 kV was employed to obtain the size and shape of the synthesized particles. The X-ray diffraction patterns were recorded by a Bruker D2 diffractometer at 40 kV and 50 mA. A secondary graphite monochromated Co K alpha radiation ($\lambda = 1.7902\text{ \AA}$) was used, and the measurements were taken at high angle 2θ in a range of 5° – 90° with a scan speed of $0.01^\circ\ 2\theta\ \text{s}^{-1}$. The elemental composition of chitosan capped silver nanoparticles was determined using energy-dispersive X-ray spectroscopy FEI TECNAI SPIRIT (TEM-EDS).

3.9 BIOLOGICAL STUDIES

3.9.1 Bacterial strains

Bacterial strains used in this study were *Staphylococcus aureus* (ATCC 25923) and *Enterococcus faecalis* (ATCC 29212) (Gram-positive bacteria strains). *Klebsiella pneumoniae* (ATCC 13883) and *Pseudomonas aeruginosa* (ATCC 15442) (Gram-negative bacteria strains).

3.9.2 Fungal strains

Fungal strains used in this study were *Candida albicans* (ATCC 14053) and *Cryptococcus neoformans* (ATCC14116) (yeasts).

3.9.3 Antibacterial studies

Minimum inhibitory concentrations (MIC) of the plant extracts, chitosan, copper nanoparticles and silver nanoparticles were each determined using the microdilution bioassay as described by (Eloff, 1998). Overnight cultures (incubated at 37 °C) of *Staphylococcus aureus*, *Enterococcus faecalis*, *Klebsiella pneumonia* and *Pseudomonas aeruginosa* bacterial strains were each diluted with sterile Mueller-Hinton (MH) broth to give final inocula of approximately 10^6 CFU/ml (colony forming units). The plant extract, chitosan, copper and silver nanoparticles were each dissolved in distilled water to make a concentration of 25 mg/ml. One hundred (100) microliters of each solution were serially diluted two-fold with sterile distilled water in a 96-well microliter plate for each of the four bacterial strains. Positive and negative controls were prepared similarly to the samples by using neomycin solution and water respectively. One hundred microliters of each bacterial culture were added to each well. Bacterial growth was indicated by adding 50 μ l of 0.2 mg/ml p-iodonitrotetrazolium chloride (INT). The plates were covered with Para-film and incubated at 37 °C for 24 hrs. Since the colourless tetrazolium salt is biologically reduced to a red product due to the presence of active organisms, the MIC values were determined as the concentration in the last wells where no colour change was observed. Bacterial growth in the wells was indicated by a reddish-pink colour. The assay was repeated twice with two replicates per assay.

3.9.4 Antifungal studies

A modified microdilution method for fungi was used as described by (Masoko and Eloff, 2007a). To determine the antifungal activity of the plant extract, chitosan, copper and silver nanoparticles against *Candida albicans* and *Cryptococcus neoformans*. An overnight fungal culture was prepared in yeast malt (YM) broth. Four hundred microliters of the overnight culture were added to 4 ml of sterile saline and absorbance was read at 530 nm. The absorbance was adjusted with sterile saline to match that of a 0.5 M McFarland standard solution. From this standardized fungal stock, a 1:1000 dilution with sterile YM broth was prepared to give a final inoculum of approximately 10^6 CFU/ml. Aqueous solutions of the plant extract, chitosan, copper and silver

nanoparticles were each prepared at the concentration of 25 mg/ml. One hundred microliters of each solution was serially diluted two-fold with sterile water in a 96-well microtitre plate. A similar two-fold dilution of amphotericin B (25 mg/ml) was used as the positive control while water was used as negative control. One hundred microliters of the diluted fungal culture was added to each well. 50 µl (0.2 mg/ml) INT was added, and the plates were covered with Para-film and incubated for 24 hours at 37 °C. The wells remained clear where there was inhibition of fungal growth, while the colour changed to pink where there was a continuation of fungal growth. The MIC values were recorded as the lowest concentration that inhibited fungal growth after 24 hrs. The assay was repeated twice with two replicates per assay.

3.9.5 Antioxidants studies

The free radical scavenging activity of plant extracts, copper and silver nanoparticles was measured using 2,2-diphenyl-1-picrylhydrazyl (DPPH) as a free radical model with some modifications (Prasad et al., 2016). Briefly, to a 3.0 mL of 50 ppm DPPH in absolute methanol, different volumes of the plant extract, silver or copper nanoparticles were added to the DPPH solution. The mixture was mixed vigorously to improve the surface reaction between the DPPH and the antioxidant. After that the solution was kept in the dark for 30 min. The absorbance was measured at 517 nm. Ascorbic acid and DPPH were both used as positive and negative controls respectively. The free radical scavenging activity was calculated using the following equation:

$$\text{Scavenging activity \%} = \left[1 - \frac{\text{Absorbance of sample}}{\text{Absorbance of negative control}} \right] * 100 \quad (1)$$

3.10 REFERENCES

- AHMED, M. F., SRINIVASA RAO, A. & IBRAHIM, M. 2012. Phytochemical studies and antioxidant activity of *Melia azedarach* leaves by DPPH scavenging assay. *International Journal of pharmaceutical applications*, 3, 271-276.
- AL-JADIDI, H. S. K. & HOSSAIN, M. A. 2016. Determination of the total phenols, flavonoids and antimicrobial activity of the crude extracts from locally grown neem stems. *Asian Pacific Journal of Tropical Disease*, 6, 376-379.
- DEEPA, M. & PADMAJA, C. K. 2014. PRELIMINARY PHYTOCHEMICAL ANALYSIS AND THIN LAYER CHROMATOGRAPHY OF THE EXTRACTS OF *EXCOECARIA*

- AGALLOCHA L. *international journal of pharmaceutical sciences and research* 5, 1000-1007.
- ELOFF, J. N. 1998. A Sensitive and quick microplate method to determine the minimal inhibitory concentration of plant extracts for bacteria. *planta medica*, 64, 711-713.
- MASOKO, P. & ELOFF, J. N. 2007a. Resistance of animal fungal pathogens to solvents used in bioassays. *South African Journal of Botany*, 73, 667-669.
- MASOKO, P. & ELOFF, J. N. 2007b. SCREENING OF TWENTY-FOUR SOUTH AFRICAN COMBRETUM AND SIX TERMINALIA SPECIES (COMBRETACEAE) FOR ANTIOXIDANT ACTIVITIES. *African journal traditional* 4, 231-239.
- ONWUKAEME, D. N., IKUEGBVWEHA, T. B. & ASONYE, C. C. 2007. Evaluation of Phytochemical Constituents, Antibacterial Activities and Effect of Exudate of *Pycnanthus Angolensis* Wedd Warb (Myristicaceae) on Corneal Ulcers in Rabbits *Tropical Journal of Pharmaceutical Research*, 6, 725-730.
- PAREKH, J. & CHANDA, S. 2007. In vitro antimicrobial activity and phytochemical analysis of some Indian medicinal plants. *Turkish Journal of Biology*, 31, 53-58.
- PRASAD, P. R., KANCHI, S. & NAIDOO, E. B. 2016. In-vitro evaluation of copper nanoparticles cytotoxicity on prostate cancer cell lines and their antioxidant, sensing and catalytic activity: One-pot green approach. *J Photochem Photobiol B*, 161, 375-82.
- REMINGTON, J. 2008. The science and practice of pharmacy. 21 ed.: Lippincott Williams & Wilkins.
- TIWAR, P., KUMAR, B., KAUR, G., KAUR, M. & KAUR, H. 2011. Phytochemical screening and extraction: A Review. *Internationale pharmaceutica sciencia*, 1, 1-9.

Chapter 4

RESULTS AND DISCUSSION

4.1 PHYTOCHEMICAL SCREENING

4.1.1 Phytochemical screening, total phenolic, and flavonoid content

Preliminary qualitative phytochemical analysis of an aqueous extract of *Camellia sinensis*, *Combretum molle*, and *Melia azedarach linn* leaves revealed the presence of alkaloids, phenols, flavonoids, proteins, carbohydrates and saponins as shown in Table 4:1. Thin layer chromatography (TLC) was further used to identify the bioactive compounds that are present in the extracts as shown in Fig 4: 1.

Table 4:1 Phytochemical screening of plant extracts

Phytochemicals	<i>Camellia sinensis</i>	<i>Combretum molle</i>	<i>Melia azedarach linn</i>
Alkaloids	+	+	+
Phenols	+	+	+
Flavonoids	+	+	+
Cardiac glycosides	-	-	-
Triterpenes	-	-	-
Carbohydrates	+	+	+
Saponins	+	+	+
Proteins	+	+	+
Diterpenes	-	-	-

+ Present – not present

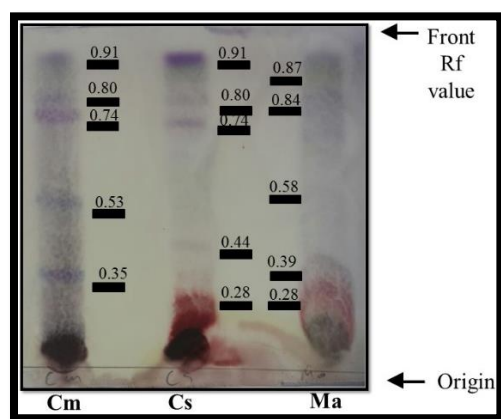


Fig 4:1 TLC of aqueous extract of *Camellia sinensis*, *Combretum molle* and *Melia azedarach linn* leaves.

The TLC plate revealed the presence of several bioactive compounds in the form of bands as represented by different colors observed. The presence of flavonoids, carbohydrates, alkaloids and phenolic compounds were shown in blue, violet, green and brown colors respectively (Madassery et al., 2015). The total phenolic compounds from the aqueous extracts were determined by the folin-calceu method. The total phenolic content is expressed as the ratio of gallic acid to dry sample (mg/g) while the ratio of quercetin to dry sample (mg/g) was used for total flavonoids content. The total phenolic contents results are plotted in Fig 4:2 (i).

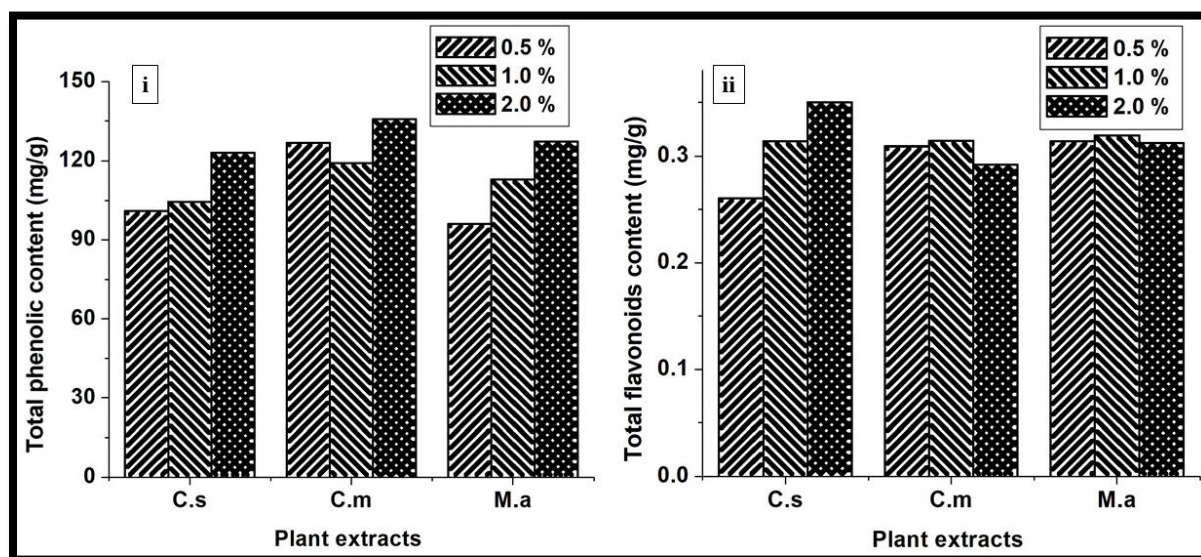


Fig 4:2 Concentration of total phenolic (i) and flavonoids (ii) content.

Key: C.s = *Camellia sinensis*, C.m = *Combretum molle*, M.a = *Melia azedarach linn*.
Concentration of plant extracts = 0.5, 1.0 and 2.0%.

The highest phenolic content was with *Combretum molle* extracts (135.81 mg/g) followed by *Camellia sinensis* (127.94 mg/g) and *Melia azedarach linn* (125.23 mg/g). The content of phenolic compounds was found to be above 20 mg/g in all extracts. This justifies the pharmacological characteristics of the three plants leaves (McGaw et al., 2001). It is of importance to mention that the method of determining the level of total phenolic compounds is not based on the absolute measurement of the amount of phenolic compounds but on the chemical reducing capacity relative

to gallic acid (Amzad Hossain and Shah, 2015), hence the total phenol and flavonoids content was calculated based on the calibration curve shown in Table 4:2.

Table 4:2 Calibration curve results

Standard	Calibration curve equation	R ²
Gallic acid	Y= 0.0008x – 0.0337	0.99810
Quercetin	Y= 0.003x + 0.0026	0.09982

The results showed that phenolic compounds were extracted from plant leaves. The presence of phenolic compounds in the extracts is essential since it supports the use of the extract as reducing and capping agent in the synthesis of metal nanoparticles because they chelate with metal ions (Iravani and Zolfaghari, 2013, Sadeghi et al., 2015). Phenols and mono-substituted phenols are hydrophilic compounds with a lower affinity towards non-polar solvents; this is the reason why high phenol content was extracted by water. The phenol content increased with an increase in the concentration of the leaves as shown in Fig 4:2 (i). Fig 4:2 (ii) shows the total flavonoid content in the aqueous extracts of *Camellia sinensis*, *Combretum molle*, and *Melia azedarach linn*. The flavonoid content was found to be 0.340 mg/g in *Camellia sinensis* and 0.300 mg/g in both *Combretum molle* and *Melia azedarach linn*. *Combretum molle* is known to have a lower concentration of flavonoids compared to phenolic compounds (Eloff et al., 2008).

4.1.2 Uv-vis spectroscopy

Spectroscopic techniques are employed for qualitative and quantitative analysis of plant extracts. In the present study, the phytochemical constituents present in the aqueous extract of *Camellia sinensis*, *Combretum molle*, and *Melia azedarach linn* leaves were also determined using Uv-Vis spectroscopy as shown in Fig 4:3 below. The presence of absorption bands in the range of 300-800 nm confirmed the presence of bioactive compounds in the plant extracts. The extracts of *Camellia sinensis*, *Combretum molle* and *Melia azedarach linn* are known to contain phenols and flavonoids. The flavonoids and terpenoids spectrum are known to have an absorption maximum in the range of 230-340 nm, the peaks that appear in this range are attributed to the presence of phenolic acids. The absorption bands in the range of 350-550 nm were attributed to derivatives of phenolic acids such as flavones and phenylpropenes. The band that appears in the range of 600-700 nm were attributed to the presence of chlorophyll.

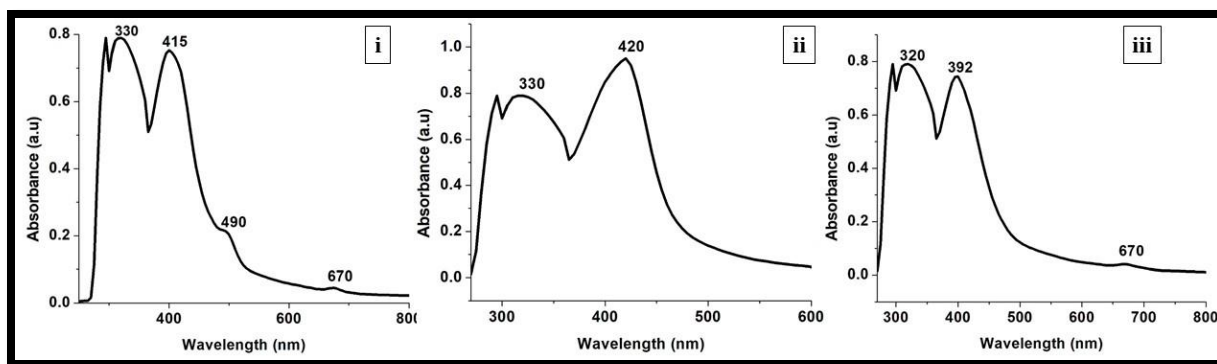


Fig 4:3 Uv-vis spectra of aqueous extract of (i) *Camellia sinensis*, (ii) *Combretum molle* and (iii) *Melia azedarach linn*.

There are several studies that have reported on the phytochemical screening of *Camellia sinensis*, *Combretum molle*, and *Melia azedarach linn* leaves. Despite all these studies it is still essential to report on the phytochemical screening of these leaves, this is because there are several factors that influence the bioactive compounds present in the plant extracts. These factors include a method of extraction, geographic location, harvest time, plant tissue and choice of solvent.

4.1.3 Fourier Infrared Spectroscopy (FTIR)

The identification of functional groups that are present in the plant extract was done using Fourier Infrared Spectroscopy (FTIR). The FTIR spectra of aqueous plant extracts are shown in Fig 4:4. As shown in figure 4:4 there are similarities between the crude leaves and the aqueous extract. *Camellia sinensis*, *Combretum molle*, and *Melia azedarach linn* leaves showed absorption peaks at 3400 cm^{-1} (-OH and N-H), 2800 cm^{-1} (-C-H), 1705 cm^{-1} (C=O), 1500 cm^{-1} (C=C) and 1050 cm^{-1} (C-O). Similar results have been reported by David et al., 2014 and Moldovan et al., 2016 in the aqueous extract of European black elderberry and *Sambucus nigra* L respectively. The presence of the hydroxyl functional group is significant since it has been established that it is an integral part of most phenolic phytochemicals such as flavonoids and tannins. Therefore, the presence of these bioactive compounds in the above-mentioned plant extracts justifies the use of plant extracts in the synthesis of metal nanoparticles through chemical reduction method. The reduction of metal ions leads to nucleation and formation of nanoparticles.

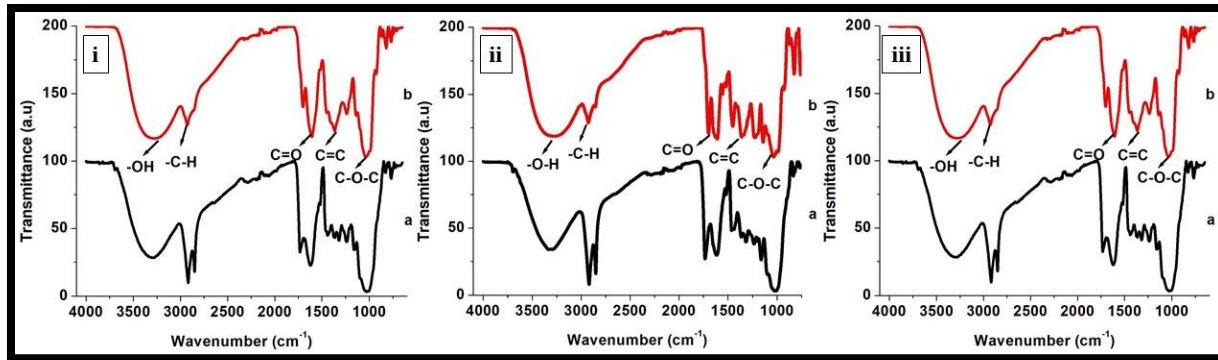


Fig 4:4 FT-IR spectra of (i) *Camellia sinensis*, (ii) *Combretum molle* and (iii) *Melia azedarach linn*. a= crude, b= aqueous extract

4.2 EFFECT OF CAPPING AGENT CONCENTRATION ON SILVER NANOPARTICLES CAPPED WITH PLANT EXTRACTS OF *CAMELLIA SINENSIS*, *COMBRETUM MOLLE*, AND *MELIA AZEDARACH LINN*.

4.2.1 Optical properties

4.2.1.1 Uv-vis absorption studies

Uv-Vis absorption spectroscopy is the commonly used method to determine the optical properties of nanoparticles; this is because the absorption bands are related to the diameters of the nanoparticles. The recorded Uv-Vis spectra of the biosynthesized silver nanoparticles are represented in Fig 4:5. The change in color of the silver solution from colorless to dark brown after addition of the plant extract indicated that the silver ions were reduced by the bioactive compounds present in the plant extract such as phenols, flavonoids, and carbohydrates. These bioactive compounds reduce silver ions by donating free electrons. Bioactive compounds from plant extracts are nucleophilic hence they are responsible for chelating with metal ions (Phull et al., 2016). The surface plasmon resonance band of silver nanoparticles approximately appeared at 425, 430 and 445 nm for *Camellia sinensis*, *Combretum molle*, and *Melia azedarach linn* capped silver nanoparticles respectively.

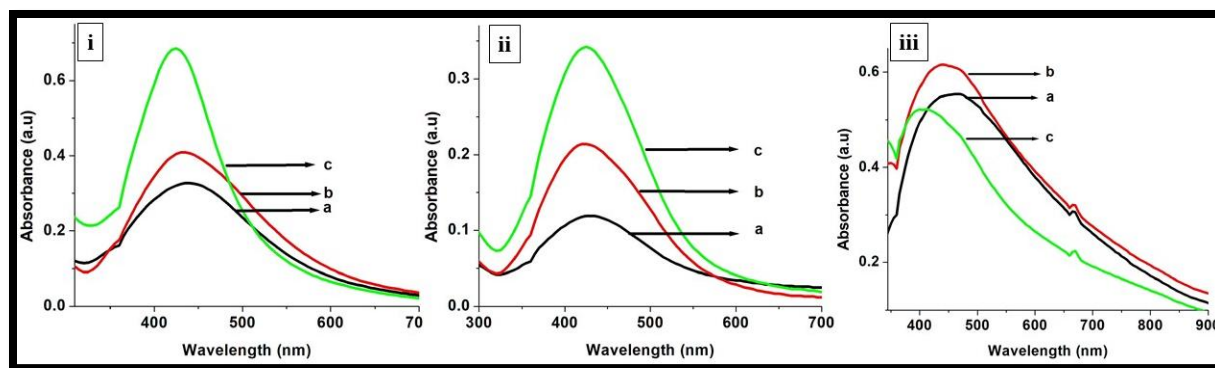


Fig 4:5 Uv-vis spectra for Ag nanoparticles capped with (i) *Camellia sinensis*, (ii) *Combretum molle* and (iii) *Melia azedarach linn* aqueous leaves extracts. $a= 0.5\%$, $b= 1.0\%$, $c= 2.0\%$ capping agent concentration.

The particles synthesized from the selected capping agent's concentration were blue shifted from the bulk silver which has a plasmon resonance band around 1000 nm. Since the absorption band is in the visible light region of 420-450 nm, it is evident that silver nanoparticles were successfully formed (Moldovan et al., 2016). It has been reported by Bhakya et al., 2015 and Krishnaraj et al., 2010 that the presence of a single surface plasmon resonance band represents particles with isotropic geometry while particles with two or more bands represent the anisotropic geometry. The presence of a single surface plasmon resonance band at 425 suggests that nanoparticles with isotropic geometry were formed. As the concentration of the capping agent was increased, a decrease in the width of the absorption band was observed as shown in Table 4:3. The obtained results are in agreement with what was obtained by Moldovan et al., 2016 in the synthesis of silver nanoparticles using *Sambucus nigra L* plant extract and Khalil et al., 2014 in the synthesis of silver nanoparticles using olive leaf extract.

Table 4:3 Effect of capping agent concentration on FWHM of silver nanoparticles

Capping molecules (%)	FWHM (nm)		
	0.5%	1.0%	2.0%
<i>Camellia sinensis</i>	175	170	115
<i>Combretum molle</i>	160	151	140
<i>Melia azedarach linn</i>	330	327	325

4.2.1.2 Photoluminescence studies

The photoluminescence properties of silver nanoparticles are shown in Fig 4:6. The nanoparticles were excited at different wavelengths as obtained in the Uv-Vis absorption bands; the excitation wavelengths were 425, 430 and 445 nm for *Camellia sinensis*, *Combretum molle* and *Melia azedarach linn* respectively. *Camellia sinensis*, *Combretum molle*, and *Melia azedarach linn* capped silver nanoparticles were found to an emission peak at 460 nm. It is observed that the emission wavelength is independent to the particles size since all concentrations gave the same wavelength. The emission peak showed a typical red shift from the absorption peaks. This is attributed to the excitation of electrons from occupied d bands into states above Fermi level (Zhao et al., 2006, Ajitha, 2013).

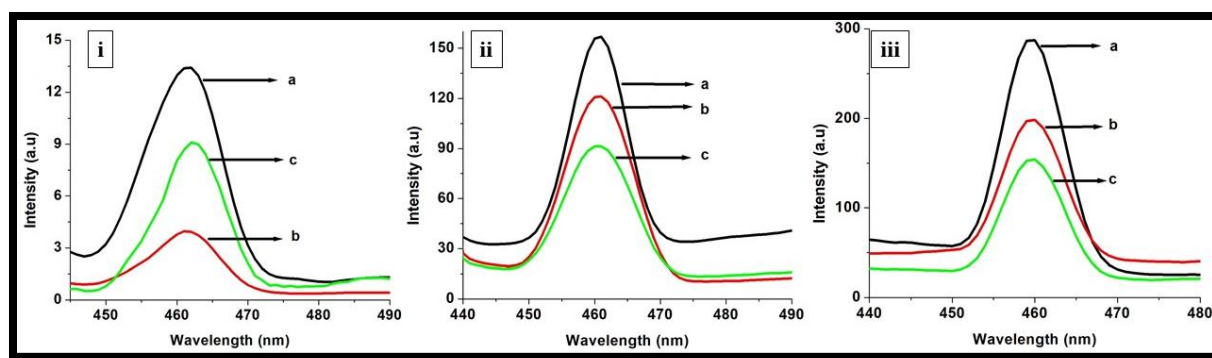


Fig 4:6 PL spectra for Ag nanoparticles capped with (i) *Camellia sinensis*, (ii) *Combretum molle* and (iii) *Melia azedarach linn* aqueous leaves extracts. *a* = 0.5%, *b* = 1.0%, *c* = 2.0% capping agent concentration.

4.2.2 Interaction of silver nanoparticles with plant extracts

4.2.2.1 FTIR analysis

FTIR spectroscopy was also used to understand the possible functional groups of the bioactive compounds that are present in the aqueous solution of *Combretum molle*, *Camellia sinensis* and *Melia azedarach linn* leaves and their role in the reduction of Ag^+ ions to stable nanoparticles. Fig 4:7 shows the FTIR spectra of aqueous extract of the three selected plants leaves and capped silver nanoparticles. The peak at 3325 cm^{-1} due to (-OH stretching, alcohol), 2899 cm^{-1} is attributed to (C-H asymmetric stretch, aromatic), 1609 cm^{-1} is due to (C=O, carbonyl), 1510 cm^{-1} (C=C symmetric stretch, aromatic), 1430 cm^{-1} (C=C asymmetric stretch, aromatic) and 1029 cm^{-1} (-C-O-C stretching). The presence of organic functional groups on the surface of the synthesized silver

nanoparticles showed that the particles were successfully capped with plant extracts through the strong affinity of their bioactive compounds to allow for reduction of silver ions to metallic silver.

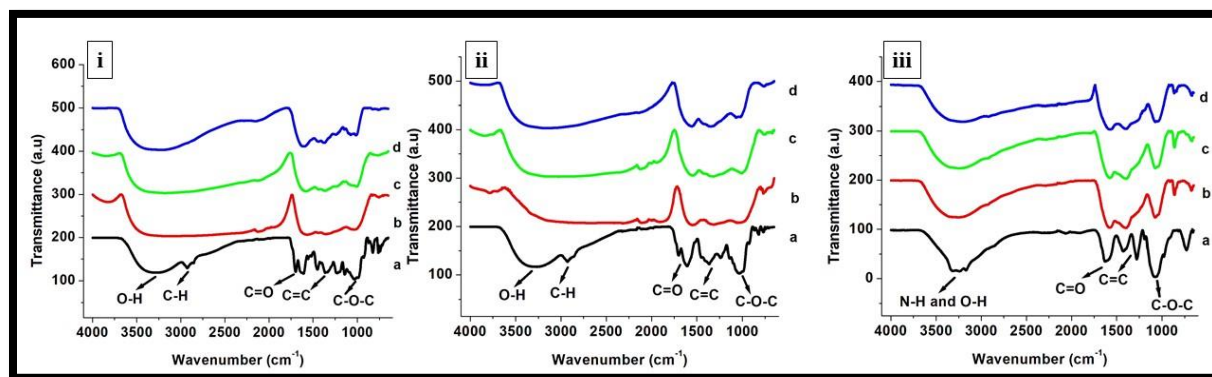


Fig 4:7 FTIR spectra for Ag nanoparticles capped with (i) *Camellia sinensis*, *Combretum molle* and (iii) *Melia azedarach linn* aqueous leaves extracts *a*= aqueous extract, *b*= 0.5%, *c*=1.0%, *d*=2.0%

Bioactive compounds such as phenolic compounds are responsible for capping the synthesized particles. This postulation is supported by the change in the peak position of the hydroxyl group for *Camellia sinensis* and *Combretum molle* capped silver nanoparticles. *Melia azedarach linn* was found to be different from the other two plants since from the FTIR spectra the presence of N-H and O-H functional groups is observed at 3272 cm^{-1} . Therefore, *Melia azedarach linn* aqueous extracts interact with silver ions using the nitrogen atom rather than the oxygen atom. This is due to the difference in electronegativity between the O and N atom. Hence a more pronounced hydroxyl functional group is observed on the surface of the particles. The presence of the hydroxyl functional group on the surface of the 2% capped silver nanoparticles for both *Combretum molle*, and *Camellia sinensis* might be due to adsorbed moisture during the drying of the particles.

4.2.2.2 Reaction pathway

The overall reaction mechanism for the synthesis of silver nanoparticles capped with phenolic compounds is represented in figure 4:8. Since aqueous extracts of different plant materials contain a wide range of bioactive compounds such as tannins and carbohydrates. There are several mechanisms that are proposed for the bio-reduction and subsequent stabilization of silver

nanoparticles.

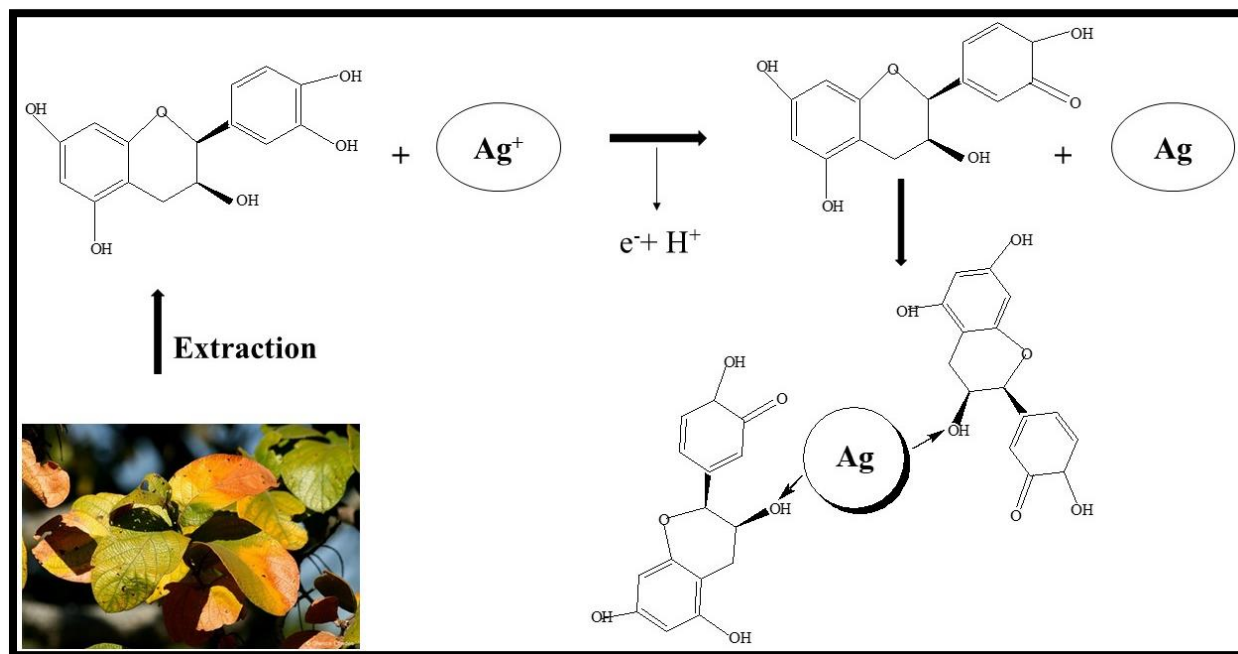


Fig 4:8 Proposed interaction of silver ions with plant extracts

The first mechanism involves the phenolic compounds in plants. Plant extracts are known to be rich in polyphenols. Thus the addition of bioactive compounds such as polyphenols created the free metallic silver atoms by reduction of silver ions. The resulting silver atoms accumulated into oligomeric clusters which later formed silver nanoparticles as confirmed by Uv-Vis spectroscopy, FTIR spectroscopy, and transmission electron microscopy. The second mechanism is based on the reduction of silver ions by proteins; this has been reported to be due to the electrostatic interaction between the protein and silver ions since proteins trap silver ions on to their surface (Rajeshkumar and Bharath, 2017). Therefore, proteins reduce the silver ions, leading to secondary structure change and formation of silver nuclei.

4.2.3 X-ray diffraction analysis

The XRD pattern of the synthesized silver nanoparticles is shown in Fig 4:9. The four distinct peaks at 38, 44, 64 and 77 are assigned to 111, 200, 220 and 311 planes of silver face-centered cubic phase (JCPDS file No 00-004-0783). The most intense diffraction peak at $2\theta = 38^\circ$ from the (111) lattice plane indicates that the silver nanoparticles might have the top basal plane with (111) facets. This observation is important for biological application of silver nanoparticles because it

suggests that smaller particles also have high atomic density (111) facets (Raza et al., 2016). The peaks that are observed in the range of 20-35° are attributed to organic compounds that are present on the surface of the particles. The average particle size as calculated by the Debye-Scherrer equation is presented in table 4:4. The broadness of the peaks indicates that the amorphous silver nanoparticles were synthesized. A decrease in particle size with an increase in capping agent concentration is observed. However this not the case with 2% *Combretum molle* capped silver nanoparticles. This is attributed to ripening effects.

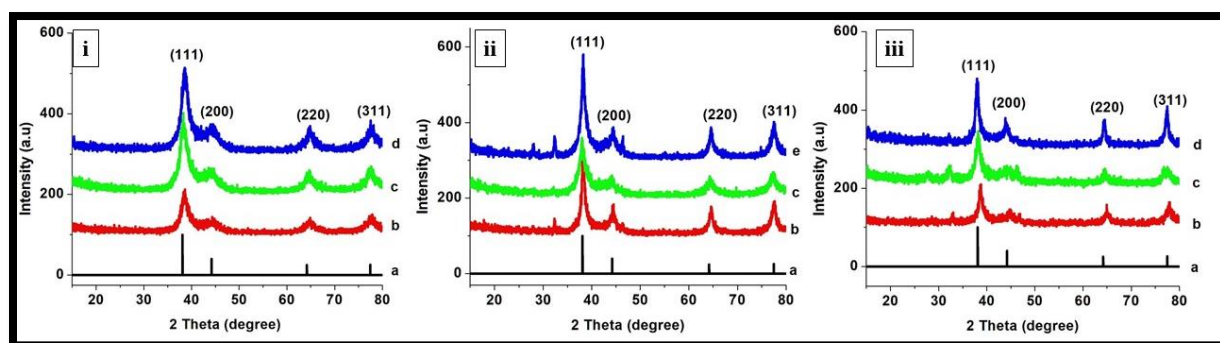


Fig 4:9 XRD micrographs for Ag nanoparticles capped with (i) *Camellia sinensis*, (ii) *Combretum molle* and (iii) *Melia azedarach linn* aqueous leaves extracts. *a*= Reference spectrum, *b*= 0.5%, *c*= 1.0% *d*= 2.0%

Table 4:4 Relationship between average particle sizes estimated using Debye-Scherrer equation and capping agent concentration

	Particle sizes (nm) for various percentages of capping agents		
Concentration	0.5%	1.0%	2.0%
Ag- <i>Camellia sinensis</i>	5.20	4.30	4.20
Ag- <i>Combretum molle</i>	4.68	2.02	5.77
Ag- <i>Melia azedarach linn</i>	8.20	7.39	1.11

4.2.4 Transmission electron microscopy (TEM) analysis

The transmission electron microscopy (TEM) micrographs and corresponding histograms of silver nanoparticles capped with *Camellia sinensis*, *Combretum molle* and *Melia azedarach linn* aqueous extracts are shown in Fig: 4:10, 4:11 and 4:12 respectively. The average particle sizes are presented

in Table 4:5. There is a decrease in particle size with an increase in capping agent concentration. The changes in particles size can be related to changes in particle formation and growth processes which are affected by the capping agent concentration.

Table 4:5 Relationship between average particle size from TEM and capping agent concentration

Concentration (%)	Particle sizes (nm)		
	0.5%	1.0%	2.0%
<i>Camellia sinensis</i>	23	10	4
<i>Combretum molle</i>	9	8	5
<i>Melia azedarach</i>	8	7	3

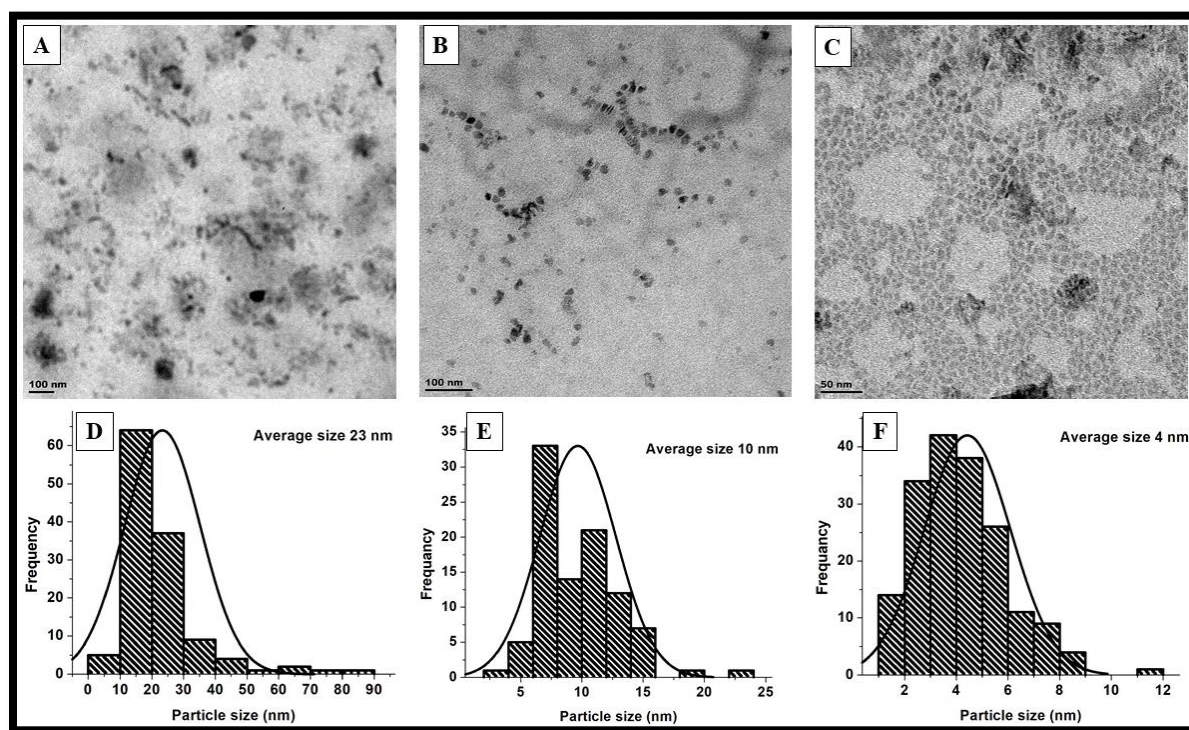


Fig 4:10 TEM micrographs of silver nanoparticles capped with (a) 0.5%, (b) 1% and (c) 2% *Camellia sinensis* leaves and the corresponding histograms (d, e and f)

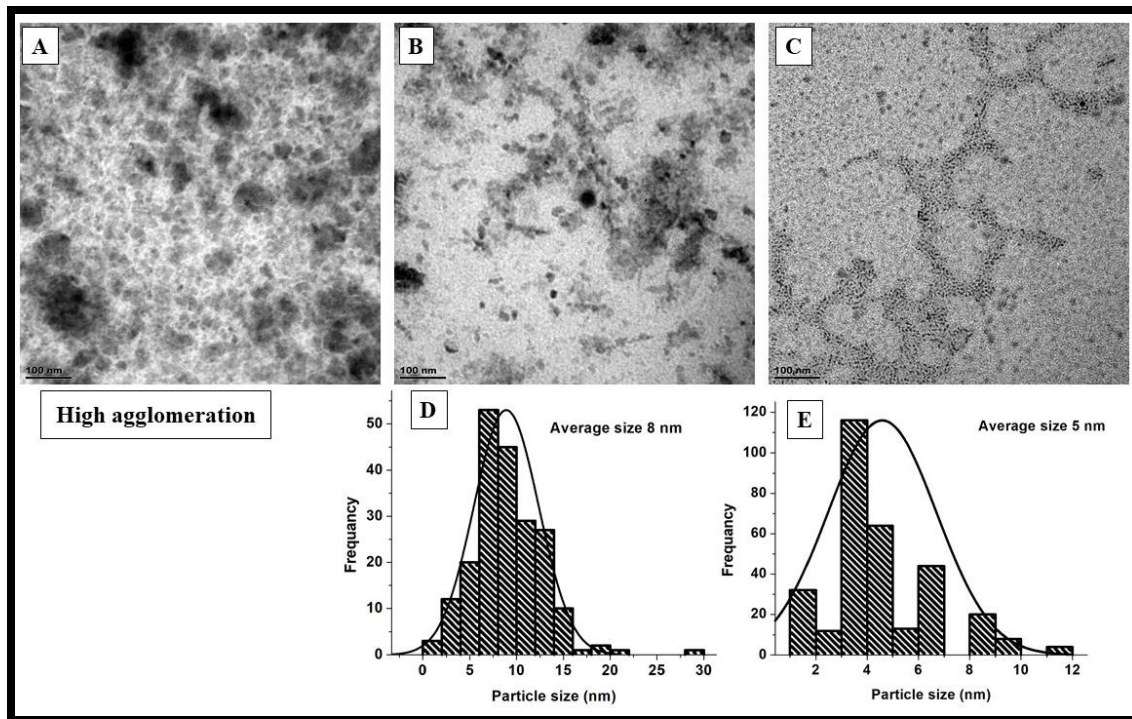


Fig 4:11 TEM micrographs of silver nanoparticles capped with (a) 0.5%, (b) 1% and (c) 2% *Combretum molle* leaves and the corresponding histograms (d and e).

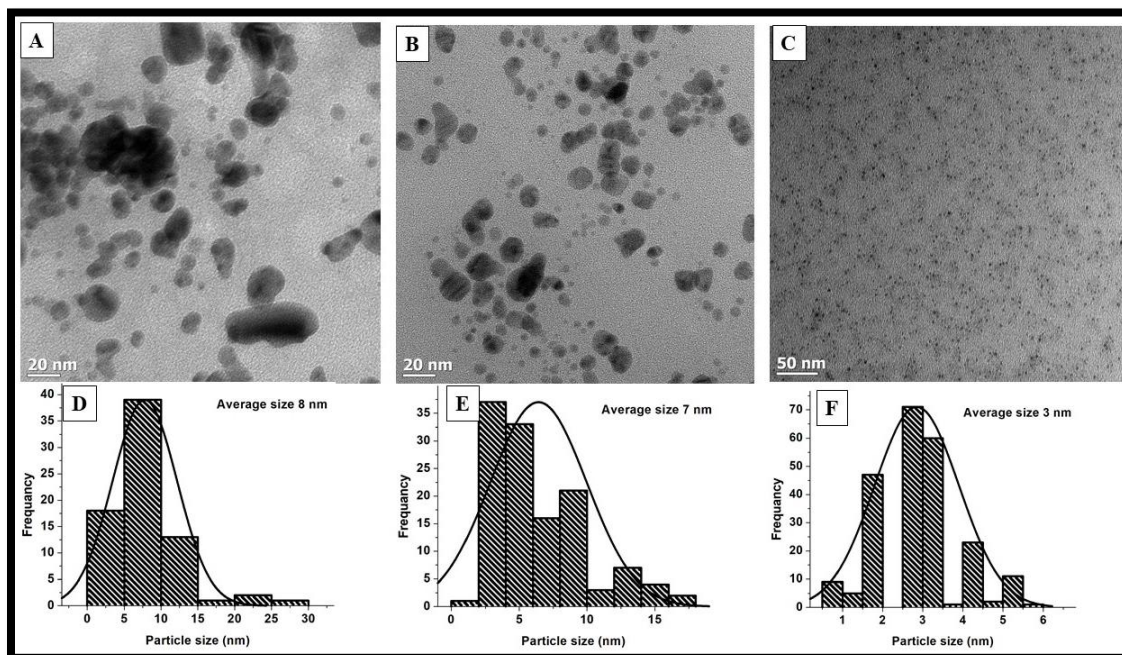


Fig 4:12 TEM micrographs of silver nanoparticles capped with (a) 0.5%, (b) 1% and (c) 2% *Melia azedarach linn* leaves and the corresponding histograms (d, e and f).

At small concentration (0.5%) of the capping agent, a mixture of spherical and belt-like structures were obtained for *Camellia sinensis*, agglomerated particles with undefined shapes were observed for *Combretum molle*, and *Melia azedarach* capped silver nanoparticles. This could be attributed to the insufficient amount of the capping agent, as a result particles agglomerated easily since the protective layer could not be formed completely. A general trend was observed for all the silver nanoparticles that were prepared at 1% capping agent concentration, a decrease in particle size with less agglomeration was observed. This might be due to the formation of the protective layer on the surface of the nanoparticles. The protective layer that is formed by the adsorption on the capping agent on the surface of the particles increases the steric hindrance effect, therefore, less agglomeration is observed. At 2% capping agent concentration, a decrease in nanoparticle size was observed, and the shape of the nanoparticle was mostly spherical. This could be influenced by many factors such as the number of nuclei formed at a given time, which favors a fast, autocatalytic growth thus giving rise to a large number of small particles. An increase in capping agent concentration also affects the distribution of the particles. At low concentration, a wide range is obtained, and at a high concentration, a narrow distribution is obtained.

4.2.5 Biological application

4.2.5.1 Antibacterial activity

To investigate the antibacterial activity of the synthesized silver nanoparticles, four bacterial strains (*Enterococcus faecalis* (*E.f*), *Staphylococcus aureus* (*S.a*), *Pseudomonas aeruginosa* (*P.a*) and *Klebsiella pneumonia* (*K.p*)) were selected. *Staphylococcus aureus* and *Enterococcus faecalis* are both gram-positive bacteria which belong to the bacterial family *Staphylococcaceae* and *Enterococcaceae* respectively. *Staphylococcus aureus* is mostly associated with skin infections, and it is resistant to several types of antibiotics, which include all antibiotics that are related to penicillin (Ansari et al., 2014). *Enterococcus faecalis* is mostly known to cause urinary tract and wound infections. *Pseudomonas aeruginosa* and *Klebsiella pneumonia* are gram-negative bacteria that are commonly associated with urinary tract and bloodstream infections.

The minimum inhibitory concentrations (MIC) of *Camellia sinensis*, *Combretum molle*, and *Melia azedarach* capped silver nanoparticles are presented in Fig 4:13. All the prepared silver nanoparticles were found to be active against bacterial strains of *Enterococcus faecalis* (*E.f*),

Staphylococcus aureus (*S.a*), *Pseudomonas aeruginosa* (*P.a*) and *Klebsiella pneumoniae* (*K.p*) but the activity was found to be dependent on the size, shape, and degree of agglomeration, this could be due to that different morphologies provides different areas to interact with the bacteria. The increase in antibacterial activity with a decrease in particle size can be attributed to the maximum reactivity of small particles since they have a high surface to volume ratio compared to larger particles (Xiu et al., 2012, Pal et al., 2007). The antibacterial activity of silver nanoparticles is also reported in the literature to be from the oligodynamic effect.

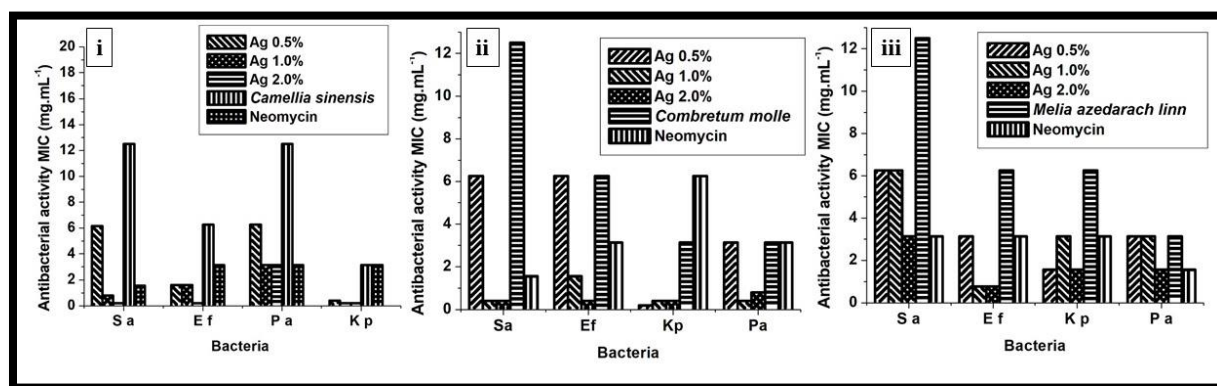


Fig 4:13 Antibacterial activity of silver nanoparticles capped with (i) *Camellia sinensis*, (ii) *Combretum molle* and (iii) *Melia azedarach linn*. *S.a* = *Staphylococcus aureus*, *E.f* = *Enterococcus faecalis*, *P.a* = *Pseudomonas aeruginosa*, *K.a* = *Klebsiella pneumoniae*

The synthesized silver nanoparticles were found to have more antibacterial activity than *Camellia sinensis*, *Combretum molle*, *Melia azedarach linn* and neomycin alone with a MIC of 0.2 mg/g for both gram positive and gram-negative bacteria. This is due to their high surface to volume ratio and an increase in surface atoms. Additionally, the presence of organic functional groups on the surface of the synthesized particles as confirmed by FTIR results in Fig 4:7 enhanced the antibacterial activity. The antibacterial activity of the plant extract may be due to the presence of tannins, proteins, flavonoids, phenols, and glycosides (de Morais Lima et al., 2012). The mechanism of action for plant extract has been reported to be due to the ability of bioactive compounds to complex with soluble proteins and bacterial cell wall (Poojary et al., 2015). Since the bioactive compounds such as flavonoids are more hydrophilic, they disrupt the cell membrane of the bacteria thus this lead to bacterial death. As shown in Fig 4:13, the synthesized silver nanoparticles were found to inhibit the growth of both gram positive and gram negative bacteria

strains. They were found to be more active against gram-negative bacteria this is due to the difference in membrane structure and composition of the cell wall. Gram-negative bacterial contain a single peptidoglycan layer, and gram-positive bacteria contain several peptidoglycan layers (Sharma et al., 2009).

Several mechanisms have been suggested for the interaction of silver with microorganisms. It is likely that the silver ions penetrate the cell membrane and interact with the nucleus, inside the bacteria silver nanoparticles being soft acids probably interact with soft bases such as sulfur and phosphorus-containing complexes like the DNA, this lead to cell death (Raza et al., 2016). It is also reported that when silver nanoparticles interact with the bacteria, silver ions are released. The released ions attack the negatively charged cell walls of the bacteria and deactivate cellular enzymes as a result the membrane permeability is disturbed thus cell death occurs.

4.2.5.2 Antifungal activity

The antifungal activity of silver nanoparticles was investigated against *Candida albicans* and *Cryptococcus neoformans* as shown in Fig 4:14. *Candida albicans* causes *Candidiasis moniliasis*, and *Cryptococcus neoformans* usually infects the lungs and central nervous system. The synthesized silver nanoparticles were found to be active against both the tested fungal strains with a MIC of 0.2 mg/ml. The high activity of nanoparticles against fungal strains compared to bacterial strains is due to particle size and composition of the microorganism. Bacteria species are prokaryotic cells; they contain a tight-knit molecular complex composed of chains of amino sugars connected by peptide linkages, while on the other hand fungi species are eukaryotic cells. This means that fungal strains do not have the peptidoglycan and their cytoplasmic membrane is not protected as a result small particles penetrate easily and disturb the activities of the cell.

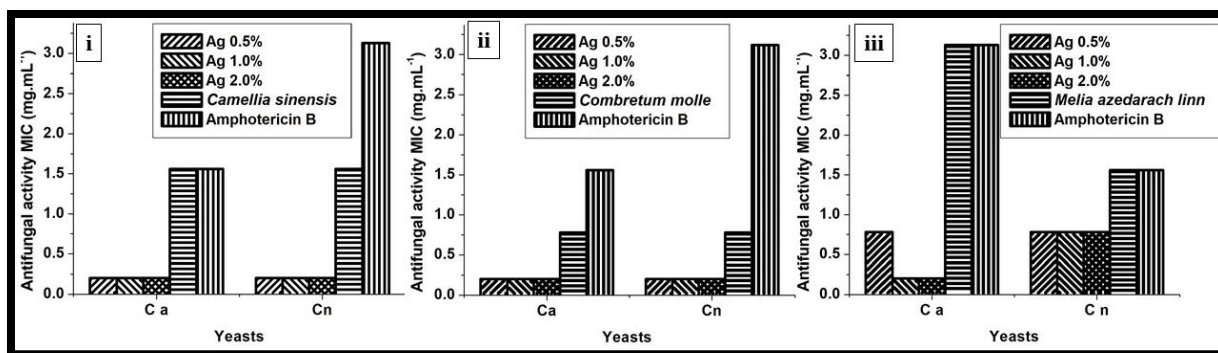


Fig 4:14 Antifungal activity of silver nanoparticles capped with (i) *Camellia sinensis*, (ii) *Combretum molle* and (iii) *Melia azedarach linn*. C.a = *Candida albicans*, C.n = *Cryptococcus neoformans*.

It is also observed in Fig 4:14 that *Camellia sinensis*, *Combretum molle*, and *Melia azedarach linn* have antifungal activity however silver nanoparticles were found to be more active than these capping agents. It is therefore proposed that the low minimum inhibitory concentration results from the synergistic effect of both silver nanoparticles and the functional groups that are present on the surface of the particles as confirmed by FTIR spectra in Fig 4:7. Silver nanoparticles showed high antifungal activity compared to amphotericin B; this is due to their mechanism of action. Amphotericin B forms transmembrane pores by binding to membrane sterols; this leads to the leakage of cell constituents thus cell death occurs (Kim et al., 2009). The mode of action for silver nanoparticles has been reported to be size dependent. The electrostatic attraction between the negatively charged cell membrane of the fungi and the positively charged nanoparticles is crucial for the antifungal activity of silver nanoparticles. Silver nanoparticles with the large surface areas can easily form silver ions; these ions, therefore, bind with the thiol functional group of the proteins thus protein denaturation occurs (Kim et al., 2009, Panacek et al., 2009). Also due to their small size, silver nanoparticles may attach to the cell surface and get into the cell directly without damaging the cell wall and causes cell death by interacting with organelles such as mitochondria and ribosomes (Xia et al., 2016).

4.2.5.3 Antioxidant activity

2,2-diphenyl-1-picrylhydrazyl. (DPPH) is a stable nitrogen-centered free radical with low deterioration rate and low reactivity towards most compounds. Upon reacting with an antioxidant,

it changes the color from violet to yellow as shown in Fig 4:15. An antioxidant is a substance that when present at a low concentration compared to the oxidizable substrate delay or inhibit the oxidation of the substrate (Moldovan et al., 2016).

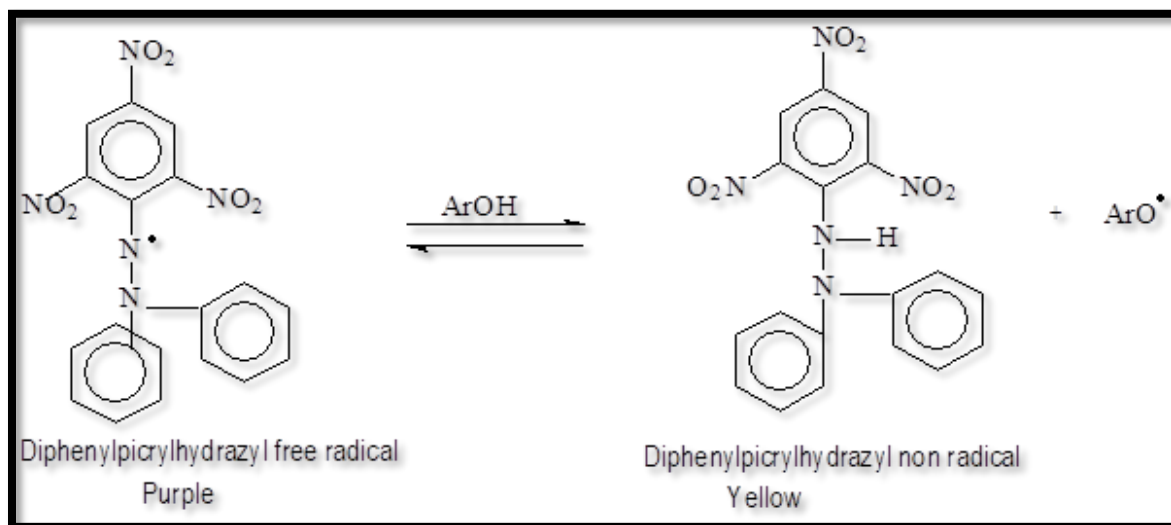


Fig 4:15 Free radical scavenging process.

The antioxidant activity of capped silver nanoparticles, *Camellia sinensis*, *Combretum molle* and *Melia azedarach* against DPPH was investigated as shown in Fig 4:16. Ascorbic acid was used as positive control. DPPH is widely used for measurements of antioxidants because it is less responsive to side reactions. The antioxidant property was found to be high in ascorbic acid (90%) and aqueous extracts (86%). The least active samples were found to be silver nanoparticles (54%). This trend may be because the bioactive compounds that are present in the aqueous extracts possess redox properties, which allow them to act as reducing agents, hydrogen donors and singlet oxygen quenchers (Reddy et al., 2014). Polyphenols are the major bioactive compounds that contribute to the antioxidant activity of plant extracts; this is due to the reactivity of the phenol moiety. The antioxidant property of silver nanoparticles may be attributed to the presence of organic functional groups on the surface of the synthesized particles (Ravichandran et al., 2016, Markus et al., 2017). The antioxidant activity was found to increase with an increase in the concentration of silver nanoparticles thus revealing its dosage-dependent nature (Bhakya et al., 2015). The dosage-dependent nature of DPPH was also reported by Prasad et al., 2016.

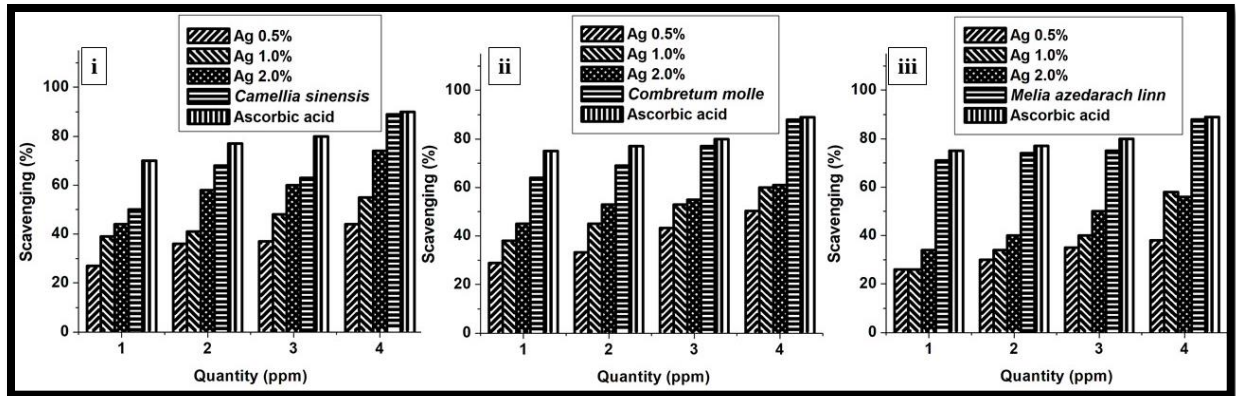


Fig 4:16 Antioxidant activity of silver nanoparticles capped with (i) *Camellia sinensis*, (ii) *Combretum molle* and (iii) *Melia azedarach linn*.

4.3 EFFECT OF CAPPING AGENT CONCENTRATION ON SILVER NANOPARTICLES CAPPED WITH CHITOSAN

4.3.1 Optical properties

4.3.1.1 Uv-vis absorption and photoluminescence studies

To investigate the effect of polymeric capping agent on the optical properties of silver nanoparticles absorption spectroscopy was done on chitosan- capped silver nanoparticles as shown by the spectra in Fig 4:17. Chitosan capped silver nanoparticles were prepared at 0.5, 1.0 and 2.0 % (w/v) of chitosan with constant silver precursor concentration of 0.1 M. Absorption peaks approximately at 385, 380 and 400 nm were obtained for 0.5, 1.0 and 2% (w/v), respectively with significant blue shifts from the bulk silver (plasma resonance around 1000 nm). Table 4:6 shows a decrease in full width at half maximum (FWHM) with an increase in capping agent concentration as also reported by Praveenkumar et al., 2014 and Zain et al., 2014. This can be attributed to quantum confinement effect.

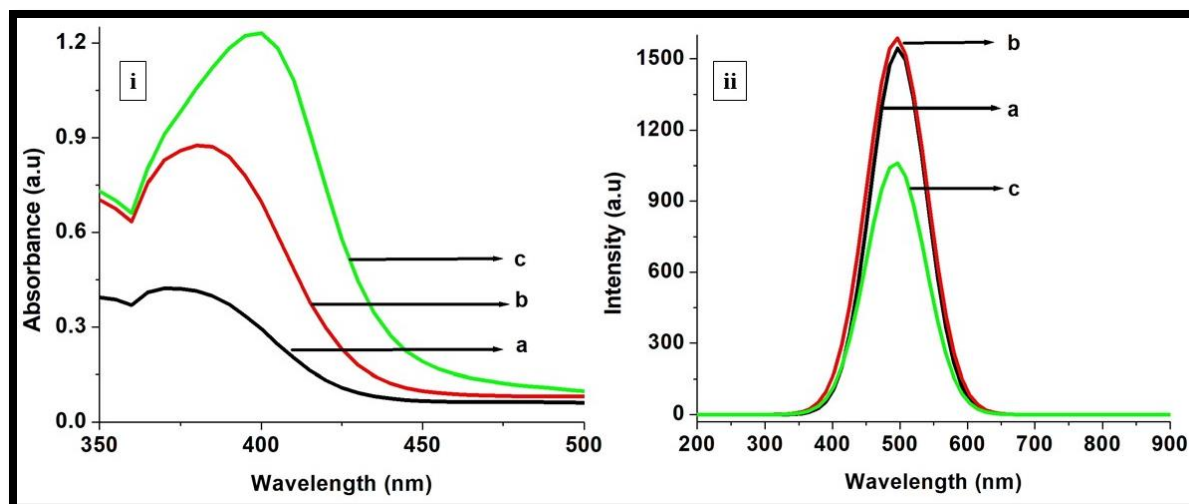


Fig 4:17 UV-vis (i) and PL (ii) spectra of chitosan capped silver nanoparticles. $a= 0.5\%$ $b= 1.0\%$ $c=2.0\%$ capping agent concentration.

Table 4:6 Effect of capping agent concentration on FWHM of silver nanoparticles based on UV-vis spectroscopy results

Capping molecules (%)	FWHM (nm)		
	0.5%	1.0%	2.0%
Chitosan	195	190	60

The photoluminescence (PL) spectra of synthesized silver nanoparticles are shown in Fig 4:17. Chitosan capped silver nanoparticles were excited at 400 nm and gave emission maxima at 500 nm for all the concentrations. The PL peaks showed a typical red shift from the absorption peaks; this is attributed to the excitation of electrons from occupied d bands into states above Fermi level (Zhao et al., 2006, Ajitha, 2013). As the concentration of chitosan was increased the peak broadness decreased. This may be due to the decrease in particle size or size distribution.

4.3.2 Interaction of silver nanoparticles with chitosan

4.3.2.1 FTIR spectral analysis

The FTIR spectral analysis was conducted to determine the molecular interaction between chitosan and silver nanoparticles and the FTIR spectra were recorded as shown in Fig 4:18. The presence

of bands at 3327 cm^{-1} (N-H and O-H stretching), 1600 cm^{-1} (NH_2 bending) and 1037 cm^{-1} (C-O-C stretching) were observed in pure chitosan. The FTIR spectra of chitosan capped silver nanoparticles (Figure 4:18 (b-d)) gave a broader peak at 3327 cm^{-1} which is indicative of more prevalence of O-H group as the N-H group is involved in binding to the silver metal. Generally, both the O-H and N-H functional groups have a strong affinity towards silver ions. The difference in electronegativity between O and N atoms plays an important role as it dictates the deprotonation site which can favor the binding of free electrons to the metal. The presence of these functional groups on the surface of the synthesized silver nanoparticles and the disappearance of the NH_2 double spike peak indicates that the nanoparticles were successfully capped by the polymer.

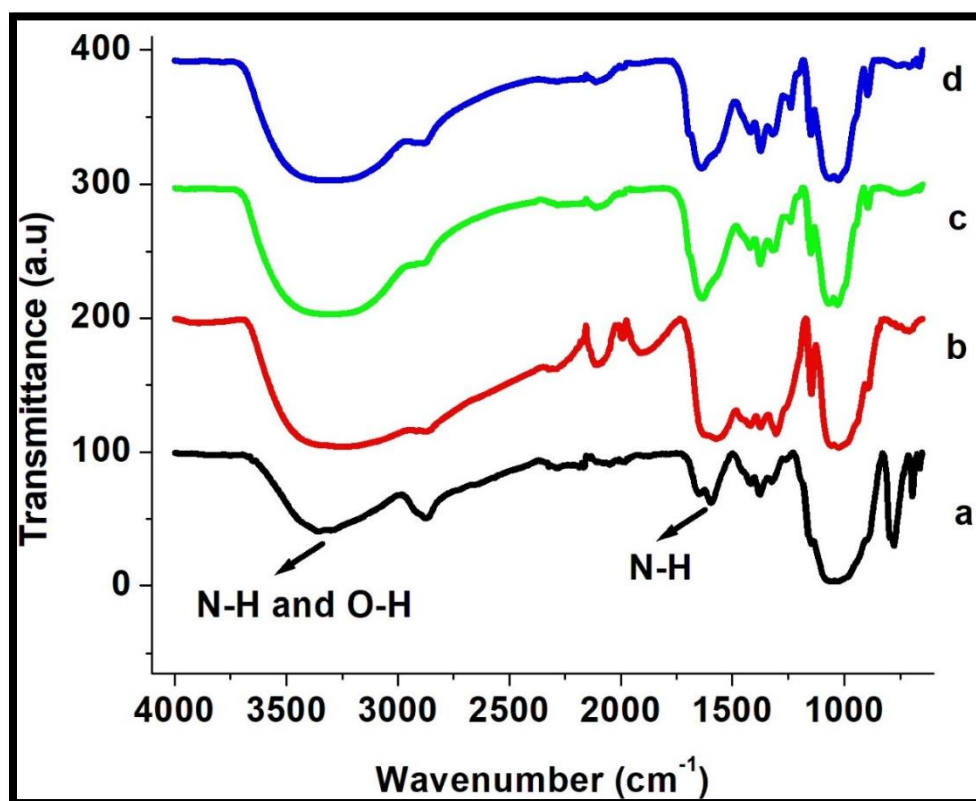


Fig 4:18 FTIR spectra of chitosan capped silver nanoparticles. *a= pure chitosan b= 0.5% c=1.0% d=2.0% capping agent concentration.*

4.3.2.2 Reaction pathway

Fig 4:19 shows the mechanism for the formation of silver nanoparticles. The formation of Ag^+ chitosan complex in the mixture of chitosan and silver nitrate enables the metal ion reduction through the amino group. The amino group of chitosan also acts as coordination sites for the release

of the metal ion (Muthukrishnan, 2015), hence it is responsible for the nucleation process in the formation of chitosan capped silver nanoparticles. Since the diffusion of Ag^+ is restricted by the polymer network, chitosan plays a crucial role as polymeric capping agent in the synthesis of silver nanoparticles.

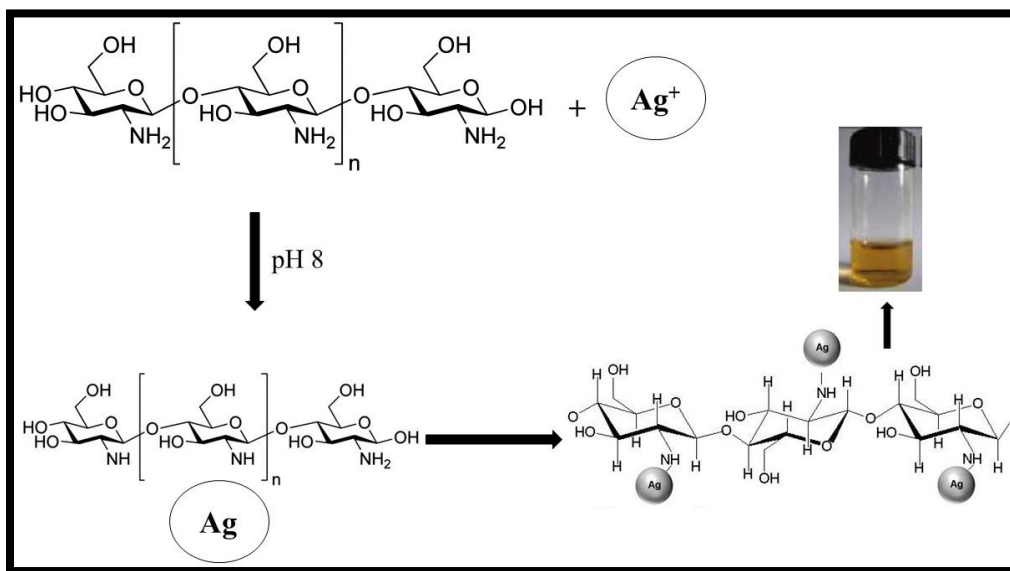


Fig 4:19 Proposed interaction of silver ions with chitosan.

4.3.3 X-ray diffraction analysis

The XRD pattern of the synthesized chitosan capped silver nanoparticles is shown in Fig 4:20. The peak at $2\theta = 22^\circ$ is due to chitosan having the cellulose structure which can possess α -type or β -type characteristic peak around that 2θ (Muthukrishnan, 2015, Ali et al., 2011). The characteristic peak of chitosan also confirms that the synthesized particles have some organic layer on their surface, this was also supported by the results from the FTIR spectra. The peaks at 2θ values of 38.5 , 44 , 64 and 77° are respectively assigned to 111, 200, 220 and 311 planes of silver face centered cubic (JCPDS file No 00-004-0783). The sharpness of these peaks indicates that the synthesized particles are highly crystalline. High crystalline particles mean that the particles were able to pack easily into an ordered structure. According to the Debye-Scherrer equation the particle size was calculated to be 9, 14, 10 nm for 0.5, 1.0 and 2.0% respectively. The most intensive peak located at $2\theta = 38.5^\circ$ corresponds to the diffraction of spherical nanoparticles crystallized in the Face centered cubic structure with basal (111) lattice plan (Raza et al., 2016). There are no peaks

of impurities such as silver oxide that were observed. This results thus confirm the reducing power of chitosan and the stabilization of the synthesized silver nanoparticles.

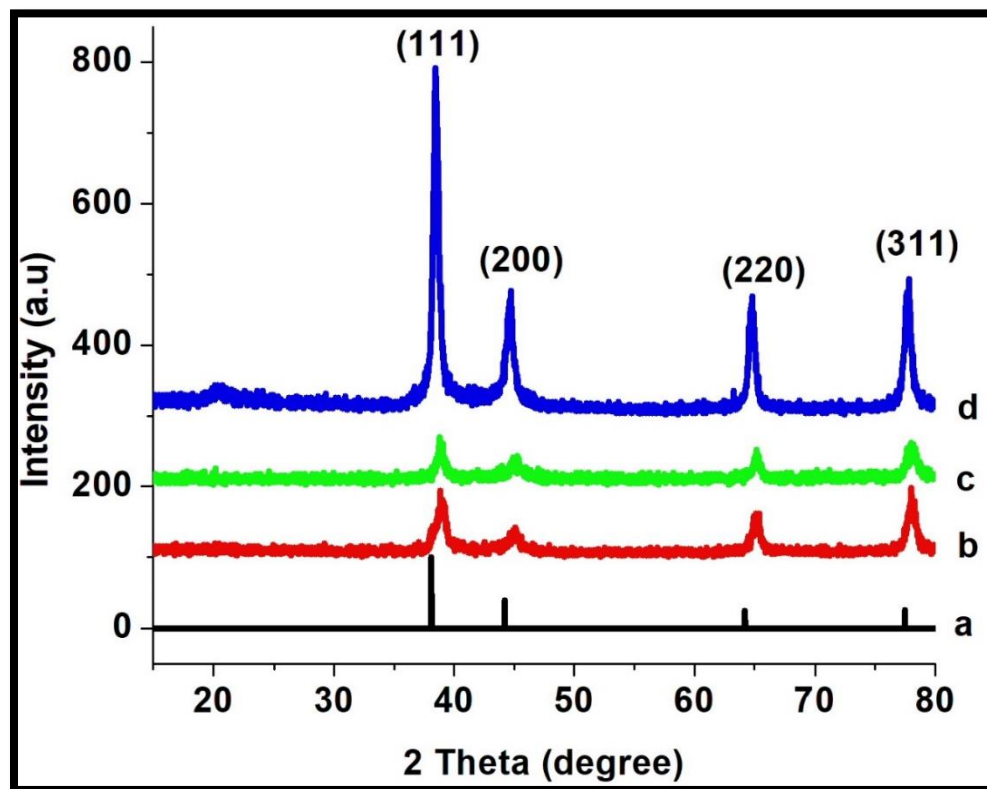


Fig 4:20 XRD micrographs of chitosan capped silver nanoparticles. *a = Reference b= 0.5 % c=1.0% and d=2.0 % capping agent concentration*

4.3.4 Transmission electron microscopy analysis

TEM analysis was conducted to study the morphology of synthesized silver nanoparticles. TEM images of synthesized Ag nanoparticles capped with chitosan are shown in Fig 4:21. The particles were formed in spherical-like shapes, and their sizes were different according to the concentration of chitosan. The particle size distribution gave average sizes of 2 ± 0.82 and 7 ± 2.69 nm for 1.0 and 2.0 % respectively. The 0.5% chitosan gave a large amorphous feature, and the nanoparticles could not be detected. This may signify incomplete growth and nucleation in this particular sample although the bulk properties could be detected by other characterization tools. This confirms that the amount of chitosan influences the size of the synthesized particles. The particle size increased as the capping agent concentration was lowered from 1% to 2%. It was expected that the particle size would decrease with an increase in capping agent since the reaction rate increase with an increase in capping agent concentration but in the current study, the slight increase in particle size

may be due to ripening effect. A similar trend is also supported by the UV-Vis spectra of the synthesized silver nanoparticles since the plasmon resonance band was found to be at a higher wavelength with an increase in capping agent concentration.

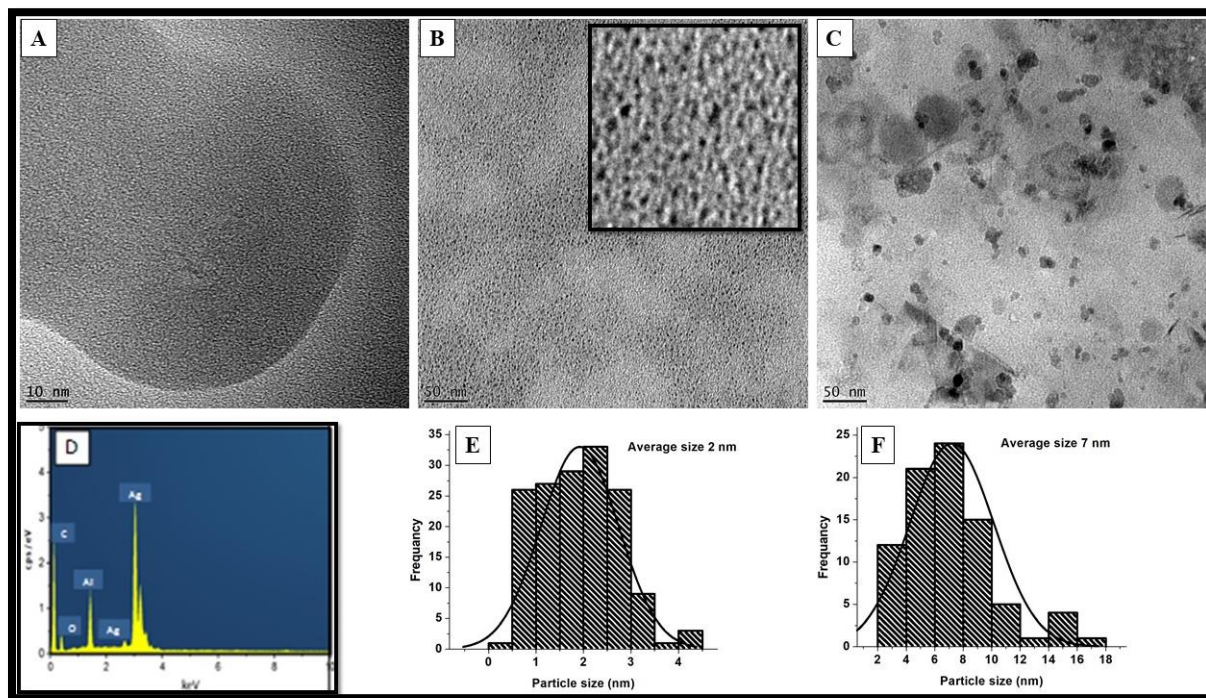


Fig 4:21 TEM micrographs of silver nanoparticles with (a) 0.5%, (b) 1% and (c) 2% chitosan and the corresponding histograms (e and f).

The elemental composition of the synthesized nanoparticles was studied using EDS, and the typical EDX spectrum of synthesised 0.5% chitosan capped silver nanoparticles is shown in Fig 4:21 (d). The presence of the silver peaks in the range of 2.4-3.2 KeV indicates that the synthesized nanoparticles contain silver. The carbon and oxygen signals may be due to chitosan that surrounds the silver nanoparticles. The carbon peak may also be due to the carbon tape. The observed aluminum peak may be due to impurities introduced during the electron microscopic sample preparation process. Aluminium peak impurities were also reported by Ajitha, 2013.

4.3.5 Biological applications

4.3.5.1 Antibacterial activity

The antibacterial activity of 0.5%, 1% and 2% chitosan-capped silver nanoparticles was investigated against the gram-positive and gram-negative bacteria Fig 4:22. The bactericidal

effects on gram-positive *Enterococcus faecalis* (E.f) showed the MIC values of 6.25, 0.4 and 1.56 mg.mL⁻¹ when using 0.5%, 1% and 2% chitosan capped silver nanoparticles respectively. For *Staphylococcus aureus* (S.a) the activity was found to be 6.25, 1.56 and 6.25 for 0.5%, 1% and 2% chitosan capped silver nanoparticles respectively. For the gram-negative bacteria, the exposure of *Pseudomonas aeruginosa* (P.a) and *Klebsiella pneumonia* (K.p) to 0.5%, 1% and 2% chitosan capped Ag nanoparticles gave the MIC values of 0.78, 1.56, 1.56 mg.mL⁻¹ respectively and 3.12, 0.2 and 1.58 mg.mL⁻¹ respectively for *Klebsiella pneumonia* (K.p).

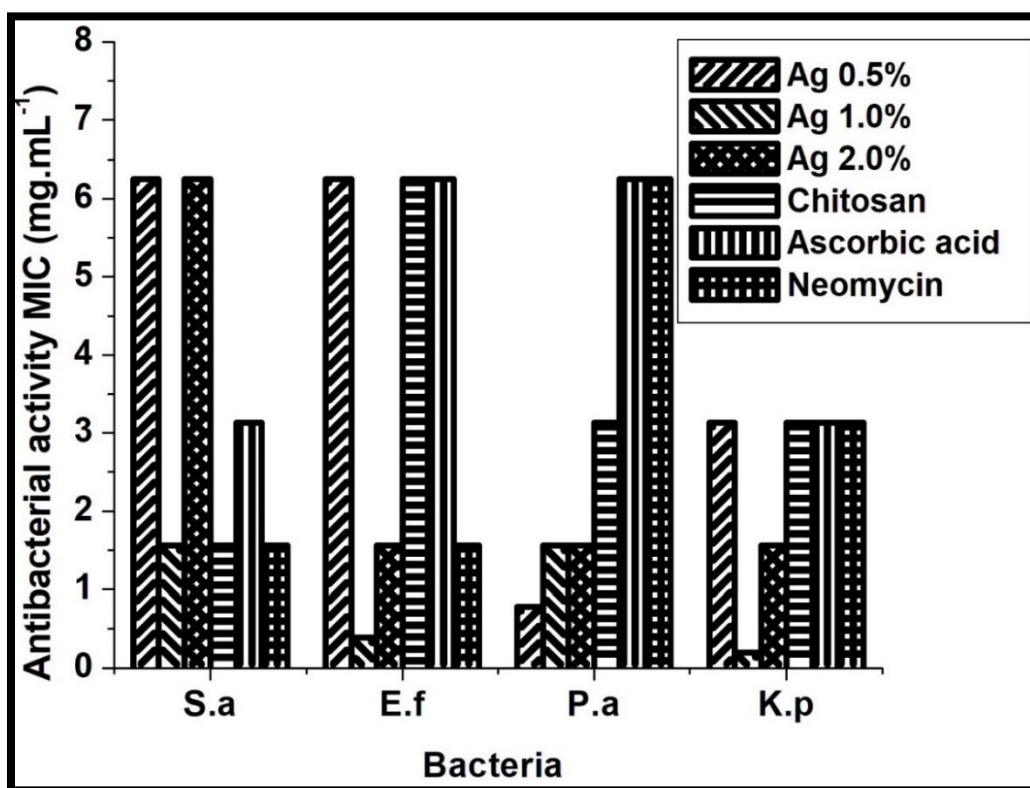


Fig 4:22 Antibacterial activity of silver nanoparticles capped with chitosan. S.a = *Staphylococcus aureus*, E.f = *Enterococcus faecalis*, P.a = *Pseudomonas aeruginosa*, K.a = *Klebsiella pneumoniae*

The synthesized nanoparticles were found to be effective in the inhibition of the chosen gram-positive and gram-negative bacteria compared to pure chitosan, ascorbic acid and neomycin B which were used as controls and exhibited relatively higher MIC values with the exclusion of *Staphylococcus aureus* (S.a). The activity of silver nanoparticles against all the tested microorganisms is presumably due to the fact that, unlike other antibacterial agents, silver nanoparticles do not target specific sites but several levels such as bacterial walls and DNA. The difference in activity between the prepared nanoparticles can be attributed to the amount of capping

agent present on the surface of the particles since the capping agent concentration affects both the size and shape of the nanoparticles as observed in the TEM images in Fig 4:21. The high antibacterial activity of 1% chitosan capped silver nanoparticles compared to 0.5%, and 2% might be due to high surface to volume ratio since smaller particles release more silver ions compared to larger and agglomerated particles.

The MIC decreased as exposure shifted from gram-positive to gram-negative bacteria. This is due to the difference in the constitution of the cell walls of the two types of bacteria (Masoko and Eloff, 2007, Howe et al., 1965). On the other hand, chitosan was found to be active against the microorganisms to some extent and similar results were obtained by Jiang, 2011, which can be attributed to the presence of the amine and hydroxyl functional groups but the synthesized particles were more effective compared to chitosan alone this is due to their high to surface volume ratio. The mechanism of the bactericidal effect of silver nanoparticles is still under investigation. However, studies suggest that as the silver ions are attached to the surface of the cell membrane, they disturb permeability and respiration functions of the cell (Raza et al., 2016, Abdel-Aziz et al., 2014). The suggested mechanism for antibacterial activity of chitosan is based on the binding of cationic chitosan to sialic acid in phospholipids (Lima et al., 2017). This binding results in a disturbance of the cell membrane. It is also reported that the penetration of oligomeric chitosan into the cell also results in bacteria death.

4.3.5.2 Antifungal activity

The antifungal activity of chitosan capped silver nanoparticles was investigated against *Candida albicans* and *Cryptococcus neoformans* as shown in Fig 4:23. The synthesized silver nanoparticles were found to be active against both the tested fungal strains with a minimum inhibitory concentration of 0.2 mg/ml. The high activity of nanoparticles against fungal strains compared to bacterial strains is due to particle size and composition of the microorganism. It is also observed in Fig 4:23 that chitosan has antifungal activity. It is therefore proposed that the low minimum inhibitory concentration results from the synergistic effect of both silver nanoparticles and the functional groups that are present on the surface of the particles.

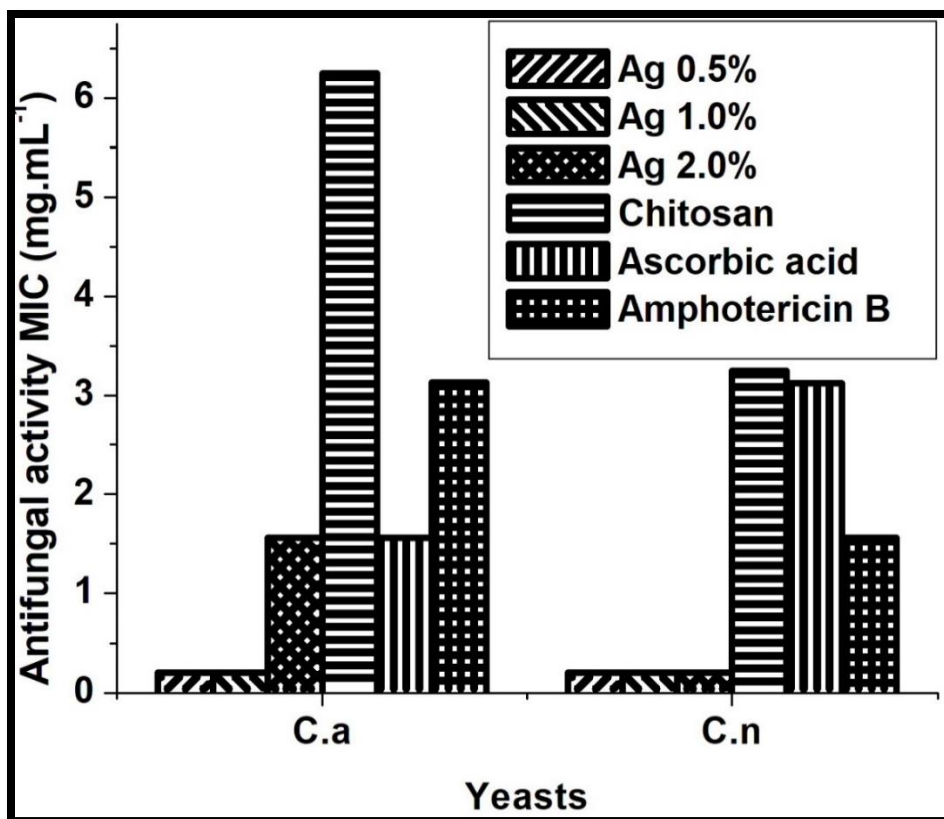


Fig 4:23 Antifungal activity of silver nanoparticles capped with chitosan. C.a = *Candida albicans*, C.n = *Cryptococcus neoformans*.

4.3.5.3 Antioxidant activity

The antioxidant activity of chitosan and chitosan capped silver nanoparticles against DPPH was investigated as shown in Fig 4:24. Ascorbic acid was used as positive control. The antioxidant property was found to be high in chitosan (82%) and ascorbic acid (90%). The least active samples were found to be silver nanoparticles (60%). The high antioxidant activity of chitosan is due to the lone pairs that are present in the nitrogen and oxygen atoms. The antioxidant property of silver nanoparticles may be attributed to the presence of organic functional groups on the surface of the synthesized particles (Ravichandran et al., 2016, Markus et al., 2017). The antioxidant activity was found to increase with an increase in the concentration of silver nanoparticles thus revealing its dosage-dependent nature (Bhakya et al., 2015). The dosage-dependent nature of DPPH was also reported by Prasad et al., 2016.

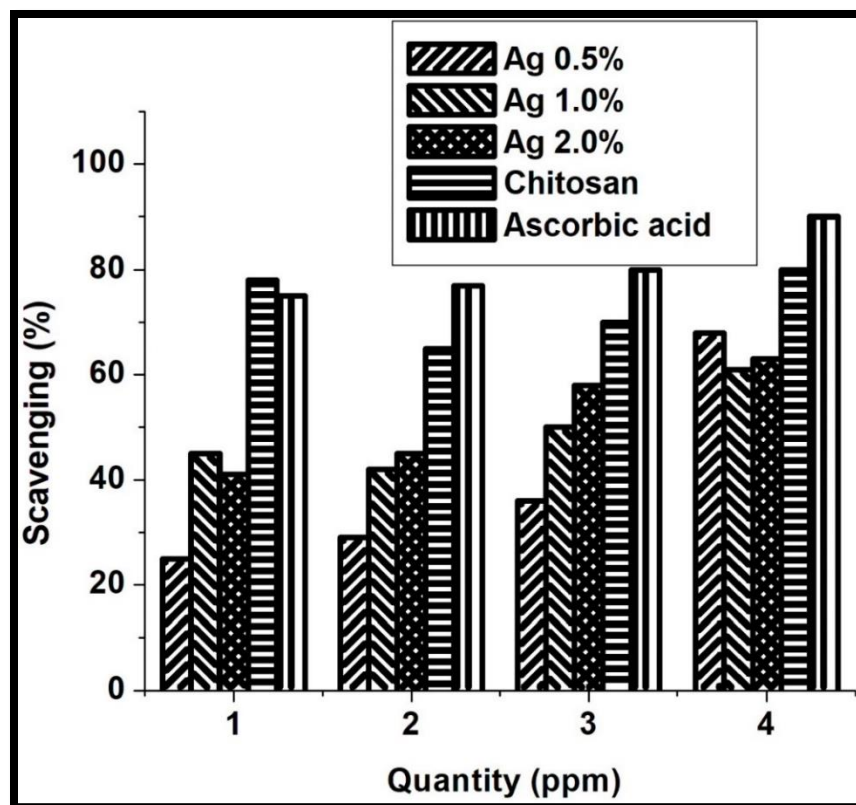


Fig 4:24 Antioxidant activity of silver nanoparticles capped with chitosan.

4.4 INFLUENCE OF PRECURSOR CONCENTRATION ON THE PROPERTIES OF SILVER NANOPARTICLES

4.4.1 Introduction

The optimum capping agent concentration was used to investigate the influence of silver nitrate concentration on the properties of silver nanoparticles. Chitosan 1%, *Camellia sinensis* 2%, *Combretum molle* 2% and *Melia azedarach linn* 2%.

4.4.2 Optical properties

4.4.2.1 Uv-vis absorption studies

To investigate the effect of silver nitrate concentration on the optical properties of silver nanoparticles, Uv-Vis spectroscopy was used. The concentration of silver nitrate was varied from 0.1 to 0.3 M with constant capping agent concentration at 2% for *Camelia Sinensis*, *Combretum molle* and *Melia azedarach linn* and 1% for chitosan. The prepared silver nanoparticles were found to be blue shifted compared to their bulk counterpart as shown in Fig 4:25. The characteristic plasmon absorption bands of the prepared silver nanoparticles are presented in table 4:7 below.

From Table 4:7 it is observed that as the concentration of silver nitrate increases the absorption peak wavelength is also increasing. This might suggest that the particle size is increasing. Similar results were obtained by Zuber et al., 2016. It is reported in the literature that bigger particles absorb towards longer wavelength, this is attributed to the difference in frequency of surface plasmon oscillation of the free electrons (Zuber et al., 2016, Barnes et al., 2003).

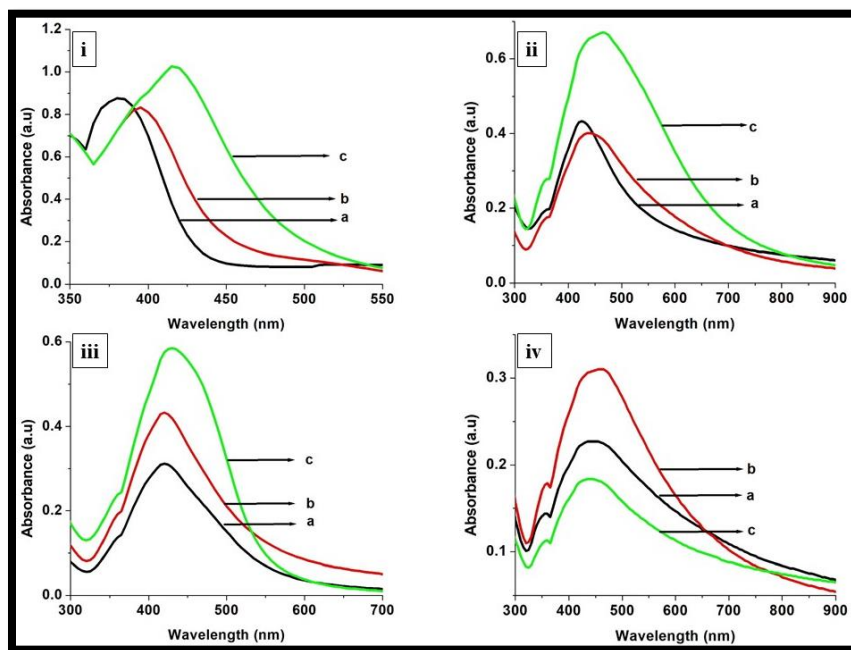


Fig 4:25 Uv-vis spectra for Ag nanoparticles capped with (i) chitosan, (ii) *Camellia sinensis*, (iii) *Combretum molle* and (iv) *Melia azedarach linn*. $a= 0.1 M$, $b= 0.2 M$, $c= 0.3 M$ silver nitrate concentration.

Table 4:7 Relationship between characteristic plasmon absorption bands and precursor concentration

Silver nitrate (M)	Absorption wavelength (nm)		
	0.1	0.2	0.3
Chitosan	380	400	417
<i>Camellia sinensis</i>	427	446	468
<i>Combretum molle</i>	421	422	434
<i>Melia Azedarach linn</i>	449	446	461

4.4.2.2 Photoluminescence studies

The emission spectra of silver nanoparticles prepared at different silver nitrate concentrations (0.1, 0.2, 0.3 M) are shown in Fig 4:26. Silver nanoparticles were excited at 380, 430, 420 and 450 nm for chitosan, *Camellia sinensis*, *Combretum molle* and *Melia azedarach linn* capped silver nanoparticles respectively. The particles were found to emit at different wavelengths as shown in Fig 4:24, all the emission peaks were red-shifted compared to their respective Uv-Vis absorption peaks. The calculated FWHM results indicated a slight increase in FWHM with an increase in silver nitrate concentration as shown in Table 4:8. This increase in FWHM suggests that polydispersed particles that are not well passivated are formed (Moloto et al., 2009). The emission property of metal nanoparticles varies with different shapes and structures (Zhang et al., 2010).

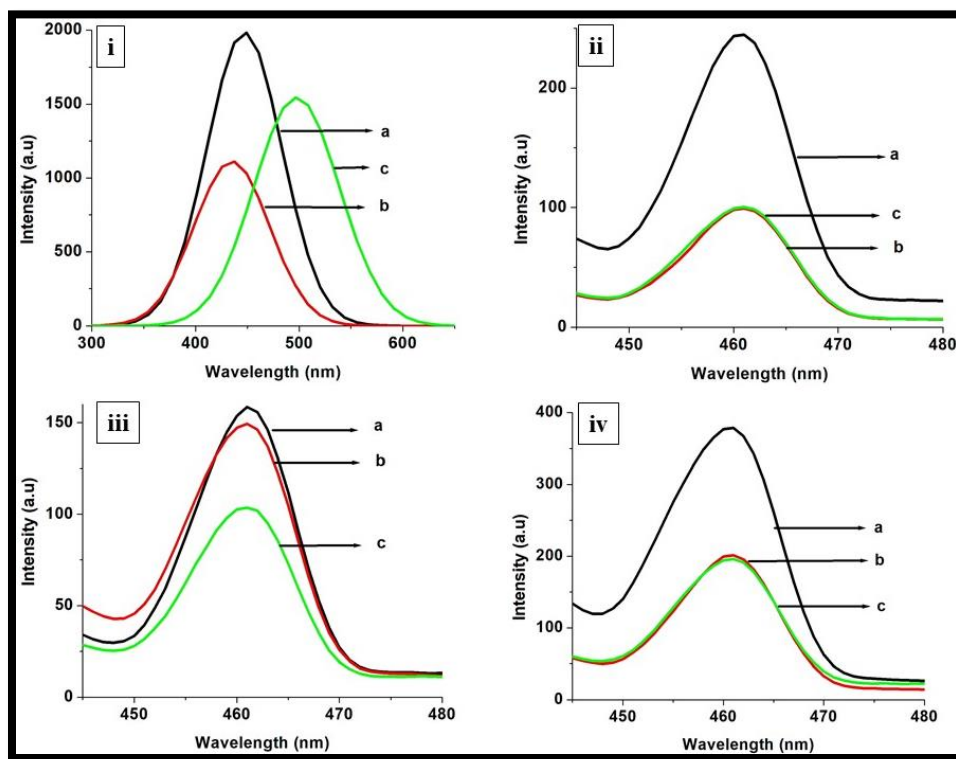


Fig 4:26 PL spectra for Ag nanoparticles capped with (i) chitosan, (ii) *Camellia sinensis*, (iii) *Combretum molle* and (iv) *Melia azedarach linn*. *a* = 0.1 M, *b* = 0.2 M, *c* = 0.3 M silver nitrate concentration.

Table 4:8 Relationship between precursor concentration and FWHM

Silver nitrate (M)	Absorption wavelength (nm)		
	0.1	0.2	0.3
Chitosan	83	83	107
<i>Camellia sinensis</i>	11	11	12
<i>Combretum molle</i>	11	12	13
<i>Melia Azedarach linn</i>	10	12	12

4.4.3 FTIR spectral analysis

To investigate the possible functional groups involved in the biosynthesis of silver nanoparticles FTIR spectroscopy was used as shown in Fig 4:27. The main difference between the spectra of pure chitosan, bioactive compounds from extracts and that of silver nanoparticles is the disappearance of the N-H and O-H stretching vibration. This observation suggests that there is an interaction between the nanoparticles and the organic functional groups.

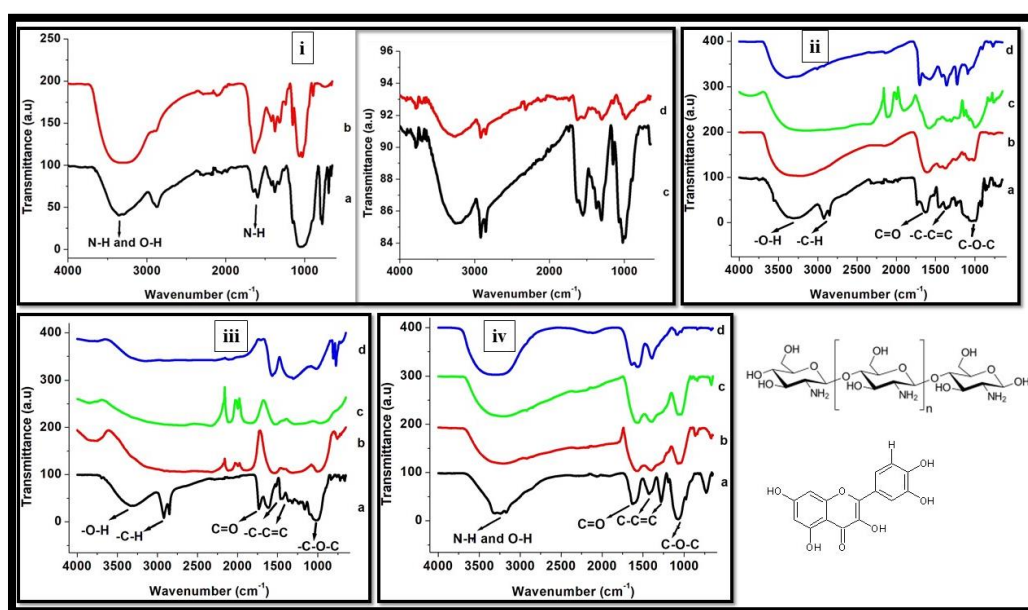


Fig 4:27 FTIR spectra for Ag nanoparticles capped with (i) chitosan, (ii) *Camellia sinensis*, (iii) *Combretum molle* and (iv) *Melia azedarach linn*. a= capping agent, b= 0.1 M, b= 0.2 M, c= 0.3 M silver nitrate concentration.

The FT-IR spectra show the presence of bands at 3327 cm^{-1} (N-H and O-H stretching), 1600 cm^{-1} (NH_2 bending) and 1037 cm^{-1} (C-O-C stretching) for chitosan and bands at 3325 cm^{-1} due to (-OH stretching, alcohol), 2899 cm^{-1} is attributed to (C=C-H asymmetric stretch, aromatic), 1609 cm^{-1} is due to (C=O, carbonyl), 1510 cm^{-1} (C-C=C symmetric stretch, aromatic), 1430 cm^{-1} (C-C=C asymmetric stretch, aromatic) and 1029 cm^{-1} (-C-O-C stretching) for bioactive plant extracts. The presence of prominent hydroxyl groups on the surface of the particles indicates that the particles are protected by the organic layer through the interaction with the free nitrogen that was created by the deprotonation of the amine group in the chitosan molecule. Also, the shift in the peak position of the hydroxyl functional group indicates that there was an interaction between the hydroxyl group and silver nanoparticles.

4.4.4 X-Ray diffraction studies

The phase purity of silver nanoparticles was confirmed by X-ray diffraction studies. Fig 4:28 shows the XRD micrographs of silver nanoparticles prepared at different molar concentrations of aqueous silver nitrate solution. Chitosan, *Camellia sinensis*, *Combretum molle* and *Melia azedarach* were used as reducing and capping agents. With all the prepared silver nanoparticles four distinct peaks at 38, 44, 64 and 77 were observed these peaks are assigned to 111, 200, 220 and 311 planes of silver face-centered cubic phase (JCPDS file No 00-004-0783). At 0.1 M silver nitrate concentration, the peaks in the range of 20-35 ° are attributed to organic compounds that are present on the surface of the particles. The absence of a chitosan peak at $2\theta = 22^\circ$ and the organic impurities from plant extracts with an increase in precursor concentration indicates that there are excess silver nuclei compared to capping molecules.

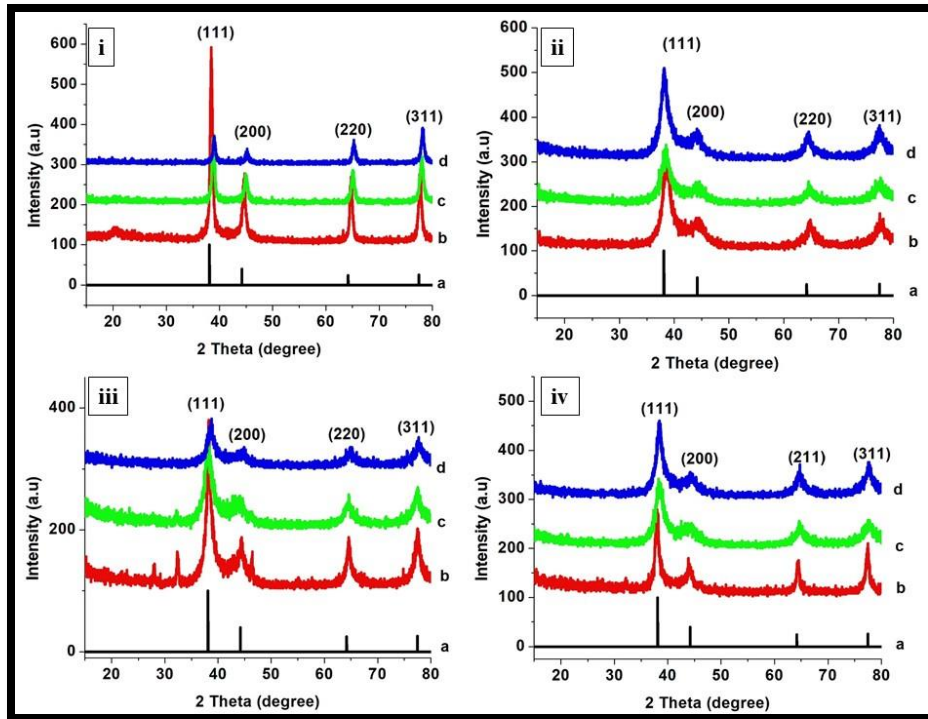


Fig 4:28 XRD micrographs for Ag nanoparticles capped with (i) chitosan, (ii) *Camellia sinensis*, (iii) *Combretum molle* and (iv) *Melia azedarach linn*. *a*= Reference, *b*= 0.1 M, *c*= 0.2 M, *d*= 0.3M silver nitrate concentration.

4.4.5 TEM analysis

To investigate the influence of precursor concentration on the size and shape of silver nanoparticles capped with chitosan, *Camellia sinensis*, *Combretum molle* and *Melia azedarach* leaves, TEM analysis was used. Figure 4:29 shows the TEM images of chitosan capped silver nanoparticles prepared at a different concentration of aqueous silver nitrate. At low concentration of 0.1 M, uniform spherical particles with average size of 2 nm were obtained. The size distribution was in the range of 1-4 nm. These results show that sufficient capping molecules were available to protect the formed silver atoms. Thus no agglomeration was observed.

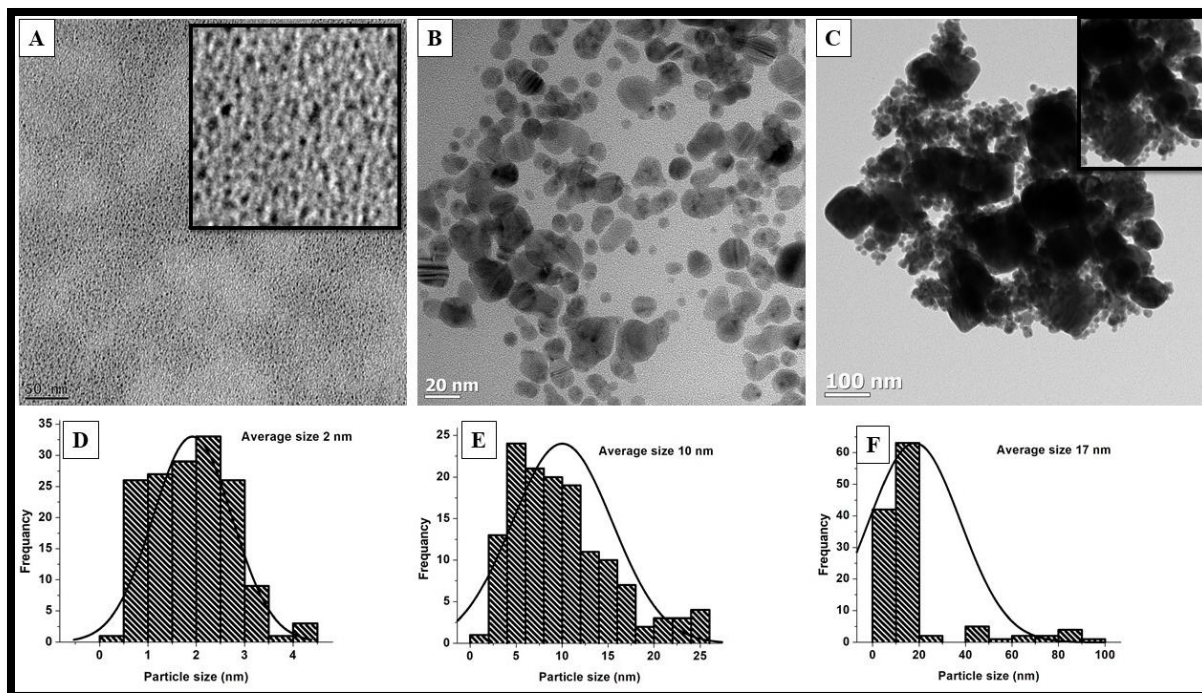


Fig 4:29 TEM micrographs and the corresponding histograms (e and f) of chitosan capped silver nanoparticles prepared at different silver nitrate concentrations (a) 0.1 M, (b) 0.2 M and (c) 0.3 M.

As the concentration of silver ions was increased to 0.2 M, spherical and bipodal nanoparticles with some fingerprint lines were obtained. The average particles size was calculated to be 10 nm, a wide distribution compared to 0.1 M particles was observed. A further increase in particle size was observed when the precursor concentration was at 0.3 M. At a high concentration a mixed shape of spheres and diamonds was observed however the dominating shape was spherical. Also at high concentration, the particles started to be agglomerated with a wide size distribution. An increase in particle size with an increase in precursor concentration was also reported by Sobczak-Kupiec et al., 2011, Sibiya and Moloto, 2014. This observation can be explained using the reaction pathways; high concentration of silver nitrate favors the kinetic growth of nanoparticles. This is supported by the formation of anisotropic shapes such as diamonds. A decrease in silver nitrate concentration favors the thermodynamic growth of silver nanoparticles. This is because the thermodynamic growth is driven by sufficient supply of thermal energy and low concentration. The degree of aggregation was found to be directly proportional to the concentration of silver ions. This can be attributed to the high surface energy and collision frequency of the nanoparticles (Ahmad et al., 2014). The effect of precursor concentration on the shape of nanoparticles is yet to

be elucidated however it has been reported that different shapes arise from the chemical potential of the nanoparticles (Sibokoza et al., 2017). This is because the chemical potential of the reaction is determined by the monomer concentration at a fixed temperature.

When plant extracts were used as capping agents and the concentration of silver ions was varied from 0.1 to 0.3M the following trend was observed: the particle size increased with an increase in silver nitrate concentration. For silver nanoparticles capped with *Combretum molle* (Fig 4:30), spherical particles with average size of 5, 9 and 11 nm were obtained for 0.1, 0.2 and 0.3 M respectively. The particle size distribution was found to increase with an increase in silver ions concentration as shown in Fig 4:30. This indicates that the particles became polydispersed with an increase in the concentration of the precursor. Also, a slight increase in average particle size is observed. However the shape remained spherical with some particles starting to agglomerate at high concentration.

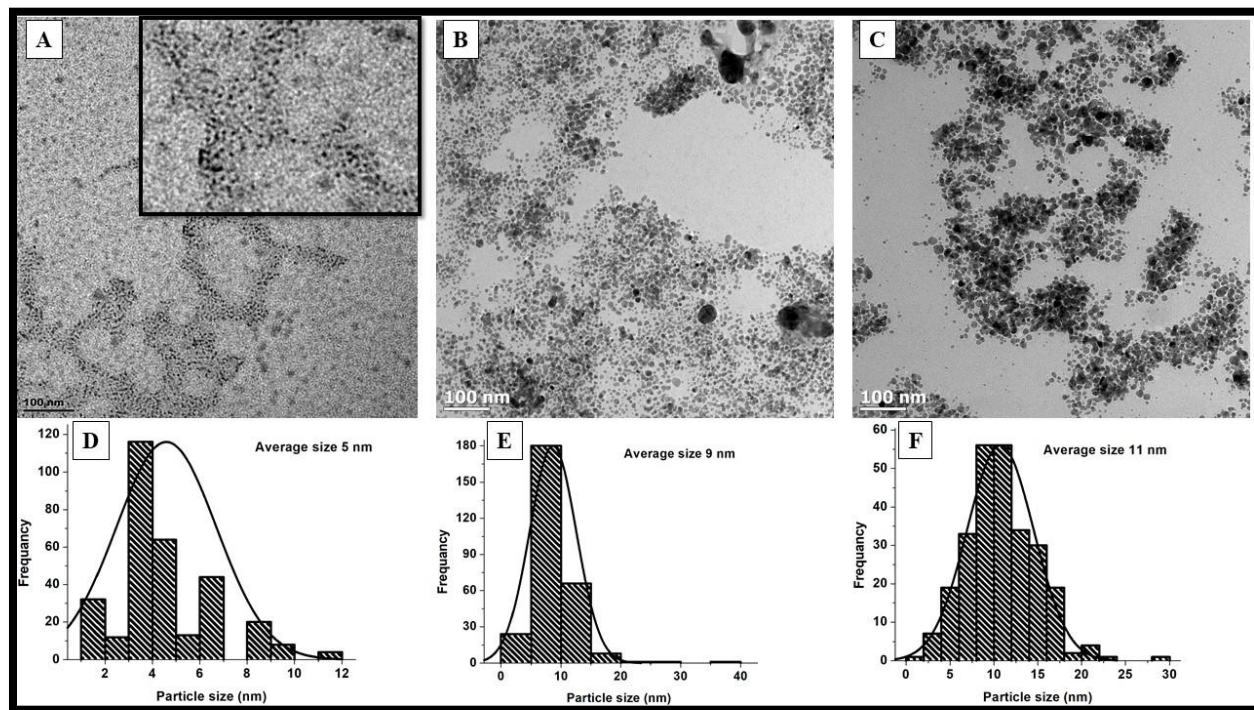


Fig 4:30 TEM micrographs and the corresponding histograms (d, e and f) of *Combretum molle* capped silver nanoparticles prepared at different silver nitrate concentrations (a) 0.1 M, (b) 0.2 M and (c) 0.3 M

For silver nanoparticles capped with *Camellia sinensis* (Fig 4:31). At 0.1 M spherical particles were obtained as the concentration was increased to 0.2 M, the dominating shape was spherical with some diamonds and rods starting to form. A further increase in the concentration of silver nitrate to 0.3 M resulted in the formation of spherical particles. An average particle size of 4, 10, and 11nm was obtained.

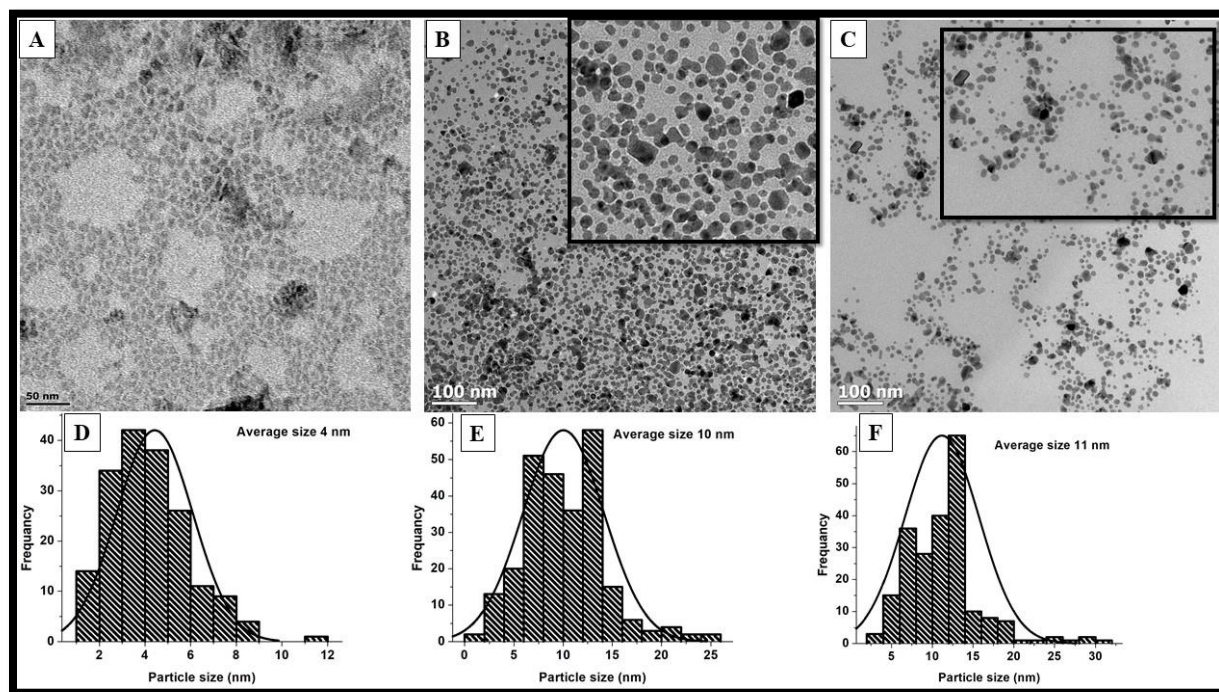


Fig 4:31 TEM micrographs and the corresponding histograms (d, e and f) of *Camellia sinensis* capped silver nanoparticles prepared at different silver nitrate concentration (a) 0.1 M, (b) 0.2 M and (c) 0.3 M.

A significant increase in average particle size is observed in the *Melia azedarach* capped silver nanoparticles (Fig 4:32). It is observed that at low precursor concentration uniform spherical particles with average size of 3 nm are obtained, and the size distribution is not wide. As the concentration is increased bipods and spherical particles with average size of 7 nm were obtained. A further increase to 0.3M resulted in the formation hexagonal and spherical particles with average size of 15 nm. The size distribution increases with an increase in precursor concentration.

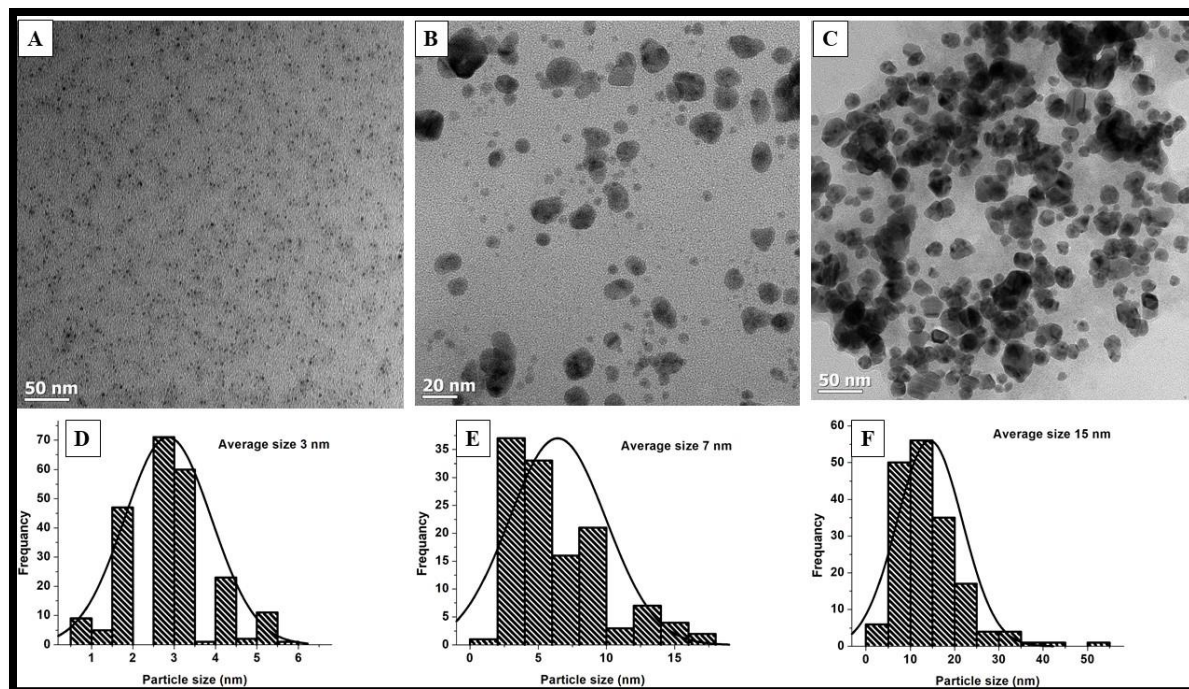
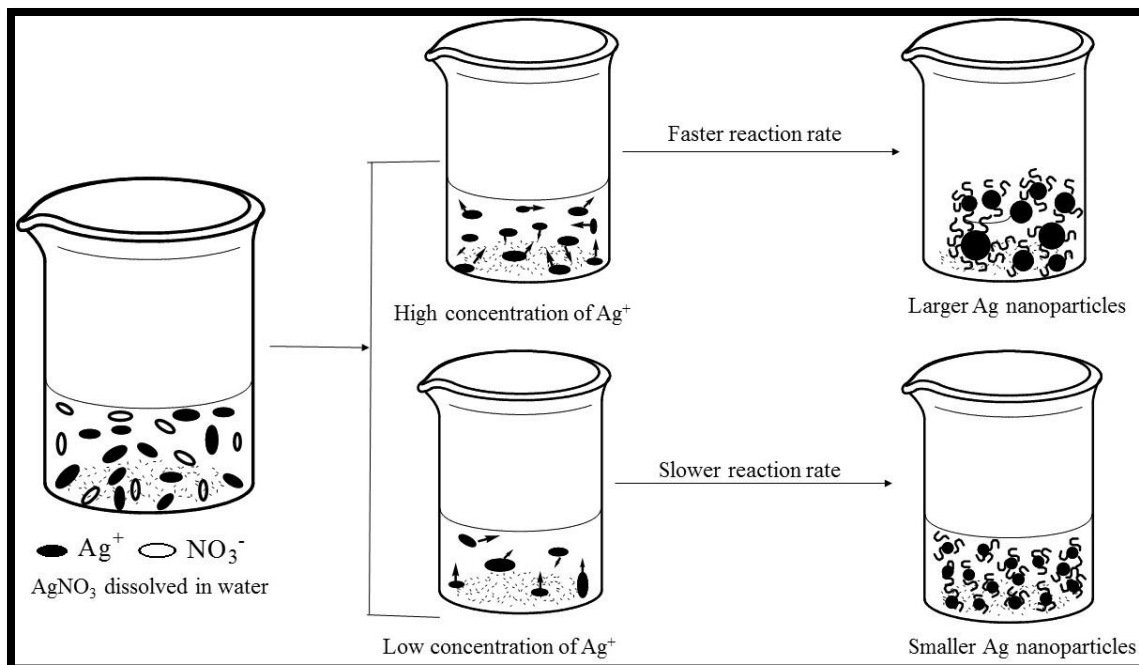


Fig 4:32 TEM micrographs and the corresponding histograms (d, e and f) of *Melia azedarach linn* capped silver nanoparticles prepared at different silver nitrate concentrations (a) 0.1M, (b) 0.2 M and (c) 0.3 M

The above-mentioned observations may be explained using the collision theory. For a chemical reaction to occur molecules must collide with sufficient energy for the reaction to proceed. At high concentration of silver nitrate the probability of silver molecules to collide is high. Thus the reaction rate is high as shown in Scheme 4:1. This rapid reduction process means that an excess number of nuclei will be generated thus larger particles are formed due to aggregation of smaller particles to larger ones (Sobczak-Kupiec et al., 2011, Ahmad et al., 2014). Also, the increase in particle size may be due to an insufficient amount of the capping molecules. Therefore this means that more silver ions were competing for the functional groups present in the capping agent. As the concentration of silver ions is decreased, the number of colliding silver nanoparticles decreased hence this resulted in the formation of uniform and mono-dispersed nanoparticles.



Scheme 4:1 Schematic diagram for the formation of silver nanoparticles at different concentrations.

4.5 EFFECT OF CAPPING AGENT CONCENTRATION ON THE PROPERTIES OF COPPER NANOPARTICLES AND THEIR ANTIBACTERIAL ACTIVITY

4.5.1 Optical properties

To investigate the optical properties of copper nanoparticles prepared at different capping molecules, Uv-Vis spectroscopy was used. The formation of copper nanoparticles was confirmed by the change in color of the reaction mixture from blue to brown; this is attributed to surface plasmon resonance of copper nanoparticles. The absorption peak of capped copper nanoparticles was found to be at 421, 425, 425, and 448 nm for chitosan, *Camellia sinensis*, *Combretum molle*, and *Melia azedarach linn* respectively as shown in Fig 4:33. The synthesized copper nanoparticles were found to be blue shifted from the bulk copper which absorbs at around 600 nm (Biçer and Şişman, 2010, Dhas et al., 1998). The absence of a peak at 800 nm which is normally attributed to copper oxide nanoparticles is noted, this, therefore, suggests that only copper nanoparticles were

formed (Biçer and Şişman, 2010, Lisiecki et al., 1996, DeAlba-Montero et al., 2017). The formation of copper nanoparticles is attributed to the reaction temperature of 85° C which favors the formation of copper nanoparticles rather than copper oxide. Also the use of capping molecules contributed this results.

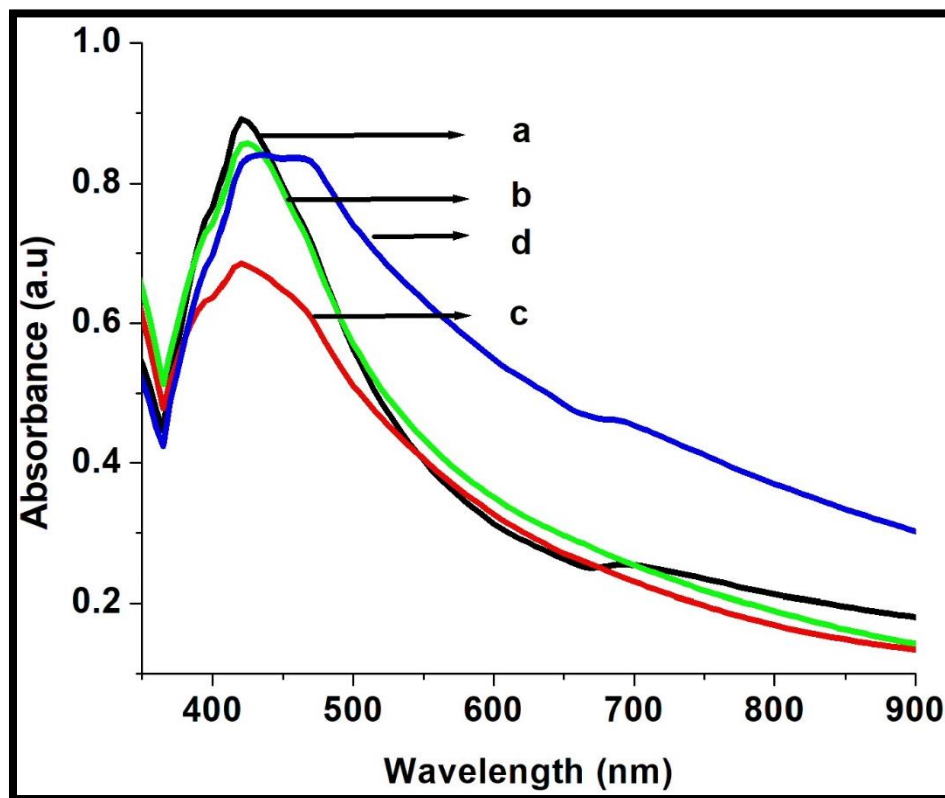


Fig 4:33 Uv-vis spectra of copper nanoparticles capped with (a) chitosan, (b) *Camellia sinensis*, (c) *Combretum molle* and (d) *Melia azedarach linn*.

4.5.2 FTIR spectral analysis

To understand the possible functional groups that are responsible for capping copper nanoparticles, FTIR spectroscopy was used. Fig 4:34 shows the FTIR spectra of copper nanoparticles synthesized with different capping agents. Table 4:9 shows different peaks that were obtained. For chitosan capped copper nanoparticles there is a well defined hydroxyl functional group on the surface of the particles, this suggests that the interaction of chitosan with copper nanoparticles was through the amine functional group. Similar results were reported by Muthukrishnan, 2015. When plant extracts were used as capping agents, peak broadening and a shift in hydroxyl functional group were observed, this indicates that plants extracts use the hydroxyl functional group to interact with

copper nanoparticles. This interaction is mainly due to the high affinity of copper ions to the hydroxyl functional groups. The presence of different functional groups on the surface of the particles also shows that copper nanoparticles were successfully capped.

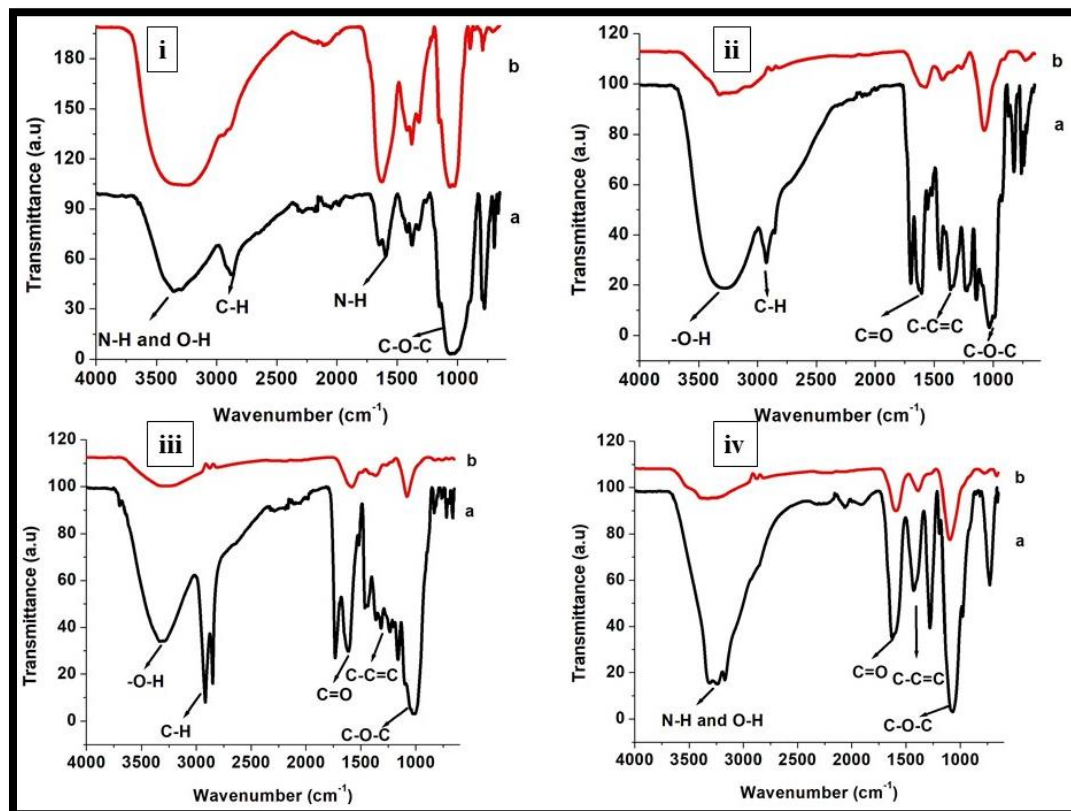


Fig 4:34 FTIR spectra of copper nanoparticles capped with (i) chitosan, (ii) *Camellia sinensis*, (iii) *Combretum molle*, (iv) *Melia azedarach* linn. *a = capping molecules b= copper nanoparticles*

Table 4:9 Functional groups present in chitosan plant extracts

Capping molecules	Functional group of interest	Wavenumber (cm ⁻¹)
Chitosan	Overlap of O-H and N-H	3340
	C-H	2900
	NH ₂	1580
	C-O-C	1050
Plant extracts	O-H	3310
	Overlap O-H and N-H	3341
	C-H	2900
	C=O	1600
	C-C=C	1288

4.5.3 TEM analysis

TEM was used to investigate the effect of capping agent on the size and shape of copper nanoparticles. TEM images are shown in Fig 4:35, when chitosan was used as a capping agent, nearly spherical agglomerated particles were obtained. Well-defined monodispersed copper nanoparticles with an average size of 3 nm were obtained when *Combretum molle* was used as a capping agent. These results illustrate the importance of the identity of the capping agent since different sizes and shapes were obtained. Also, the degree of agglomeration is different. Mixed shaped (spheres and rods) copper nanoparticles with an average size of 18 nm were obtained when *Camellia sinensis* was used as a capping agent. *Melia azedarach linn* also gave mixed (spheres, diamonds and hexagonal) shaped copper nanoparticles. Since capping agents use different functional groups to interact with copper ions, the shape is mostly influenced by the binding site of the capping molecules and the steric hindrance effect from the structure of the capping molecule.

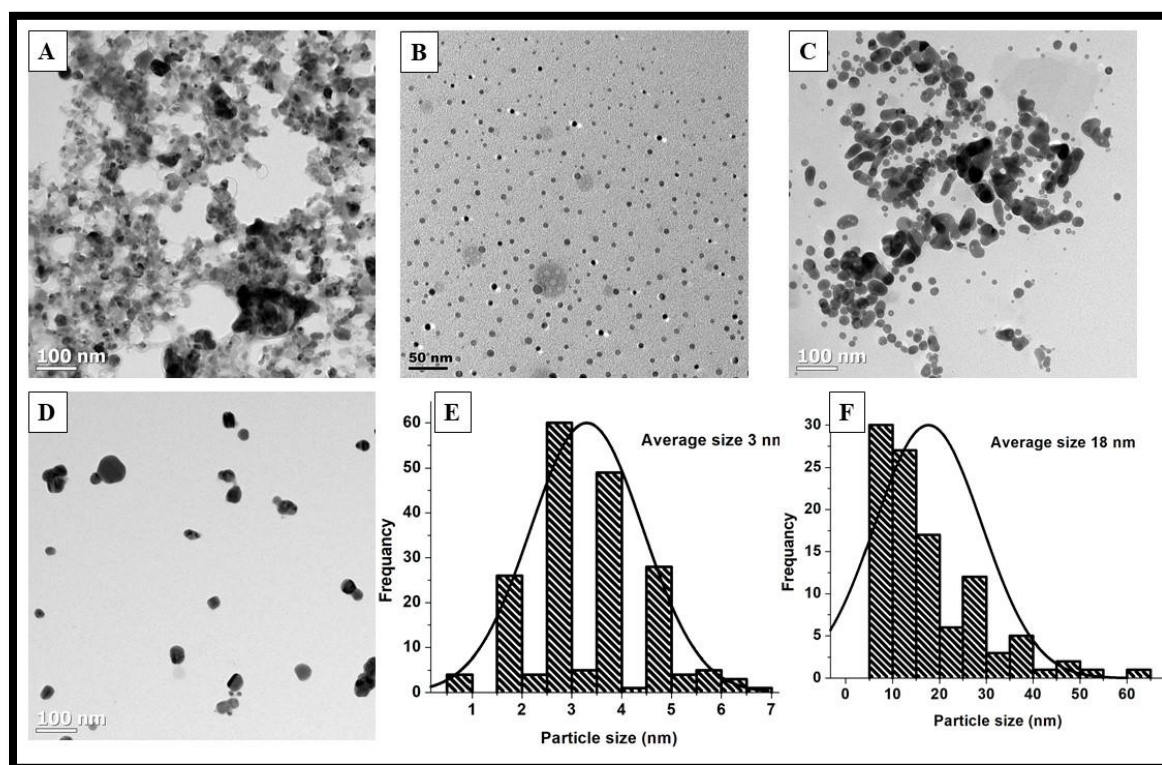


Fig 4:35 TEM micrographs and histograms (e and f) of capped copper nanoparticles prepared at different capping agents (a) chitosan, (b) *Combretum molle*, (c) *Camellia sinensis*, (d) *Melia azedarach linn*.

4.5.4 Antibacterial activity

The antibacterial activity of copper nanoparticles was investigated against *Enterococcus faecalis* (*E.f*), *Staphylococcus aureus* (*S.a*), *Pseudomonas aeruginosa* (*P.a*), and *Klebsiella pneumonia* (*K.p*) as shown in fig 4:36. The synthesized copper nanoparticles were found to be active against all the tested microorganisms with different MIC values as shown in table 4:10. Neomycin was used at positive control. It can be seen that *Combretum molle* capped copper nanoparticles were found to have high antibacterial activity compared to the other samples. This is attributed to their small size and less degree of agglomeration as shown in Fig 4:36 above. The least active particles were found to be *Melia azedarach linn* capped copper nanoparticles, this is due to their larger size. The antibacterial activity of copper nanoparticles was found to be high in *Pseudomonas aeruginosa* and *Klebsiella pneumonia* compared to *Enterococcus faecalis* and *Staphylococcus aureus*. This is attributed to the difference in the cell wall of each microorganism. The mechanism of action for copper nanoparticles is yet to be fully explained. However, there are studies in the literature that propose a similar mechanism to that of silver nanoparticles (Kruk et al., 2015).

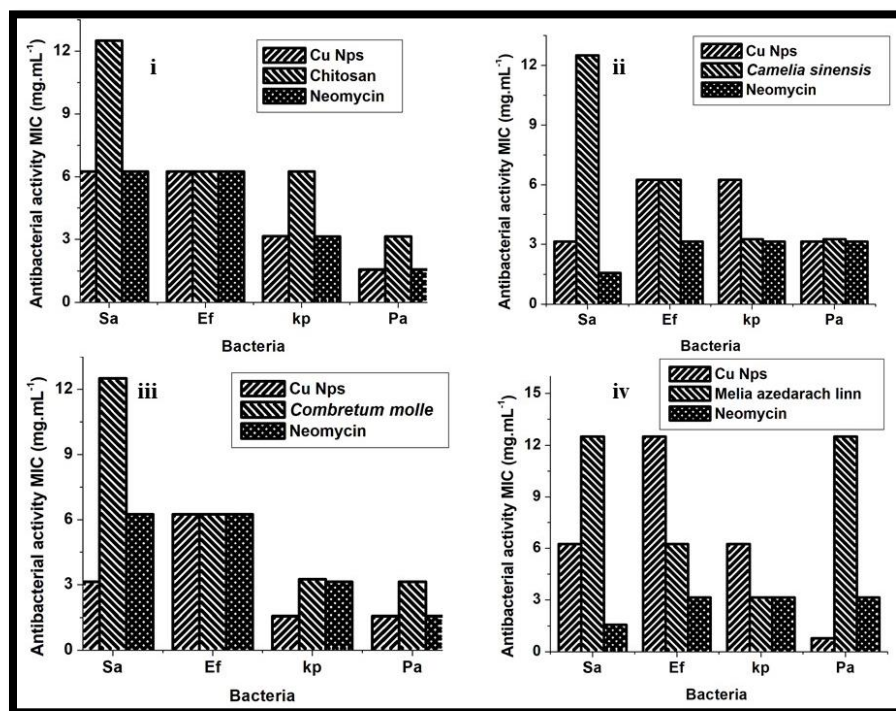


Fig 4:36 Antibacterial activity of copper nanoparticles capped with (i) chitosan, (ii) *Camellia sinensis*, (iii) *Combretum molle* and (iv) *Melia azedarach linn*. *S.a* = *Staphylococcus aureus*, *E.f* = *Enterococcus faecalis*, *P.a* = *Pseudomonas aeruginosa*, *K.a* = *Klebsiella pneumoniae*

Table 4:10 MIC values for copper nanoparticles

Bacteria	Cu Chitosan	Cu <i>Camellia sinensis</i>	Cu <i>Combretum molle</i>	Cu <i>Melia azedarach</i>
Sa	6.25	3.25	3.25	6.25
Ef	6.25	6.25	6.25	12.5
Pa	1.56	3.25	1.56	0.78
Kp	3.25	6.25	1.56	6.25

4.6 REFERENCES

- ABDEL-AZIZ, M. S., SHAHEEN, M. S., EL-NEKEETY, A. A. & ABDEL-WAHHAB, M. A. 2014. Antioxidant and antibacterial activity of silver nanoparticles biosynthesized using *Chenopodium murale* leaf extract. *Journal of Saudi Chemical Society*, 18, 356-363.
- AHMAD, T., WANI, I. A., AHMED, J. & AL-HARTOMY, O. A. 2014. Effect of gold ion concentration on size and properties of gold nanoparticles in TritonX-100 based inverse microemulsions. *Applied Nanoscience*, 4, 491-498.
- AJITHA, B. D., A. HARISH, G.S. SREEDHARA REDDY, P. 2013. The influence of silver precursor concentration on size of silver nanoparticles grown by soft chemical route. *Research Journal of Physical sciences*, 1, 11-14.
- ALI, S. W., RAJENDRAN, S. & JOSHI, M. 2011. Synthesis and characterization of chitosan and silver loaded chitosan nanoparticles for bioactive polyester. *Carbohydrate Polymers*, 83, 438-446.
- AMZAD HOSSAIN, M. & SHAH, M. D. 2015. A study on the total phenols content and antioxidant activity of essential oil and different solvent extracts of endemic plant *Merremia borneensis*. *Arabian Journal of Chemistry*, 8, 66-71.
- ANSARI, S., NEPAL, H. P., GAUTAM, R., RAYAMAJHI, N., SHRESTHA, S., UPADHYAY, G., ACHARYA, A. & CHAPAGAIN, M. L. 2014. Threat of drug resistant *Staphylococcus aureus* to health in Nepal. *BMC Infectious Diseases*, 14, 157.
- BARNES, W. L., DEREUX, A. & EBBESEN, T. W. 2003. Surface plasmon subwavelength optics. *Nature*, 424, 824-830.
- BHAKYA, S., MUTHUKRISHNAN, S., SUKUMARAN, M. & MUTHUKUMAR, M. 2015. Biogenic synthesis of silver nanoparticles and their antioxidant and antibacterial activity. *Applied Nanoscience*, 6, 755-766.

- BIÇER, M. & ŞIŞMAN, İ. 2010. Controlled synthesis of copper nano/microstructures using ascorbic acid in aqueous CTAB solution. *Powder Technology*, 198, 279-284.
- DAVID, L., MOLDOVAN, B., VULCU, A., OLENIC, L., PERDE-SCHREPLER, M., FISCHER-FODOR, E., FLOREA, A., CRISAN, M., CHIOREAN, I., CLICHICI, S. & FILIP, G. A. 2014. Green synthesis, characterization and anti-inflammatory activity of silver nanoparticles using European black elderberry fruits extract. *Colloids and Surfaces B: Biointerfaces*, 122, 767-777.
- DEALBA-MONTERO, I., GUAJARDO-PACHECO, J., MORALES-SANCHEZ, E., ARAUJO-MARTINEZ, R., LOREDO-BECERRA, G. M., MARTINEZ-CASTANON, G. A., RUIZ, F. & COMPEAN JASSO, M. E. 2017. Antimicrobial Properties of Copper Nanoparticles and Amino Acid Chelated Copper Nanoparticles Produced by Using a Soya Extract. *Bioinorg Chem Appl*, 2017, 1064918.
- DE MORAIS LIMA, G. R., DE SALES, I. R., CALDAS FILHO, M. R., DE JESUS, N. Z., DE SOUSA FALCAO, H., BARBOSA-FILHO, J. M., CABRAL, A. G., SOUTO, A. L., TAVARES, J. F. & BATISTA, L. M. 2012. Bioactivities of the genus *Combretum* (Combretaceae): a review. *Molecules*, 17, 9142-206.
- DESARKAR, H. S., KUMBHAKAR, P. & MITRA, A. K. 2013. Synthesis of silver hollow nanoparticles and observation of photoluminescence emission properties. *Journal of Luminescence*, 134, 1-7.
- DHAS, N. A., RAJ, C. P. & GEDANKEN, A. 1998. Synthesis, Characterization, and Properties of Metallic Copper Nanoparticles. *Chemistry of Materials*, 10, 1446-1452.
- ELOFF, J. N., KATERERE, D. R. & MCGAW, L. J. 2008. The biological activity and chemistry of the southern African Combretaceae. *J Ethnopharmacol*, 119, 686-99.
- HOWE, J. M., FEATHERSTON, W. R., STADELMAN, W. J. & BANWART, G. J. 1965. Amino Acid Composition of Certain Bacterial Cell-Wall Proteins. *Applied Microbiology*, 13, 650-652.
- IRAVANI, S. & ZOLFAGHARI, B. 2013. Green Synthesis of Silver Nanoparticles Using *Pinus eldarica* Bark Extract. *BioMed Research International*, 2013, 1-5.
- JIANG, L. 2011. *Comparison of disk diffusion, agar dilution and broth microdilution for antimicrobial susceptibility testing of five chitosans*. MSc Dissertation, Louisiana State University and

Agricultural and Mechanical College.

- KHALIL, M. M. H., ISMAIL, E. H., EL-BAGHDADY, K. Z. & MOHAMED, D. 2014. Green synthesis of silver nanoparticles using olive leaf extract and its antibacterial activity. *Arabian Journal of Chemistry*, 7, 1131-1139.
- KIM, K. J., SUNG, W. S., SUH, B. K., MOON, S. K., CHOI, J. S., KIM, J. G. & LEE, D. G. 2009. Antifungal activity and mode of action of silver nano-particles on *Candida albicans*. *Biometals*, 22, 235-42.
- KRISHUARAJ, C., JAGAN, E. G., RAJASEKAR, S., SELVAKUMAR, P., KALAICHELVAN, P. T. & MOHAN, N. 2010. Synthesis of silver nanoparticles using *acalypha indica* leaf extract and its antibacterial activity against water borne pathogens *Colloids and Surfaces B: Biointerfaces* 76, 50-56.
- KRUK, T., SZCZEPANOWICZ, K., STEFANSKA, J., SOCHA, R. P. & WARSZYNSKI, P. 2015. Synthesis and antimicrobial activity of monodisperse copper nanoparticles. *Colloids Surf B Biointerfaces*, 128, 17-22.
- LIMA, D. D. S., GULLON, B., CARDELLE-COBAS, A., BRITO, L. M., RODRIGUES, K. A. F., QUELEMES, P. V., RAMOS-JESUS, J., ARCANJO, D. D. R., PLÁCIDO, A., BATZIOU, K., QUARESMA, P., EATON, P., DELERUE-MATOS, C., CARVALHO, F. A. A., DA SILVA, D. A., PINTADO, M. & LEITE, J. R. D. S. A. 2017. Chitosan-based silver nanoparticles: A study of the antibacterial, antileishmanial and cytotoxic effects. *Journal of Bioactive and Compatible Polymers*, 32, 397-410.
- LISIECKI, I., BILLOUDET, F. & PILENI, M. P. 1996. Control of the Shape and the Size of Copper Metallic Particles. *The Journal of Physical Chemistry*, 100, 4160-4166.
- MADASSERY, J., CHERIYAMUN, S. & RAGHAVAN, R. 2015. DPPH Radical Scavenging Property of Methanol Leaf Extract from *Pogostemon quadrifolius* (Benth.). *Research Journal of Medicinal Plant*, 9, 361-367.
- MARKUS, J., WANG, D., KIM, Y. J., AHN, S., MATHIYALAGAN, R., WANG, C. & YANG, D. C. 2017. Biosynthesis, Characterization, and Bioactivities Evaluation of Silver and Gold Nanoparticles Mediated by the Roots of Chinese Herbal *Angelica pubescens* Maxim. *Nanoscale Res Lett*, 12, 46.
- MASOKO, P. & ELOFF, J. N. 2007. Resistance of animal fungal pathogens to solvents used in bioassays. *South African Journal of Botany*, 73, 667-669.

- MCGAW, L. J., RABE, T., SPARG, S. G., JAGER, A. K., ELOFF, J. N. & VAN STADEN, J. 2001. An investigation on the biological activity of Combretum species. *J Ethnopharmacol*, 75, 45-50.
- MOLDOVAN, B., DAVID, L., ACHIM, M., CLICHICI, S. & FILIP, G. A. 2016. A green approach to phytomediated synthesis of silver nanoparticles using Sambucus nigra L. fruits extract and their antioxidant activity. *Journal of Molecular Liquids*, 221, 271-278.
- MOLOTO, N., REVAPRASADU, N., MUSEETHA, P. L. & MOLOTO, M. J. 2009. The effect of precursor concentration, temperature and capping group on the morphology of CdS nanoparticles. *J Nanosci Nanotechnol*, 9, 4760-6.
- MUTHUKRISHNAN, A. M. 2015. Green Synthesis of Copper-Chitosan Nanoparticles and Study of its Antibacterial Activity. *Journal of Nanomedicine & Nanotechnology*, 06.
- PAL, S., TAK, Y. K. & SONG, J. M. 2007. Does the Antibacterial Activity of Silver Nanoparticles Depend on the Shape of the Nanoparticle? A Study of the Gram-Negative Bacterium Escherichia coli. *Applied and Environmental Microbiology*, 73, 1712-1720.
- PANACEK, A., KOLAR, M., VECEROVA, R., PRUCEK, R., SOUKUPOVA, J., KRYSTOF, V., HAMAL, P., ZBORIL, R. & KVITEK, L. 2009. Antifungal activity of silver nanoparticles against Candida spp. *Biomaterials*, 30, 6333-40.
- PHULL, A.-R., ABBAS, Q., ALI, A., RAZA, H., KIM, S. J., ZIA, M. & HAQ, I.-U. 2016. Antioxidant, cytotoxic and antimicrobial activities of green synthesized silver nanoparticles from crude extract of Bergenia ciliata. *Future Journal of Pharmaceutical Sciences*, 2, 31-36.
- POOJARY, M. M., VISHNUMURTHY, K. A. & VASUDEVA ADHIKARI, A. 2015. Extraction, characterization and biological studies of phytochemicals from Mammea suriga. *Journal of Pharmaceutical Analysis*, 5, 182-189.
- PRASAD, P. R., KANCHI, S. & NAIDOO, E. B. 2016. In-vitro evaluation of copper nanoparticles cytotoxicity on prostate cancer cell lines and their antioxidant, sensing and catalytic activity: One-pot green approach. *J Photochem Photobiol B*, 161, 375-82.
- PRAVEENKUMAR, K., ROBINAL, M. K., KALASAD, M. D., SANKARAPPA, T. & MASSHESH, D. 2014. Chitosan capped silver nanoparticles used as pressure sensors. *Journal of applied physics* 5, 43-51.

- RAJESHKUMAR, S. & BHARATH, L. V. 2017. Mechanism of plant-mediated synthesis of silver nanoparticles - A review on biomolecules involved, characterisation and antibacterial activity. *Chem Biol Interact*, 273, 219-227.
- RAVICHANDRAN, V., VASANTHI, S., SHALINI, S., ALI SHAH, S. A. & HARISH, R. 2016. Green synthesis of silver nanoparticles using *Atrocarpus altilis* leaf extract and the study of their antimicrobial and antioxidant activity. *Materials Letters*, 180, 264-267.
- RAZA, M. A., KANWAL, Z., RAUF, A., SABRI, A. N., RIAZ, S. & NASEEM, S. 2016. Size- and Shape-Dependent Antibacterial Studies of Silver Nanoparticles Synthesized by Wet Chemical Routes. *Nanomaterials (Basel)*, 6.
- REDDY, N. J., NAGOOR VALI, D., RANI, M. & RANI, S. S. 2014. Evaluation of antioxidant, antibacterial and cytotoxic effects of green synthesized silver nanoparticles by *Piper longum* fruit. *Mater Sci Eng C Mater Biol Appl*, 34, 115-22.
- SADEGHI, Z., VALIZADEH, J., AZYZIAN SHERMEH, O. & AKABERI, M. 2015. Antioxidant activity and total phenolic content of *Boerhavia elegans* (choisy) grown in Baluchestan, Iran. *Avicenna Journal of Phytomedicine*, 5, 1-9.
- SHARMA, V. K., YNGARD, R. A. & LIN, Y. 2009. Silver nanoparticles: green synthesis and their antimicrobial activities. *Adv Colloid Interface Sci*, 145, 83-96.
- SIBIYA, P. N. & MOLOTO, M. J. 2014. Effect of precursor concentration and pH on the shape and size of starch capped silver Selenide nanoparticles. *Chalcogenide letters* 11, 577-588.
- SIBOKOZA, S. B., MOLOTO, M. J., MOLOTO, N. & SIBIYA, P. N. 2017. The effect of temperature and precursor concentration on the synthesis of cobalt sulphide nanoparticles using cobalt diethyldithiocarbamate complex. *Chalcogenide Letters*, 14, 69-78.
- SOBCZAK-KUPIEC, A., MALINA, D., WZOREK, Z. & ZIMOWSKA, M. 2011. Influence of silver nitrate concentration on the properties of silver nanoparticles. *IET Micro & Nano Letters*, 6, 656-660.
- XIA, Z. K., MA, Q. H., LI, S. Y., ZHANG, D. Q., CONG, L., TIAN, Y. L. & YANG, R. Y. 2016. The antifungal effect of silver nanoparticles on *Trichosporon asahii*. *J Microbiol Immunol Infect*, 49, 182-8.
- XIU, Z. M., ZHANG, Q. B., PUPPALA, H. L., COLVIN, V. L. & ALVAREZ, P. J. 2012. Negligible particle-specific antibacterial activity of silver nanoparticles. *Nano Lett*, 12, 4271-5.

- ZAIN, N. M., STAPLEY, A. G. & SHAMA, G. 2014. Green synthesis of silver and copper nanoparticles using ascorbic acid and chitosan for antimicrobial applications. *Carbohydr Polym*, 112, 195-202.
- ZHANG, A., ZHANG, J. & FANG, Y. 2008. Photoluminescence from colloidal silver nanoparticles. *Journal of Luminescence*, 128, 1635-1640.
- ZHANG, X., HE, T., WANG, C. & ZHANG, J. 2010. Nonlinear-Optical and Fluorescent Properties of Ag Aqueous Colloid Prepared by Silver Nitrate Reduction. *Journal of Nanomaterials*, 2010, 1-7.
- ZHAO, Y., JIANG, Y. & FANG, Y. 2006. Spectroscopy property of Ag nanoparticles. *Spectrochim Acta A Mol Biomol Spectrosc*, 65, 1003-6.
- ZUBER, A., PURDEY, M., SCHATNER, E., FORBES, C., VAN DER HOEK, B., GILES, D., ABELL, A., MONRO, T. & EBENDORFF-HEIDEPRIEM, H. 2016. Detection of gold nanoparticles with different sizes using absorption and fluorescence based method. *Sensors and Actuators B: Chemical*, 227, 117-127.

Chapter 5

Conclusions and Future work

5.1 Conclusions

Preliminary phytochemical screening revealed that secondary metabolites from the leaves of *Camellia sinensis*, *Combretum molle*, and *Melia azedarach linn* were successfully extracted using decoction method. The characterization of the aqueous extracts using qualitative preliminary phytochemical screening methods, TLC, Uv-vis spectroscopy, and FTIR spectroscopy revealed that secondary metabolites such as phenols, flavonoids, saponins and carbohydrates were extracted. The total phenolic content was found to be in the following order *Combretum molle* > *Camellia sinensis* > *Melia azedarach linn*, while the total flavonoid content was found to be high in *Camellia sinensis* followed by *Combretum molle* and *Melia azedarach linn*.

A simple and eco-friendly method for synthesis of silver nanoparticles using chitosan, aqueous extracts of *Camellia sinensis*, *Combretum molle* and *Melia azedarach linn* was successfully developed. The influence of capping agent concentration on the properties of silver nanoparticles was investigated. The optical properties of the synthesized silver nanoparticles were influenced by the capping agent concentration. All the prepared silver nanoparticles were blue shifted from the bulk silver metal which has a plasmon resonance band at 1000 nm. A decrease in peak width with an increase in capping agent concentration was observed, this is attributed to quantum confinement effect. It was also observed that all the prepared silver nanoparticles have photoluminescence properties. The presence of different functional groups on the surface of the synthesized nanoparticles indicates that the particles were successfully capped with chitosan and the bioactive compounds from three different plant leaves. These functional groups uses the amine and hydroxyl functional groups to bond with silver nanoparticles. A face-centered cubic symmetry was obtained for the synthesized silver nanoparticles.

A decrease in particle size with an increase in capping agent concentration was the general trend that was observed, however this was not the case with chitosan capped silver nanoparticles, this is because an increase in capping agent concentration resulted in a decrease in particles size however a further increase in capping agent concentration to 2 % resulted in a slight increase in particle size. The slight increase in particle size may be due to ripening effects. A change in the shape of

the particles was observed with the variation in capping agent concentration, at low concentration (0.5%) mixed particles with a high degree of agglomeration were obtained for the particles capped with plant materials. An increase in capping concentration resulted in the formation of well-defined particles with a low degree of agglomeration.

All the prepared silver nanoparticles showed satisfactory antifungal activity against *Candida albicans* and *Cryptococcus neoformans*. The antibacterial activity of all the synthesized silver nanoparticles was investigated against *Staphylococcus aureus*, *Enterococcus faecalis*, *Klebsiella pneumonia*, and *Pseudomonas aeruginosa*. Silver nanoparticles were found to be active against all the selected bacterial strains, with more activity towards the gram-negative bacteria compared to gram-positive bacteria. The capping molecules used in this study also showed some antibacterial and antifungal activity against selected strains however silver nanoparticles performed better than these capping molecules. Silver nanoparticles were found to have some antioxidant activity, however, the capping molecules were found to be more active than silver nanoparticles.

The investigation of the influence of precursor concentrations revealed that the particle size is directly proportional to the precursor concentration. All the prepared silver nanoparticles were blue shifted from the bulk silver. An increase in precursor concentration resulted in the formation of various shapes which includes spheres, bipods, and diamonds. A face-centered cubic geometry was obtained from XRD, and the phase remained the same with an increase in precursor concentration.

Copper nanoparticles were successfully synthesized using the green synthesis method. The influence of the identity of the capping agent on the size and shape of copper nanoparticles was revealed by the TEM results. The identity of the capping agent was found to affect both the size and shape of copper nanoparticles. All the prepared copper nanoparticles were found to be active against the selected bacterial strains.

5.2 Future work and Recommendations

Isolation of bioactive compounds: Different bioactive compounds were obtained from the aqueous extracts of *Camellia sinensis*, *Combretum molle*, and *Melia azedarach* leaves. Therefore, it was not possible to state without a reasonable doubt which bioactive compounds were responsible for the reduction and capping of silver nanoparticles. It is therefore recommended that isolation and separation of the bioactive compound be done using preparative or column chromatography. This will help in identifying the structure of the capping molecule using gas chromatography-mass spectroscopy and nuclear magnetic resonance.

Effect of molecular weight on the properties of nanoparticles: The physicochemical nature of chitosan is mostly affected by factors such as pH and temperature. Other factors that affect the properties of chitosan includes the degree of quaternization of the amino group, the degree of N-Acetylation and molecular weight. It is recommended that the influence of chitosan molecular weight be investigated on the size and shape of metal nanoparticles.

Mechanism for interaction of nanoparticles with microorganisms: Since silver and copper nanoparticles were found to have antibacterial activity; it is recommended that the mechanism in which nanoparticles interact with bacterial strains be investigated.

Cytotoxicity of silver nanoparticles: Due to high antibacterial and antifungal activity of the prepared silver nanoparticles against the selected six test microorganisms, it is recommended that the cytotoxicity study of the prepared silver nanoparticles be conducted against some selected cells. This is will also assist in understanding the influence of particle size and shape on the cytotoxicity of nanoparticles.

